7

AC Equivalent Circuit Modeling

7.1 INTRODUCTION

Converter systems invariably require feedback. For example, in a typical dc–dc converter application, the output voltage $v(t)$ must be kept constant, regardless of changes in the input voltage $v_g(t)$ or in the effective load resistance R. This is accomplished by building a circuit that varies the converter control input [i.e., the duty cycle $d(t)$] in such a way that the output voltage $v(t)$ is regulated to be equal to a desired reference value v_{ref}. In inverter systems, a feedback loop causes the output voltage to follow a sinusoidal reference voltage. In modern low-harmonic rectifier systems, a control system causes the converter input current to be proportional to the input voltage, such that the input port presents a resistive load to the ac source. So feedback is commonly employed.

A typical dc–dc system incorporating a buck converter and feedback loop block diagram is illustrated in Fig. 7.1. It is desired to design this feedback system in such a way that the output voltage is accurately regulated, and is insensitive to disturbances in $v_g(t)$ or in the load current. In addition, the feedback system should be stable, and properties such as transient overshoot, settling time, and steady-state regulation should meet specifications. The ac modeling and design of converters and their control systems such as Fig. 7.1 is the subject of Part II of this book.

To design the system of Fig. 7.1, we need a dynamic model of the switching converter. How do variations in the power input voltage, the load current, or the duty cycle affect the output voltage? What are the small-signal transfer functions? To answer these questions, we will extend the steady-state models developed in Chapters 2 and 3 to include the dynamics introduced by the inductors and capacitors of the converter. Dynamics of converters operating in the continuous conduction mode can be modeled using techniques quite similar to those of Chapters 2 and 3; the resulting ac equivalent circuits bear a strong resemblance to the dc equivalent circuits derived in Chapter 3.

Modeling is the representation of physical phenomena by mathematical means. In engineering,

R. W. Erickson et al., *Fundamentals of Power Electronics*

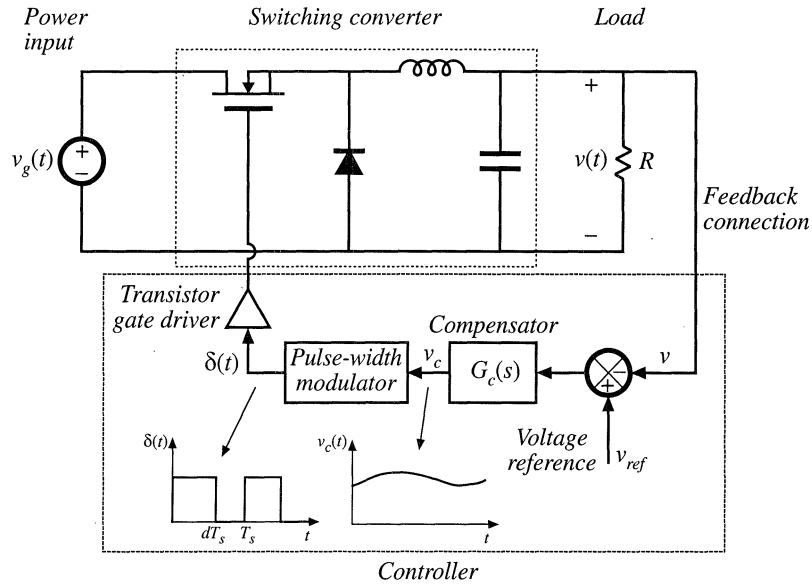

Fig. 7.1 A simple dc–dc regulator system, including a buck converter power stage and a feedback network.

it is desired to model the important dominant behavior of a system, while neglecting other insignificant phenomena. Simplified terminal equations of the component elements are used, and many aspects of the system response are neglected altogether, that is, they are "unmodeled." The resulting simplified model yields physical insight into the system behavior, which aids the engineer in designing the system to operate in a given specified manner. Thus, the modeling process involves use of approximations to neglect small but complicating phenomena, in an attempt to understand what is most important. Once this basic insight is gained, it may be desirable to carefully refine the model, by accounting for some of the previously ignored phenomena. It is a fact of life that real, physical systems are complex, and their detailed analysis can easily lead to an intractable and useless mathematical mess. Approximate models are an important tool for gaining understanding and physical insight.

As discussed in Chapter 2, the switching ripple is small in a well-designed converter operating in continuous conduction mode (CCM). Hence, we should ignore the switching ripple, and model only the underlying ac variations in the converter waveforms. For example, suppose that some ac variation is introduced into the converter duty cycle $d(t)$, such that

$$d(t) = D + D_m \cos\omega_m t \tag{7.1}$$

where D and D_m are constants, $| D_m | \ll D$, and the modulation frequency ω_m is much smaller than the converter switching frequency $\omega_s = 2\pi f_s$. The resulting transistor gate drive signal is illustrated in Fig. 7.2(a), and a typical converter output voltage waveform $v(t)$ is illustrated in Fig. 7.2(b). The spectrum of $v(t)$ is illustrated in Fig. 7.3. This spectrum contains components at the switching frequency as well as its harmonics and sidebands; these components are small in magnitude if the switching ripple is small. In addition, the spectrum contains a low-frequency component at the modulation frequency ω_m. The magnitude and phase of this component depend not only on the duty cycle variation, but also on the frequency response of the converter. If we neglect the switching ripple, then this low-frequency compo-

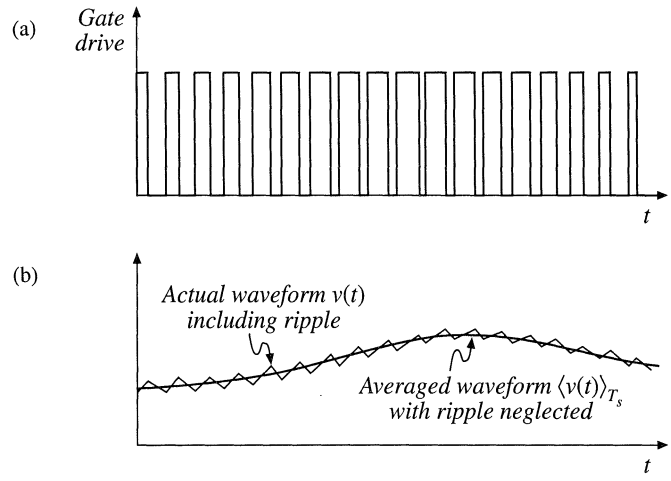

Fig. 7.2 Ac variation of the converter signals: (a) transistor gate drive signal, in which the duty cycle varies slowly, and (b) the resulting converter output voltage waveform. Both the actual waveform $v(t)$ (including high frequency switching ripple) and its averaged, low-frequency component, $\langle v(t)\rangle_{T_s}$, are illustrated.

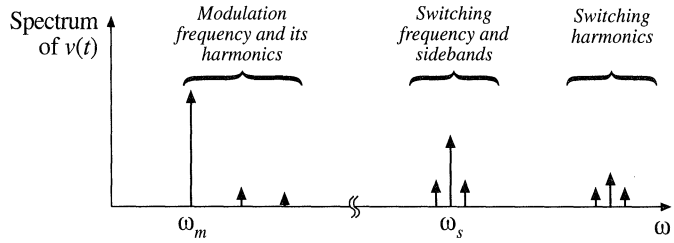

Fig. 7.3 Spectrum of the output voltage waveform $v(t)$ of Fig. 7.2.

nent remains [also illustrated in Fig. 7.2(b)]. The objective of our ac modeling efforts is to predict this low-frequency component.

A simple method for deriving the small-signal model of CCM converters is explained in Section 7.2. The switching ripples in the inductor current and capacitor voltage waveforms are removed by averaging over one switching period. Hence, the low-frequency components of the inductor and capacitor waveforms are modeled by equations of the form

$$\begin{aligned} L\frac{d\langle i_L(t)\rangle_{T_s}}{dt} &= \langle v_L(t)\rangle_{T_s} \\ C\frac{d\langle v_C(t)\rangle_{T_s}}{dt} &= \langle i_C(t)\rangle_{T_s} \end{aligned} \tag{7.2}$$

where $\langle x(t)\rangle_{T_s}$ denotes the average of $x(t)$ over an interval of length T_s:

$$\langle x(t)\rangle_{T_s} = \frac{1}{T_s}\int_t^{t+T_s} x(\tau)d\tau \tag{7.3}$$

So we will employ the basic approximation of removing the high-frequency switching ripple by averaging over one switching period. Yet the average value is allowed to vary from one switching period to the next, such that low-frequency variations are modeled. In effect, the "moving average" of Eq. (7.3) constitutes low-pass filtering of the waveform. A few of the numerous references on averaged modeling of switching converters are listed at the end of this chapter [1–20].

Note that the principles of inductor volt-second balance and capacitor charge balance predict that the right-hand sides of Eqs. (7.2) are zero when the converter operates in equilibrium. Equations (7.2) describe how the inductor currents and capacitor voltages change when nonzero average inductor voltage and capacitor current are applied over a switching period.

The averaged inductor voltage and capacitor currents of Eq. (7.2) are, in general, nonlinear functions of the signals in the converter, and hence Eqs. (7.2) constitute a set of nonlinear differential equations. Indeed, the spectrum in Fig. 7.3 also contains harmonics of the modulation frequency ω_m. In most converters, these harmonics become significant in magnitude as the modulation frequency ω_m approaches the switching frequency ω_s, or as the modulation amplitude D_m approaches the quiescent duty cycle D. Nonlinear elements are not uncommon in electrical engineering; indeed, all semiconductor devices exhibit nonlinear behavior. To obtain a linear model that is easier to analyze, we usually construct a small-signal model that has been linearized about a quiescent operating point, in which the harmonics of the modulation or excitation frequency are neglected. As an example, Fig. 7.4 illustrates linearization of the familiar diode i–v characteristic shown in Fig. 7.4(b). Suppose that the diode current $i(t)$ has a quiescent (dc) value I and a signal component $\hat{i}(t)$. As a result, the voltage $v(t)$ across the diode has a quiescent value V and a signal component $\hat{v}(t)$. If the signal components are small compared to the quiescent values,

$$|\hat{v}| \ll |V|, \quad |\hat{i}| \ll |I| \tag{7.4}$$

then the relationship between $\hat{v}(t)$ and $\hat{i}(t)$ is approximately linear, $\hat{v}(t) = r_D\hat{i}(t)$. The conductance $1/r_D$

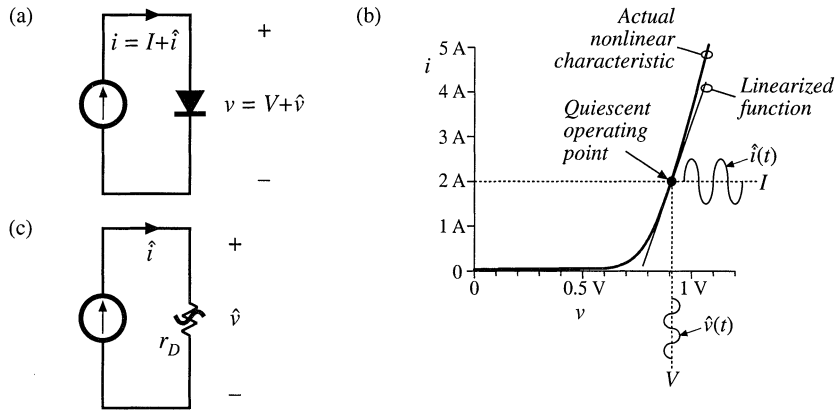

Fig. 7.4 Small-signal equivalent circuit modeling of the diode: (a) a nonlinear diode conducting current i; (b) linearization of the diode characteristic around a quiescent operating point; (c) a linearized small-signal model.

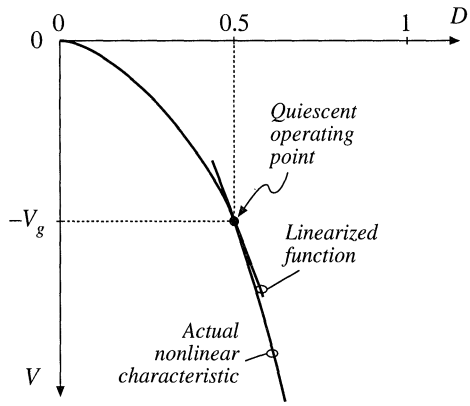

Fig. 7.5 Linearization of the static control-to-output characteristic of the buck-boost converter about the quiescent operating point $D = 0.5$.

represents the slope of the diode characteristic, evaluated at the quiescent operating point. The small-signal equivalent circuit model of Fig. 7.4(c) describes the diode behavior for small variations around the quiescent operating point.

An example of a nonlinear converter characteristic is the dependence of the steady-state output voltage V of the buck-boost converter on the duty cycle D, illustrated in Fig. 7.5. Suppose that the converter operates with some dc output voltage, say, $V = -V_g$, corresponding to a quiescent duty cycle of $D = 0.5$. Duty cycle variations $\hat{d}$ about this quiescent value will excite variations $\hat{v}$ in the output voltage. If the magnitude of the duty cycle variation is sufficiently small, then we can compute the resulting output voltage variations by linearizing the curve. The slope of the linearized characteristic in Fig. 7.5 is chosen to be equal to the slope of the actual nonlinear characteristic at the quiescent operating point; this slope is the dc control-to-output gain of the converter. The linearized and nonlinear characteristics are approximately equal in value provided that the duty cycle variations $\hat{d}$ are sufficiently small.

Although it illustrates the process of small-signal linearization, the buck-boost example of Fig. 7.5 is oversimplified. The inductors and capacitors of the converter cause the gain to exhibit a frequency response. To correctly predict the poles and zeroes of the small-signal transfer functions, we must linearize the converter averaged differential equations, Eqs. (7.2). This is done in Section 7.2. A small-signal ac equivalent circuit can then be constructed using the methods developed in Chapter 3. The resulting small-signal model of the buck-boost converter is illustrated in Fig. 7.6; this model can be solved using conventional circuit analysis techniques, to find the small-signal transfer functions, output impedance, and other frequency-dependent properties. In systems such as Fig. 7.1, the equivalent circuit model can be inserted in place of the converter. When small-signal models of the other system elements (such as the

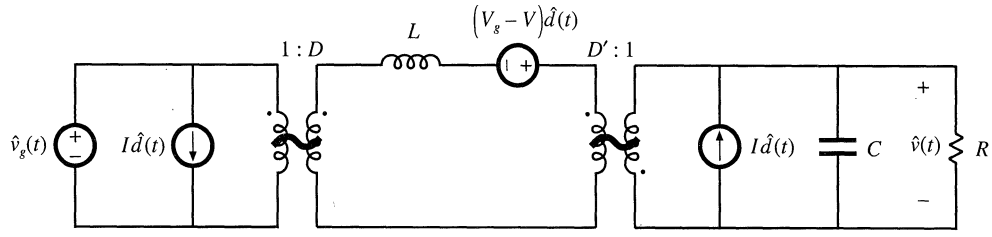

Fig. 7.6 Small-signal ac equivalent circuit model of the buck-boost converter.

pulse-width modulator) are inserted, then a complete linearized system model is obtained. This model can be analyzed using standard linear techniques, such as the Laplace transform, to gain insight into the behavior and properties of the system.

Two well-known variants of the ac modeling method, state-space averaging and circuit averaging, are explained in Sections 7.3 and 7.4. An extension of circuit averaging, known as *averaged switch modeling*, is also discussed in Section 7.4. Since the switches are the only elements that introduce switching harmonics, equivalent circuit models can be derived by averaging only the switch waveforms. The converter models suitable for analysis or simulation are obtained simply by replacing the switches with the averaged switch model. The averaged switch modeling technique can be extended to other modes of operation such as the discontinuous conduction mode, as well as to current programmed control and to resonant converters. In Section 7.5, it is shown that the small-signal model of any dc–dc pulse-width modulated CCM converter can be written in a standard form. Called the *canonical model*, this equivalent circuit describes the basic physical functions that any of these converters must perform. A simple model of the pulse-width modulator circuit is described in Section 7.6.

These models are useless if you don't know how to apply them. So in Chapter 8, the frequency response of converters is explored, in a design-oriented and detailed manner. Small-signal transfer functions of the basic converters are tabulated. Bode plots of converter transfer functions and impedances are derived in a simple, approximate manner, which allows insight to be gained into the origins of the frequency response of complex converter systems.

These results are used to design converter control systems in Chapter 9 and input filters in Chapter 10. The modeling techniques are extended in Chapters 11 and 12 to cover the discontinuous conduction mode and the current programmed mode.

7.2 THE BASIC AC MODELING APPROACH

Let us derive a small-signal ac model of the buck-boost converter of Fig. 7.7. The analysis begins as usual, by determining the voltage and current waveforms of the inductor and capacitor. When the switch is in position 1, the circuit of Fig. 7.8(a) is obtained. The inductor voltage and capacitor current are:

$$v_L(t) = L\frac{di(t)}{dt} = v_g(t) \tag{7.5}$$

$$i_C(t) = C\frac{dv(t)}{dt} = -\frac{v(t)}{R} \tag{7.6}$$

We now make the small-ripple approximation. But rather than replacing $v_g(t)$ and $v(t)$ with their dc components V_g and V as in Chapter 2, we now replace them with their low-frequency averaged values $\langle v_g(t)\rangle_{T_s}$ and $\langle v(t)\rangle_{T_s}$, defined by Eq. (7.3). Equations (7.5) and (7.6) then become

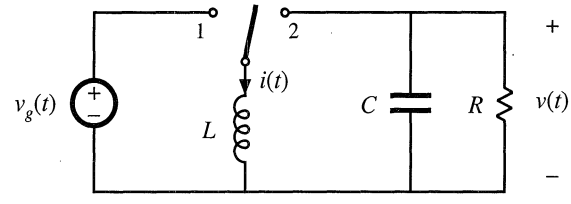

Fig. 7.7 Buck-boost converter example.

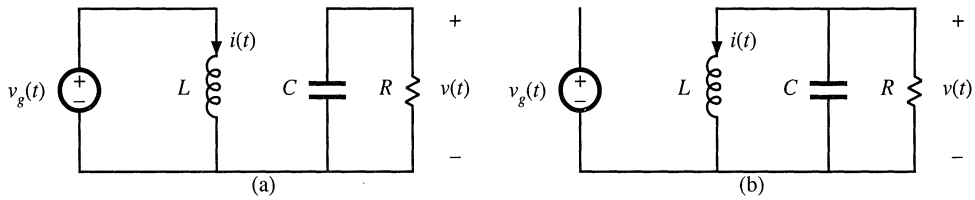

Fig. 7.8 Buck-boost converter circuit: (a) when the switch is in position 1, (b) when the switch is in position 2.

$$v_L(t) = L\frac{di(t)}{dt} \approx \langle v_g(t)\rangle_{T_s} \tag{7.7}$$

$$i_C(t) = C\frac{dv(t)}{dt} \approx -\frac{\langle v(t)\rangle_{T_s}}{R} \tag{7.8}$$

Hence, during the first subinterval, the inductor current $i(t)$ and the capacitor voltage $v(t)$ change with the essentially constant slopes given by Eqs. (7.7) and (7.8). With the switch in position 2, the circuit of Fig. 7.8(b) is obtained. Its inductor voltage and capacitor current are:

$$v_L(t) = L\frac{di(t)}{dt} = v(t) \tag{7.9}$$

$$i_C(t) = C\frac{dv(t)}{dt} = -i(t) - \frac{v(t)}{R} \tag{7.10}$$

Use of the small-ripple approximation, to replace $i(t)$ and $v(t)$ with their averaged values, yields

$$v_L(t) = L\frac{di(t)}{dt} \approx \langle v(t)\rangle_{T_s} \tag{7.11}$$

$$i_C(t) = C\frac{dv(t)}{dt} \approx -\langle i(t)\rangle_{T_s} - \frac{\langle v(t)\rangle_{T_s}}{R} \tag{7.12}$$

During the second subinterval, the inductor current and capacitor voltage change with the essentially constant slopes given by Eqs. (7.11) and (7.12).

7.2.1 Averaging the Inductor Waveforms

The inductor voltage and current waveforms are sketched in Fig. 7.9. The low-frequency average of the inductor voltage is found by evaluation of Eq. (7.3)—the inductor voltage during the first and second subintervals, given by Eqs. (7.7) and (7.11), are averaged:

$$\langle v_L(t)\rangle_{T_s} = \frac{1}{T_s}\int_t^{t+T_s} v_L(\tau)d\tau \approx d(t)\langle v_g(t)\rangle_{T_s} + d'(t)\langle v(t)\rangle_{T_s} \tag{7.13}$$

where $d'(t) = 1 - d(t)$. The right-hand side of Eq. (7.13) contains no switching harmonics, and models

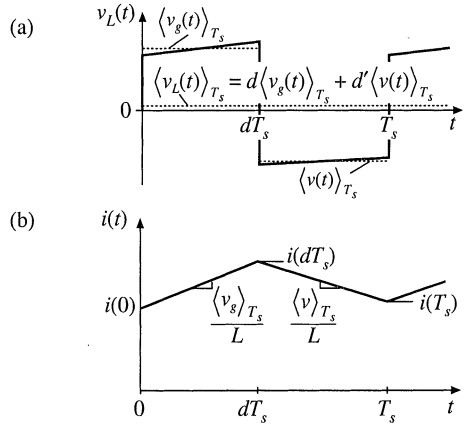

Fig. 7.9 Buck-boost converter waveforms: (a) inductor voltage, (b) inductor current.

only the low-frequency components of the inductor voltage waveform. Insertion of this equation into Eq. (7.2) leads to

$$L\frac{d\langle i(t)\rangle_{T_s}}{dt} = d(t)\langle v_g(t)\rangle_{T_s} + d'(t)\langle v(t)\rangle_{T_s} \tag{7.14}$$

This equation describes how the low-frequency components of the inductor current vary with time.

7.2.2 Discussion of the Averaging Approximation

In steady-state, the actual inductor current waveform $i(t)$ is periodic with period equal to the switching period T_s: $i(t + T_s) = i(t)$. During transients, there is a net change in $i(t)$ over one switching period. This net change in inductor current is correctly predicted by use of the average inductor voltage. We can show that this is true, based on the inductor equation

$$L\frac{di(t)}{dt} = v_L(t) \tag{7.15}$$

Divide by L, and integrate both sides from t to $t + T_s$:

$$\int_t^{t+T_s} di = \frac{1}{L}\int_t^{t+T_s} v_L(\tau)d\tau \tag{7.16}$$

The left-hand side of Eq. (7.16) is $i(t + T_s) - i(t)$, while the right-hand side can be expressed in terms of the definition of $\langle v_L(t)\rangle_{T_s}$, Eq. (7.3), by multiplying and dividing by T_s to obtain

$$i(t + T_s) - i(t) = \frac{1}{L}T_s\langle v_L(t)\rangle_{T_s} \tag{7.17}$$

The left-hand side of Eq. (7.17) is the net change in inductor current over one complete switching period. Equation (7.17) states that this change is exactly equal to the switching period T_s multiplied by the aver-

age slope $\langle v_L(t)\rangle_{T_s}/L$.

Equation (7.17) can be rearranged to obtain

$$L\frac{i(t+T_s)-i(t)}{T_s} = \langle v_L(t)\rangle_{T_s} \tag{7.18}$$

Let us now find the derivative of $\langle i(t)\rangle_{T_s}$:

$$\frac{d\langle i(t)\rangle_{T_s}}{dt} = \frac{d}{dt}\left(\frac{1}{T_s}\int_t^{t+T_s} i(\tau)d\tau\right) = \frac{i(t+T_s)-i(t)}{T_s} \tag{7.19}$$

Substitution of Eq. (7.19) into (7.18) leads to

$$L\frac{d\langle i(t)\rangle_{T_s}}{dt} = \langle v_L(t)\rangle_{T_s} \tag{7.20}$$

which coincides with Eq. (7.2).

Let us next compute how the inductor current changes over one switching period in our buck-boost example. The inductor current waveform is sketched in Fig. 7.9(b). Assume that the inductor current begins at some arbitrary value $i(0)$. During the first subinterval, the inductor current changes with the essentially constant value given by Eq. (7.7). The value at the end of the first subinterval is

$$\underbrace{i(dT_s)}_{\text{(final value)}} = \underbrace{i(0)}_{\text{(initial value)}} + \underbrace{(dT_s)}_{\text{(length of interval)}} \underbrace{\left(\frac{\langle v_g(t)\rangle_{T_s}}{L}\right)}_{\text{(average slope)}} \tag{7.21}$$

During the second subinterval, the inductor current changes with the essentially constant value given by Eq. (7.11). Hence, the value at the end of the second subinterval is

$$\underbrace{i(T_s)}_{\text{(final value)}} = \underbrace{i(dT_s)}_{\text{(initial value)}} + \underbrace{(d'T_s)}_{\text{(length of interval)}} \underbrace{\left(\frac{\langle v(t)\rangle_{T_s}}{L}\right)}_{\text{(average slope)}} \tag{7.22}$$

By substitution of Eq. (7.21) into Eq. (7.22), we can express $i(T_s)$ in terms of $i(0)$,

$$i(T_s) = i(0) + \frac{T_s}{L}\underbrace{\left(d(t)\langle v_g(t)\rangle_{T_s} + d'(t)\langle v(t)\rangle_{T_s}\right)}_{\langle v_L(t)\rangle_{T_s}} \tag{7.23}$$

Equations (7.21) to (7.23) are illustrated in Fig. 7.10. Equation (7.23) expresses the final value $i(T_s)$ directly in terms of $i(0)$, without the intermediate step of calculating $i(DT_s)$. This equation can be interpreted in the same manner as Eqs. (7.21) and (7.22): the final value $i(T_s)$ is equal to the initial value $i(0)$, plus the length of the interval T_s multiplied by the average slope $\langle v_L(t)\rangle_{T_s}/L$. But note that the interval length is chosen to coincide with the switching period, such that the switching ripple is effectively

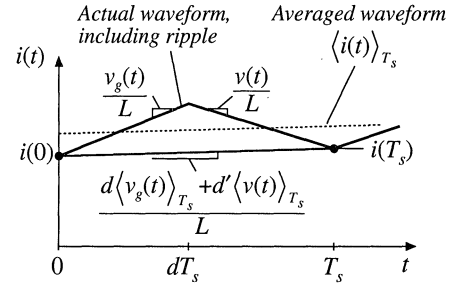

Fig. 7.10 Use of the average slope to predict how the inductor current waveform changes over one switching period. The actual waveform $i(t)$ and its low-frequency component $\langle i(t)\rangle_{T_s}$ are illustrated.

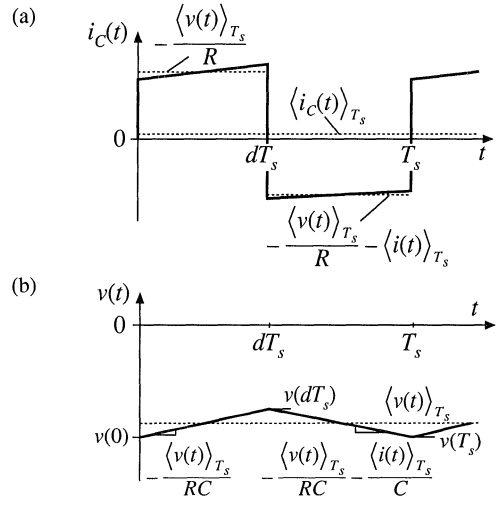

Fig. 7.11 Buck-boost converter waveforms: (a) capacitor current, (b) capacitor voltage.

removed. Also, the use of the average slope leads to correct prediction of the final value $i(T_s)$. It can be easily verified that, when Eq. (7.23) is inserted into Eq. (7.19), the previous result (7.14) is obtained.

7.2.3 Averaging the Capacitor Waveforms

A similar procedure leads to the capacitor dynamic equation. The capacitor voltage and current waveforms are sketched in Fig. 7.11. The average capacitor current can be found by averaging Eqs. (7.8) and (7.12); the result is

$$\langle i_C(t)\rangle_{T_s} = d(t)\left(-\frac{\langle v(t)\rangle_{T_s}}{R}\right) + d'(t)\left(-\langle i(t)\rangle_{T_s} - \frac{\langle v(t)\rangle_{T_s}}{R}\right) \tag{7.24}$$

Upon inserting this equation into Eq. (7.2) and collecting terms, one obtains

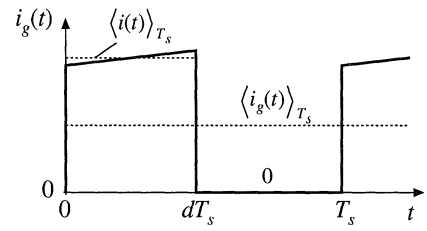

Fig. 7.12 Buck-boost converter waveforms: input source current $i_g(t)$.

$$C \frac{d\langle v(t) \rangle_{T_s}}{dt} = -d'(t) \langle i(t) \rangle_{T_s} - \frac{\langle v(t) \rangle_{T_s}}{R} \tag{7.25}$$

This is the basic averaged equation which describes dc and low-frequency ac variations in the capacitor voltage.

7.2.4 The Average Input Current

In Chapter 3, it was found to be necessary to write an additional equation that models the dc component of the converter input current. This allowed the input port of the converter to be modeled by the dc equivalent circuit. A similar procedure must be followed here, so that low-frequency variations at the converter input port are modeled by the ac equivalent circuit.

For the buck-boost converter example, the current $i_g(t)$ drawn by the converter from the input source is equal to the inductor current $i(t)$ during the first subinterval, and zero during the second subinterval. By neglecting the inductor current ripple and replacing $i(t)$ with its averaged value $\langle i(t) \rangle_{T_s}$, we can express the input current as follows:

$$i_g(t) = \begin{cases} \langle i(t) \rangle_{T_s} & \text{during subinterval 1} \\ 0 & \text{during subinterval 2} \end{cases} \tag{7.26}$$

The input current waveform is illustrated in Fig. 7.12. Upon averaging over one switching period, one obtains

$$\langle i_g(t) \rangle_{T_s} = d(t) \langle i(t) \rangle_{T_s} \tag{7.27}$$

This is the basic averaged equation which describes dc and low-frequency ac variations in the converter input current.

7.2.5 Perturbation and Linearization

The buck-boost converter averaged equations, Eqs. (7.14), (7.25), and (7.27), are collected below:

$$
\begin{aligned}
L\frac{d\langle i(t)\rangle_{T_s}}{dt} &= d(t)\langle v_g(t)\rangle_{T_s} + d'(t)\langle v(t)\rangle_{T_s} \\
C\frac{d\langle v(t)\rangle_{T_s}}{dt} &= -d'(t)\langle i(t)\rangle_{T_s} - \frac{\langle v(t)\rangle_{T_s}}{R} \\
\langle i_g(t)\rangle_{T_s} &= d(t)\langle i(t)\rangle_{T_s}
\end{aligned}
\tag{7.28}
$$

These equations are nonlinear because they involve the multiplication of time-varying quantities. For example, the capacitor current depends on the product of the control input $d'(t)$ and the low-frequency component of the inductor current, $\langle i(t)\rangle_{T_s}$. Multiplication of time-varying signals generates harmonics, and is a nonlinear process. Most of the techniques of ac circuit analysis, such as the Laplace transform and other frequency-domain methods, are not useful for nonlinear systems. So we need to linearize Eqs. (7.28) by constructing a small-signal model.

Suppose that we drive the converter at some steady-state, or quiescent, duty ratio $d(t) = D$, with quiescent input voltage $v_g(t) = V_g$. We know from our steady-state analysis of Chapters 2 and 3 that, after any transients have subsided, the inductor current $\langle i(t)\rangle_{T_s}$, the capacitor voltage $\langle v(t)\rangle_{T_s}$, and the input current $\langle i_g(t)\rangle_{T_s}$ will reach the quiescent values I, V, and I_g, respectively, where

$$
\begin{aligned}
V &= -\frac{D}{D'}V_g \\
I &= -\frac{V}{D'R} \\
I_g &= DI
\end{aligned}
\tag{7.29}
$$

Equations (7.29) are derived as usual via the principles of inductor volt-second and capacitor charge balance. They could also be derived from Eqs. (7.28) by noting that, in steady state, the derivatives must equal zero.

To construct a small-signal ac model at a quiescent operating point (I, V), one assumes that the input voltage $v_g(t)$ and the duty cycle $d(t)$ are equal to some given quiescent values V_g and D, plus some superimposed small ac variations $\hat{v}_g(t)$ and $\hat{d}(t)$. Hence, we have

$$
\begin{aligned}
\langle v_g(t)\rangle_{T_s} &= V_g + \hat{v}_g(t) \\
d(t) &= D + \hat{d}(t)
\end{aligned}
\tag{7.30}
$$

In response to these inputs, and after any transients have subsided, the averaged inductor current $\langle i(t)\rangle_{T_s}$, the averaged capacitor voltage $\langle v(t)\rangle_{T_s}$, and the averaged input current $\langle i_g(t)\rangle_{T_s}$ waveforms will be equal to the corresponding quiescent values I, V, and I_g, plus some superimposed small ac variations $\hat{i}(t)$, $\hat{v}(t)$, and $\hat{i}_g(t)$:

$$
\begin{aligned}
\langle i(t)\rangle_{T_s} &= I + \hat{i}(t) \\
\langle v(t)\rangle_{T_s} &= V + \hat{v}(t) \\
\langle i_g(t)\rangle_{T_s} &= I_g + \hat{i}_g(t)
\end{aligned}
\tag{7.31}
$$

With the assumptions that the ac variations are small in magnitude compared to the dc quiescent values, or

$$\begin{aligned} |\hat{v}_g(t)| &\ll |V_g| \\ |\hat{d}(t)| &\ll |D| \\ |\hat{i}(t)| &\ll |I| \\ |\hat{v}(t)| &\ll |V| \\ |\hat{i}_g(t)| &\ll |I_g| \end{aligned} \tag{7.32}$$

then the nonlinear equations (7.28) can be linearized. This is done by inserting Eqs. (7.30) and (7.31) into Eq. (7.28). For the inductor equation, one obtains

$$L\frac{d\left(I+\hat{i}(t)\right)}{dt} = \left(D+\hat{d}(t)\right)\left(V_g+\hat{v}_g(t)\right) + \left(D'-\hat{d}(t)\right)\left(V+\hat{v}(t)\right) \tag{7.33}$$

It should be noted that the complement of the duty cycle is given by

$$d'(t) = \left(1-d(t)\right) = 1-\left(D+\hat{d}(t)\right) = D'-\hat{d}(t) \tag{7.34}$$

where $D' = 1 - D$. The minus sign arises in the expression for $d'(t)$ because a $d(t)$ variation that causes $d(t)$ to increase will cause $d'(t)$ to decrease.

By multiplying out Eq. (7.33) and collecting terms, one obtains

$$L\left(\frac{dI}{dt}+\frac{d\hat{i}(t)}{dt}\right) = \underbrace{\left(DV_g+D'V\right)}_{\text{Dc terms}} + \underbrace{\left(D\hat{v}_g(t)+D'\hat{v}(t)+\left(V_g-V\right)\hat{d}(t)\right)}_{1^{st}\text{ order ac terms (linear)}} + \underbrace{\hat{d}(t)\left(\hat{v}_g(t)-\hat{v}(t)\right)}_{2^{nd}\text{ order ac terms (nonlinear)}} \tag{7.35}$$

The derivative of I is zero, since I is by definition a dc (constant) term. For the purposes of deriving a small-signal ac model, the dc terms can be considered known constant quantities. On the right-hand side of Eq. (7.35), three types of terms arise:

Dc terms: These terms contain dc quantities only.

First-order ac terms: Each of these terms contains a single ac quantity, usually multiplied by a constant coefficient such as a dc term. These terms are linear functions of the ac variations.

Second-order ac terms: These terms contain the products of ac quantities. Hence they are nonlinear, because they involve the multiplication of time-varying signals.

It is desired to neglect the nonlinear ac terms. Provided that the small-signal assumption, Eq. (7.32), is satisfied, then each of the second-order nonlinear terms is much smaller in magnitude that one or more of the linear first-order ac terms. For example, the second-order ac term $\hat{d}(t)\hat{v}_g(t)$ is much smaller in magnitude than the first-order ac term $D\hat{v}_g(t)$ whenever $|\hat{d}(t)| \ll D$. So we can neglect the second-order terms. Also, by definition [or by use of Eq. (7.29)], the dc terms on the right-hand side of the equation are equal to the dc terms on the left-hand side, or zero.

We are left with the first-order ac terms on both sides of the equation. Hence,

$$L\frac{d\hat{i}(t)}{dt} = D\hat{v}_g(t) + D'\hat{v}(t) + \left(V_g-V\right)\hat{d}(t) \tag{7.36}$$

This is the desired result: the small-signal linearized equation that describes variations in the inductor current.

The capacitor equation can be linearized in a similar manner. Insertion of Eqs. (7.30) and (7.31) into the capacitor equation of Eq. (7.28) yields

$$C\frac{d\left(V+\hat{v}(t)\right)}{dt} = -\left(D'-\hat{d}(t)\right)\left(I+\hat{i}(t)\right) - \frac{\left(V+\hat{v}(t)\right)}{R} \tag{7.37}$$

Upon multiplying out Eq. (7.37) and collecting terms, one obtains

$$C\left(\frac{dV}{dt}+\frac{d\hat{v}(t)}{dt}\right) = \underbrace{\left(-D'I-\frac{V}{R}\right)}_{\text{Dc terms}} + \underbrace{\left(-D'\hat{i}(t)-\frac{\hat{v}(t)}{R}+I\hat{d}(t)\right)}_{1^{st}\text{ order ac terms (linear)}} + \underbrace{\hat{d}(t)\hat{i}(t)}_{2^{nd}\text{ order ac term (nonlinear)}} \tag{7.38}$$

By neglecting the second-order terms, and noting that the dc terms on both sides of the equation are equal, we again obtain a linearized first-order equation, containing only the first-order ac terms of Eq. (7.38):

$$C\frac{d\hat{v}(t)}{dt} = -D'\hat{i}(t) - \frac{\hat{v}(t)}{R} + I\hat{d}(t) \tag{7.39}$$

This is the desired small-signal linearized equation that describes variations in the capacitor voltage.

Finally, the equation of the average input current is also linearized. Insertion of Eqs. (7.30) and (7.31) into the input current equation of Eq. (7.28) yields

$$I_g + \hat{i}_g(t) = \left(D+\hat{d}(t)\right)\left(I+\hat{i}(t)\right) \tag{7.40}$$

By collecting terms, we obtain

$$\underbrace{I_g}_{\text{Dc term}} + \underbrace{\hat{i}_g(t)}_{1^{st}\text{ order ac term}} = \underbrace{\left(DI\right)}_{\text{Dc term}} + \underbrace{\left(D\hat{i}(t)+I\hat{d}(t)\right)}_{1^{st}\text{ order ac terms (linear)}} + \underbrace{\hat{d}(t)\hat{i}(t)}_{2^{nd}\text{ order ac term (nonlinear)}} \tag{7.41}$$

We again neglect the second-order nonlinear terms. The dc terms on both sides of the equation are equal. The remaining first-order linear ac terms are

$$\hat{i}_g(t) = D\hat{i}(t) + I\hat{d}(t) \tag{7.42}$$

This is the linearized small-signal equation that describes the low-frequency ac components of the converter input current.

In summary, the nonlinear averaged equations of a switching converter can be linearized about a quiescent operating point. The converter independent inputs are expressed as constant (dc) values, plus small ac variations. In response, the converter averaged waveforms assume similar forms. Insertion of Eqs. (7.30) and (7.31) into the converter averaged nonlinear equations yields dc terms, linear ac terms, and nonlinear terms. If the ac variations are sufficiently small in magnitude, then the nonlinear terms are

much smaller than the linear ac terms, and so can be neglected. The remaining linear ac terms comprise the small-signal ac model of the converter.

7.2.6 Construction of the Small-Signal Equivalent Circuit Model

Equations (7.36), (7.39), and (7.42) are the small-signal ac description of the ideal buck-boost converter, and are collected below:

$$\begin{aligned} L\frac{d\hat{i}(t)}{dt} &= D\hat{v}_g(t) + D'\hat{v}(t) + \left(V_g - V\right)\hat{d}(t) \\ C\frac{d\hat{v}(t)}{dt} &= -D'\hat{i}(t) - \frac{\hat{v}(t)}{R} + I\hat{d}(t) \\ \hat{i}_g(t) &= D\hat{i}(t) + I\hat{d}(t) \end{aligned} \tag{7.43}$$

In Chapter 3, we collected the averaged dc equations of a converter, and reconstructed an equivalent circuit that modeled the dc properties of the converter. We can use the same procedure here, to construct averaged small-signal ac models of converters.

The inductor equation of (7.43), or Eq. (7.36), describes the voltages around a loop containing the inductor. Indeed, this equation was derived by finding the inductor voltage via loop analysis, then averaging, perturbing, and linearizing. So the equation represents the voltages around a loop of the small-signal model, which contains the inductor. The loop current is the small-signal ac inductor current $\hat{i}(t)$. As illustrated in Fig. 7.13, the term $L\,d\hat{i}(t)/dt$ represents the voltage across the inductor L in the small-signal model. This voltage is equal to three other voltage terms. $D\hat{v}_g(t)$ and $D'\hat{v}(t)$ represent dependent sources as shown. These terms will be combined into ideal transformers. The term $(V_g - V)\hat{d}(t)$ is driven by the control input $\hat{d}(t)$, and is represented by an independent source as shown.

The capacitor equation of (7.43), or Eq. (7.39), describes the currents flowing into a node attached to the capacitor. This equation was derived by finding the capacitor current via node analysis, then averaging, perturbing, and linearizing. Hence, this equation describes the currents flowing into a node of the small-signal model, attached to the capacitor. As illustrated in Fig. 7.14, the term $C\,d\hat{v}(t)/dt$ represents the current flowing through capacitor C in the small-signal model. The capacitor voltage is $\hat{v}(t)$. According to the equation, this current is equal to three other terms. The term $-D'\hat{i}(t)$ represents a dependent source, which will eventually be combined into an ideal transformer. The term $-\hat{v}(t)/R$ is rec-

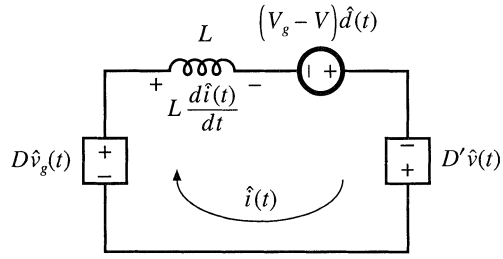

Fig. 7.13 Circuit equivalent to the small-signal ac inductor loop equation of Eq. (7.43) or (7.36).

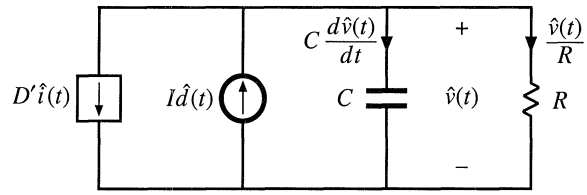

Fig. 7.14 Circuit equivalent to the small-signal ac capacitor node equation of Eq. (7.43) or (7.39).

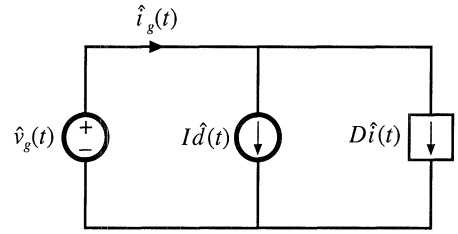

Fig. 7.15 Circuit equivalent to the small-signal ac input source current equation of Eq. (7.43) or (7.42).

ognized as the current flowing through the load resistor in the small-signal model. The resistor is connected in parallel with the capacitor, such that the ac voltage across the resistor R is $\hat{v}(t)$ as expected. The term $I\hat{d}(t)$ is driven by the control input $\hat{d}(t)$, and is represented by an independent source as shown.

Finally, the input current equation of (7.43), or Eq. (7.42), describes the small-signal ac current $\hat{i}_g(t)$ drawn by the converter out of the input voltage source $\hat{v}_g(t)$. This is a node equation which states that $\hat{i}_g(t)$ is equal to the currents in two branches, as illustrated in Fig. 7.15. The first branch, corresponding to the $D\hat{i}(t)$ term, is dependent on the ac inductor current $\hat{i}(t)$. Hence, we represent this term using a dependent current source; this source will eventually be incorporated into an ideal transformer. The second branch, corresponding to the $I\hat{d}(t)$ term, is driven by the control input $\hat{d}(t)$, and is represented by an independent source as shown.

The circuits of Figs. 7.13, 7.14, and 7.15 are collected in Fig. 7.16(a). As discussed in Chapter 3, the dependent sources can be combined into effective ideal transformers, as illustrated in Fig. 7.16(b). The sinusoid superimposed on the transformer symbol indicates that the transformer is ideal, and is part of the averaged small-signal ac model. So the effective dc transformer property of CCM dc-dc converters also influences small-signal ac variations in the converter signals.

The equivalent circuit of Fig. 7.16(b) can now be solved using techniques of conventional linear circuit analysis, to find the converter transfer functions, input and output impedances, etc. This is done in detail in the next chapter. Also, the model can be refined by inclusion of losses and other nonidealities—an example is given in Section 7.2.9.

7.2.7 Discussion of the Perturbation and Linearization Step

In the perturbation and linearization step, it is assumed that an averaged voltage or current consists of a constant (dc) component and a small-signal ac variation around the dc component. In Section 7.2.5, the

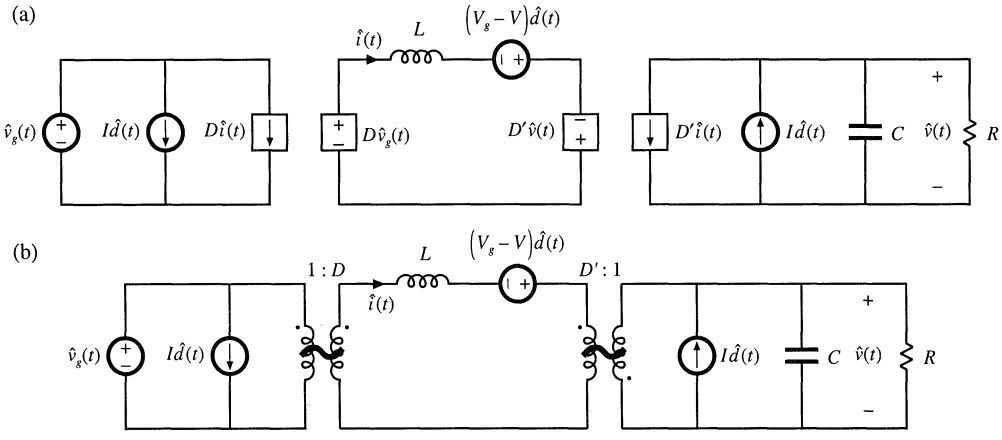

Fig. 7.16 Buck-boost converter small-signal ac equivalent circuit: (a) the circuits of Figs. 7.13 to 7.15, collected together; (b) combination of dependent sources into effective ideal transformer, leading to the final model.

linearization step was completed by neglecting nonlinear terms that correspond to products of the small-signal ac variations. In general, the linearization step amounts to taking the Taylor expansion of a nonlinear relation and retaining only the constant and linear terms. For example, the large-signal averaged equation for the inductor current in Eq. (7.28) can be written as:

$$L\frac{d\langle i(t)\rangle_{T_s}}{dt} = d(t)\langle v_g(t)\rangle_{T_s} + d'(t)\langle v(t)\rangle_{T_s} = f_1\left(\langle v_g(t)\rangle_{T_s}, \langle v(t)\rangle_{T_s}, d(t)\right) \tag{7.44}$$

Let us expand this expression in a three-dimensional Taylor series, about the quiescent operating point (V_g, V, D):

$$\begin{aligned} L\left(\frac{dI}{dt} + \frac{d\hat{i}(t)}{dt}\right) = {} & f_1\left(V_g, V, D\right) + \hat{v}_g(t)\left.\frac{\partial f_1\left(v_g, V, D\right)}{\partial v_g}\right|_{v_g = V_g} \\ & + \hat{v}(t)\left.\frac{\partial f_1\left(V_g, v, D\right)}{\partial v}\right|_{v = V} + \hat{d}(t)\left.\frac{\partial f_1\left(V_g, V, d\right)}{\partial d}\right|_{d = D} \\ & + \text{higher-order nonlinear terms} \end{aligned} \tag{7.45}$$

For simplicity of notation, the angle brackets denoting average values are dropped in the above equation. The derivative of I is zero, since I is by definition a dc (constant) term. Equating the dc terms on both sides of Eq. (7.45) gives:

$$0 = f_1\left(V_g, V, D\right) \tag{7.46}$$

which is the volt-second balance relationship for the inductor. The coefficients with the linear terms on the right-hand side of Eq. (7.45) are found as follows:

$$\left.\frac{\partial f_1\left(v_g, V, D\right)}{\partial v_g}\right|_{v_g = V_g} = D \tag{7.47}$$

$$\left.\frac{\partial f_1\left(V_g, v, D\right)}{\partial v}\right|_{v = V} = D' \tag{7.48}$$

$$\left.\frac{\partial f_1\left(V_g, V, d\right)}{\partial d}\right|_{d = D} = V_g - V \tag{7.49}$$

Using (7.47), (7.48) and (7.49), neglecting higher-order nonlinear terms, and equating the linear ac terms on both sides of Eq. (7.45) gives:

$$L\frac{d\hat{i}(t)}{dt} = D\hat{v}_g(t) + D'\hat{v}(t) + \left(V_g - V\right)\hat{d}(t) \tag{7.50}$$

which is identical to Eq. (7.36) derived in Section 7.2.5. In conclusion, the linearization step can always be accomplished using the Taylor expansion.

7.2.8 Results for Several Basic Converters

The equivalent circuit models for the buck, boost, and buck-boost converters operating in the continuous conduction mode are summarized in Fig. 7.17. The buck and boost converter models contain ideal transformers having turns ratios equal to the converter conversion ratio. The buck-boost converter contains ideal transformers having buck and boost conversion ratios; this is consistent with the derivation of Section 6.1.2 of the buck-boost converter as a cascade connection of buck and boost converters. These models can be solved to find the converter transfer functions, input and output impedances, inductor current variations, etc. By insertion of appropriate turns ratios, the equivalent circuits of Fig. 7.17 can be adapted to model the transformer-isolated versions of the buck, boost, and buck-boost converters, including the forward, flyback, and other converters.

7.2.9 Example: A Nonideal Flyback Converter

To illustrate that the techniques of the previous section are useful for modeling a variety of converter phenomena, let us next derive a small-signal ac equivalent circuit of a converter containing transformer isolation and resistive losses. An isolated flyback converter is illustrated in Fig. 7.18. The flyback transformer has magnetizing inductance L, referred to the primary winding, and turns ratio $1{:}n$. MOSFET Q_1 has on-resistance R_{on}. Other loss elements, as well as the transformer leakage inductances and the switching losses, are negligible. The ac modeling of this converter begins in a manner similar to the dc converter analysis of Section 6.3.4. The flyback transformer is replaced by an equivalent circuit consisting of the magnetizing inductance L in parallel with an ideal transformer, as illustrated in Fig. 7.19(a).

During the first subinterval, when MOSFET Q_1 conducts, diode D_1 is off. The circuit then

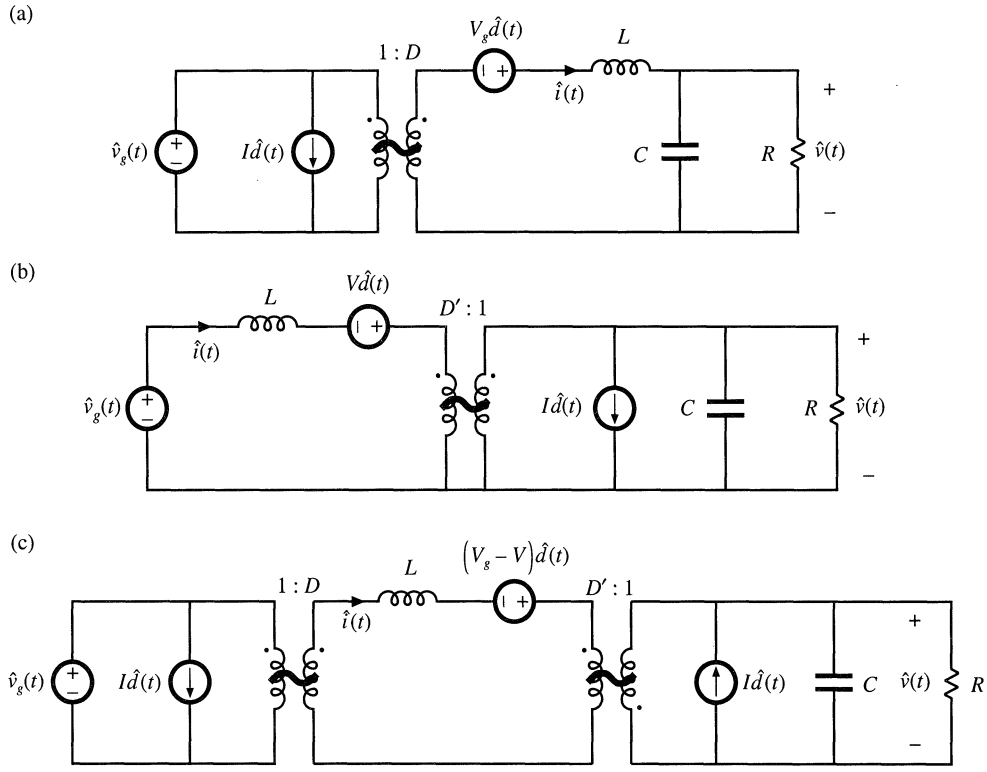

Fig. 7.17 Averaged small-signal ac models for several basic converters operating in continuous conduction mode: (a) buck, (b) boost, (c) buck-boost.

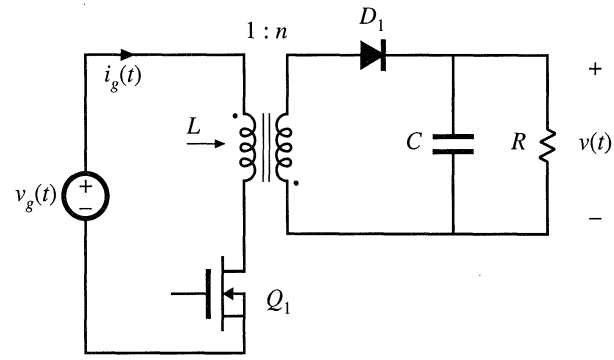

Fig. 7.18 Flyback converter example.

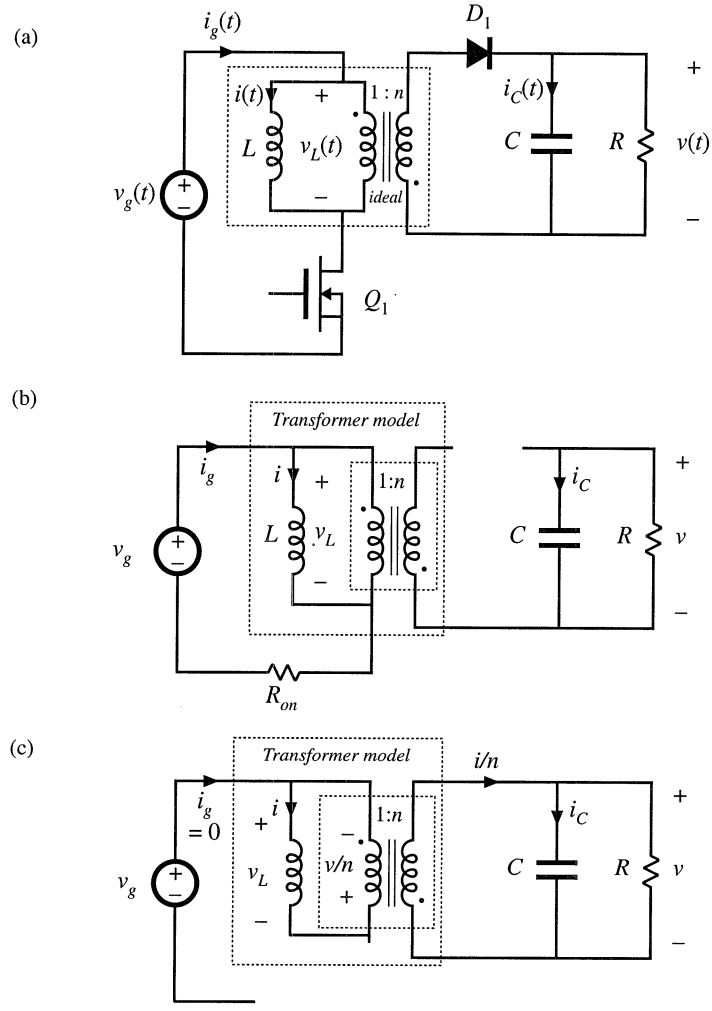

Fig. 7.19 Flyback converter example: (a) incorporation of transformer equivalent circuit, (b) circuit during subinterval 1, (c) circuit during subinterval 2.

reduces to Fig. 7.19(b). The inductor voltage $v_L(t)$, capacitor current $i_C(t)$, and converter input current $i_g(t)$ are:

$$\begin{aligned} v_L(t) &= v_g(t) - i(t)R_{on} \\ i_C(t) &= -\frac{v(t)}{R} \\ i_g(t) &= i(t) \end{aligned} \tag{7.51}$$

We next make the small ripple approximation, replacing the voltages and currents with their average val-

ues as defined by Eq. (7.3), to obtain

$$\begin{aligned} v_L(t) &= \langle v_g(t) \rangle_{T_s} - \langle i(t) \rangle_{T_s} R_{on} \\ i_C(t) &= -\frac{\langle v(t) \rangle_{T_s}}{R} \\ i_g(t) &= \langle i(t) \rangle_{T_s} \end{aligned} \tag{7.52}$$

During the second subinterval, MOSFET Q_1 is off, diode D_1 conducts, and the circuit of Fig. 7.19(c) is obtained. Analysis of this circuit shows that the inductor voltage, capacitor current, and input current are given by

$$\begin{aligned} v_L(t) &= -\frac{v(t)}{n} \\ i_C(t) &= \frac{i(t)}{n} - \frac{v(t)}{R} \\ i_g(t) &= 0 \end{aligned} \tag{7.53}$$

The small-ripple approximation leads to

$$\begin{aligned} v_L(t) &= -\frac{\langle v(t) \rangle_{T_s}}{n} \\ i_C(t) &= \frac{\langle i(t) \rangle_{T_s}}{n} - \frac{\langle v(t) \rangle_{T_s}}{R} \\ i_g(t) &= 0 \end{aligned} \tag{7.54}$$

The inductor voltage and current waveforms are sketched in Fig. 7.20. The average inductor voltage can now be found by averaging the waveform of Fig. 7.20(a) over one switching period. The result is

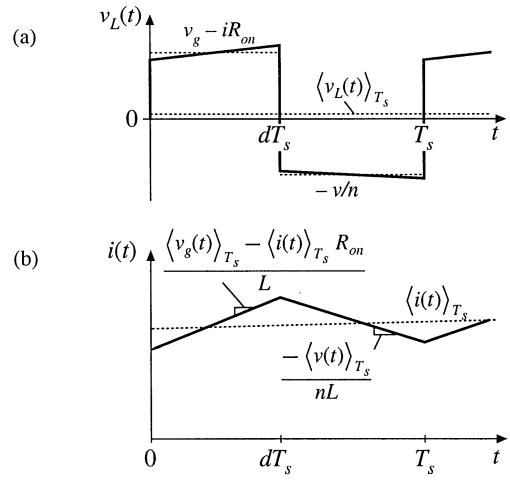

Fig. 7.20 Inductor waveforms for the flyback example: (a) inductor voltage, (b) inductor current.

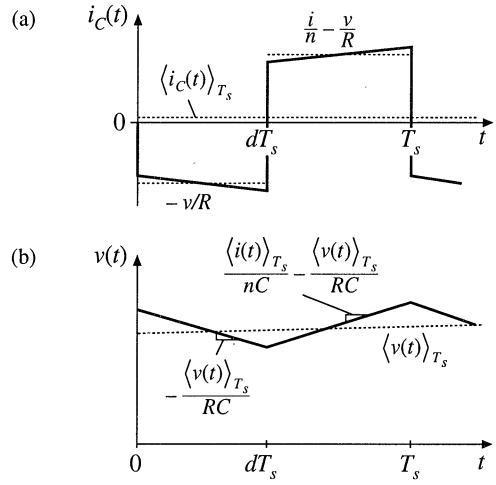

Fig. 7.21 Capacitor waveforms for the flyback example: (a) capacitor current, (b) capacitor voltage.

$$\langle v_L(t)\rangle_{T_s} = d(t)\left(\langle v_g(t)\rangle_{T_s} - \langle i(t)\rangle_{T_s} R_{on}\right) + d'(t)\left(\frac{-\langle v(t)\rangle_{T_s}}{n}\right) \tag{7.55}$$

By inserting this result into Eq. (7.20), we obtain the averaged inductor equation,

$$L\frac{d\langle i(t)\rangle_{T_s}}{dt} = d(t)\langle v_g(t)\rangle_{T_s} - d(t)\langle i(t)\rangle_{T_s} R_{on} - d'(t)\frac{\langle v(t)\rangle_{T_s}}{n} \tag{7.56}$$

The capacitor waveforms are constructed in Fig. 7.21. The average capacitor current is

$$\langle i_C(t)\rangle_{T_s} = d(t)\left(\frac{-\langle v(t)\rangle_{T_s}}{R}\right) + d'(t)\left(\frac{\langle i(t)\rangle_{T_s}}{n} - \frac{\langle v(t)\rangle_{T_s}}{R}\right) \tag{7.57}$$

This leads to the averaged capacitor equation

$$C\frac{d\langle v(t)\rangle_{T_s}}{dt} = d'(t)\frac{\langle i(t)\rangle_{T_s}}{n} - \frac{\langle v(t)\rangle_{T_s}}{R} \tag{7.58}$$

The converter input current $i_g(t)$ is sketched in Fig. 7.22. Its average is

$$\langle i_g(t)\rangle_{T_s} = d(t)\langle i(t)\rangle_{T_s} \tag{7.59}$$

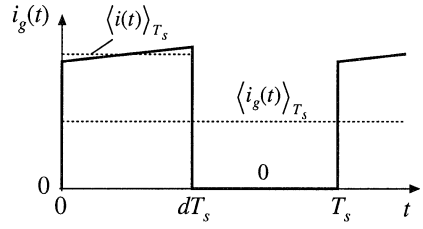

Fig. 7.22 Input source current waveform, flyback example.

The averaged converter equations (7.56), (7.58) and (7.59) are collected below:

$$
\begin{aligned}
L\frac{d\langle i(t)\rangle_{T_s}}{dt} &= d(t)\langle v_g(t)\rangle_{T_s} - d(t)\langle i(t)\rangle_{T_s} R_{on} - d'(t)\frac{\langle v(t)\rangle_{T_s}}{n} \\
C\frac{d\langle v(t)\rangle_{T_s}}{dt} &= d'(t)\frac{\langle i(t)\rangle_{T_s}}{n} - \frac{\langle v(t)\rangle_{T_s}}{R} \\
\langle i_g(t)\rangle_{T_s} &= d(t)\langle i(t)\rangle_{T_s}
\end{aligned}
\tag{7.60}
$$

This is a nonlinear set of differential equations, and hence the next step is to perturb and linearize, to construct the converter small-signal ac equations. We assume that the converter input voltage $v_g(t)$ and duty cycle $d(t)$ can be expressed as quiescent values plus small ac variations, as follows:

$$
\begin{aligned}
\langle v_g(t)\rangle_{T_s} &= V_g + \hat{v}_g(t) \\
d(t) &= D + \hat{d}(t)
\end{aligned}
\tag{7.61}
$$

In response to these inputs, and after all transients have decayed, the average converter waveforms can also be expressed as quiescent values plus small ac variations:

$$
\begin{aligned}
\langle i(t)\rangle_{T_s} &= I + \hat{i}(t) \\
\langle v(t)\rangle_{T_s} &= V + \hat{v}(t) \\
\langle i_g(t)\rangle_{T_s} &= I_g + \hat{i}_g(t)
\end{aligned}
\tag{7.62}
$$

With these substitutions, the large-signal averaged inductor equation becomes

$$
L\frac{d\left(I + \hat{i}(t)\right)}{dt} = \left(D + \hat{d}(t)\right)\left(V_g + \hat{v}_g(t)\right) - \left(D' - \hat{d}(t)\right)\frac{\left(V + \hat{v}(t)\right)}{n} - \left(D + \hat{d}(t)\right)\left(I + \hat{i}(t)\right)R_{on}
\tag{7.63}
$$

Upon multiplying this expression out and collecting terms, we obtain

$$
\begin{aligned}
L\left(\frac{dI}{dt} + \frac{d\hat{i}(t)}{dt}\right) = &\underbrace{\left(DV_g - D'\frac{V}{n} - DR_{on}I\right)}_{\text{Dc terms}} + \underbrace{\left(D\hat{v}_g(t) - D'\frac{\hat{v}(t)}{n} + \left(V_g + \frac{V}{n} - IR_{on}\right)\hat{d}(t) - DR_{on}\hat{i}(t)\right)}_{1^{st}\text{ order ac terms (linear)}} \\
&+ \underbrace{\left(\hat{d}(t)\hat{v}_g(t) + \hat{d}(t)\frac{\hat{v}(t)}{n} - \hat{d}(t)\hat{i}(t)R_{on}\right)}_{2^{nd}\text{ order ac terms (nonlinear)}}
\end{aligned}
\tag{7.64}
$$

As usual, this equation contains three types of terms. The dc terms contain no time-varying quantities. The first-order ac terms are linear functions of the ac variations in the circuit, while the second-order ac terms are functions of the products of the ac variations. If the small-signal assumptions of Eq. (7.32) are satisfied, then the second-order terms are much smaller in magnitude that the first-order terms, and hence can be neglected. The dc terms must satisfy

$$0 = DV_g - D'\frac{V}{n} - DR_{on}I \tag{7.65}$$

This result could also be derived by applying the principle of inductor volt-second balance to the steady-state inductor voltage waveform. The first-order ac terms must satisfy

$$L\frac{d\hat{i}(t)}{dt} = D\hat{v}_g(t) - D'\frac{\hat{v}(t)}{n} + \left(V_g + \frac{V}{n} - IR_{on}\right)\hat{d}(t) - DR_{on}\hat{i}(t) \tag{7.66}$$

This is the linearized equation that describes ac variations in the inductor current.

Upon substitution of Eqs. (7.61) and (7.62) into the averaged capacitor equation (7.60), one obtains

$$C\frac{d\left(V + \hat{v}(t)\right)}{dt} = \left(D' - \hat{d}(t)\right)\frac{\left(I + \hat{i}(t)\right)}{n} - \frac{\left(V + \hat{v}(t)\right)}{R} \tag{7.67}$$

By collecting terms, we obtain

$$C\left(\frac{dV}{dt} + \frac{d\hat{v}(t)}{dt}\right) = \underbrace{\left(\frac{D'I}{n} - \frac{V}{R}\right)}_{\text{Dc terms}} + \underbrace{\left(\frac{D'\hat{i}(t)}{n} - \frac{\hat{v}(t)}{R} - \frac{I\hat{d}(t)}{n}\right)}_{\substack{1^{st}\text{ order ac terms} \\ \text{(linear)}}} - \underbrace{\frac{\hat{d}(t)\hat{i}(t)}{n}}_{\substack{2^{nd}\text{ order ac term} \\ \text{(nonlinear)}}} \tag{7.68}$$

We neglect the second-order terms. The dc terms of Eq. (7.68) must satisfy

$$0 = \left(\frac{D'I}{n} - \frac{V}{R}\right) \tag{7.69}$$

This result could also be obtained by use of the principle of capacitor charge balance on the steady-state capacitor current waveform. The first-order ac terms of Eq. (7.68) lead to the small-signal ac capacitor equation

$$C\frac{d\hat{v}(t)}{dt} = \frac{D'\hat{i}(t)}{n} - \frac{\hat{v}(t)}{R} - \frac{I\hat{d}(t)}{n} \tag{7.70}$$

Substitution of Eqs. (7.61) and (7.62) into the averaged input current equation (7.60) leads to

$$I_g + \hat{i}_g(t) = \left(D + \hat{d}(t)\right)\left(I + \hat{i}(t)\right) \tag{7.71}$$

Upon collecting terms, we obtain

$$\underbrace{I_g}_{\text{Dc term}} + \underbrace{\hat{i}_g(t)}_{1^{st}\text{ order ac term}} = \underbrace{\left(DI\right)}_{\text{Dc term}} + \underbrace{\left(D\hat{i}(t) + I\hat{d}(t)\right)}_{\substack{1^{st}\text{ order ac terms} \\ \text{(linear)}}} + \underbrace{\hat{d}(t)\hat{i}(t)}_{\substack{2^{nd}\text{ order ac term} \\ \text{(nonlinear)}}} \tag{7.72}$$

The dc terms must satisfy

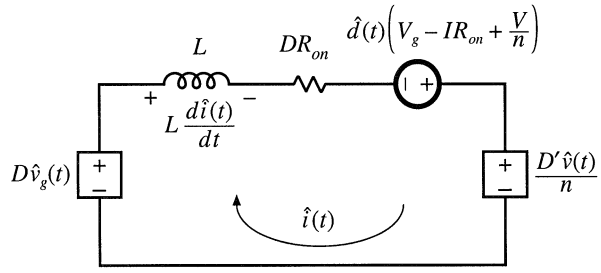

Fig. 7.23 Circuit equivalent to the small-signal ac inductor loop equation, Eq. (7.76) or (7.66).

$$I_g = DI \tag{7.73}$$

We neglect the second-order nonlinear terms of Eq. (7.72), leaving the following linearized ac equation:

$$\hat{i}_g(t) = D\hat{i}(t) + I\hat{d}(t) \tag{7.74}$$

This result models the low-frequency ac variations in the converter input current.

The equations of the quiescent values, Eqs. (7.65), (7.69), and (7.73) are collected below:

$$\begin{aligned} 0 &= DV_g - D'\frac{V}{n} - DR_{on}I \\ 0 &= \left(\frac{D'I}{n} - \frac{V}{R}\right) \\ I_g &= DI \end{aligned} \tag{7.75}$$

For given quiescent values of the input voltage V_g and duty cycle D, this system of equations can be evaluated to find the quiescent output voltage V, inductor current I, and input current dc component I_g. The results are then inserted into the small-signal ac equations.

The small-signal ac equations, Eqs. (7.66), (7.70), and (7.74), are summarized below:

$$\begin{aligned} L\frac{d\hat{i}(t)}{dt} &= D\hat{v}_g(t) - D'\frac{\hat{v}(t)}{n} + \left(V_g + \frac{V}{n} - IR_{on}\right)\hat{d}(t) - DR_{on}\hat{i}(t) \\ C\frac{d\hat{v}(t)}{dt} &= \frac{D'\hat{i}(t)}{n} - \frac{\hat{v}(t)}{R} - \frac{I\hat{d}(t)}{n} \\ \hat{i}_g(t) &= D\hat{i}(t) + I\hat{d}(t) \end{aligned} \tag{7.76}$$

The final step is to construct an equivalent circuit that corresponds to these equations.

The inductor equation was derived by first writing loop equations, to find the applied inductor voltage during each subinterval. These equations were then averaged, perturbed, and linearized, to obtain Eq. (7.66). So this equation describes the small-signal ac voltages around a loop containing the inductor. The loop current is the ac inductor current $\hat{i}(t)$. The quantity $Ld\hat{i}(t)/dt$ is the low-frequency ac voltage across the inductor. The four terms on the right-hand side of the equation are the voltages across the four other elements in the loop. The terms $D\hat{v}_g(t)$ and $-D'\hat{v}(t)/n$ are dependent on voltages elsewhere in the converter, and hence are represented as dependent sources in Fig. 7.23. The third term is driven by the duty cycle variations $\hat{d}(t)$ and hence is represented as an independent source. The fourth term, $-DR_{on}\hat{i}(t)$, is a voltage that is proportional to the loop current $\hat{i}(t)$. Hence this term obeys Ohm's law, with effective resistance DR_{on} as shown in the figure. So the influence of the MOSFET on-resistance on the converter

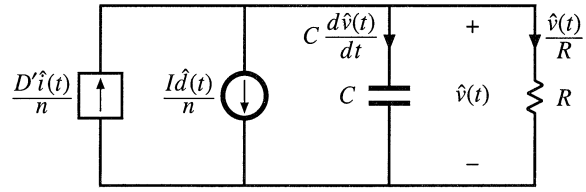

Fig. 7.24 Circuit equivalent to the small-signal ac capacitor node equation, Eq. (7.76) or (7.70).

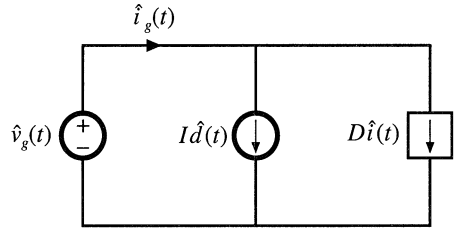

Fig. 7.25 Circuit equivalent to the small-signal ac input source current equation, Eq. (7.76) or (7.74).

small-signal transfer functions is modeled by an effective resistance of value DR_{on}.

Small-signal capacitor equation (7.70) leads to the equivalent circuit of Fig. 7.24. The equation constitutes a node equation of the equivalent circuit model. It states that the capacitor current $Cd\hat{v}(t)/dt$ is equal to three other currents. The current $D'\hat{i}(t)/n$ depends on a current elsewhere in the model, and hence is represented by a dependent current source. The term $-\hat{v}(t)/R$ is the ac component of the load current, which we model with a load resistance R connected in parallel with the capacitor. The last term is driven by the duty cycle variations $\hat{d}(t)$, and is modeled by an independent source.

The input port equation, Eq. (7.74), also constitutes a node equation. It describes the small-signal ac current $\hat{i}_g(t)$, drawn by the converter out of the input voltage source $\hat{v}_g(t)$. There are two other terms in the equation. The term $D\hat{i}(t)$ is dependent on the inductor current ac variation $\hat{i}(t)$, and is represented with a dependent source. The term $I\hat{d}(t)$ is driven by the control variations, and is modeled by an independent source. The equivalent circuit for the input port is illustrated in Fig. 7.25.

The circuits of Figs. 7.23, 7.24, and 7.25 are combined in Fig. 7.26. The dependent sources can be replaced by ideal transformers, leading to the equivalent circuit of Fig. 7.27. This is the desired result: an equivalent circuit that models the low-frequency small-signal variations in the converter waveforms. It can now be solved, using conventional linear circuit analysis techniques, to find the converter transfer functions, output impedance, and other ac quantities of interest.

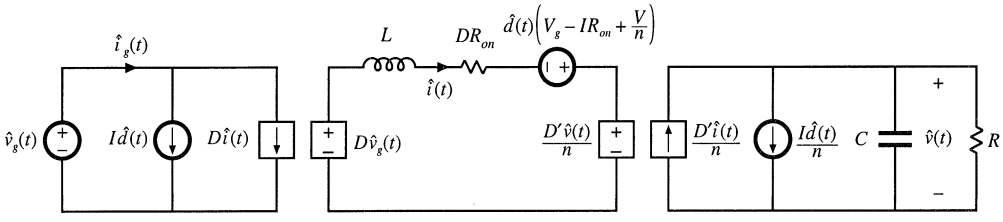

Fig. 7.26 The equivalent circuits of Figs. 7.23 to 7.25, collected together.

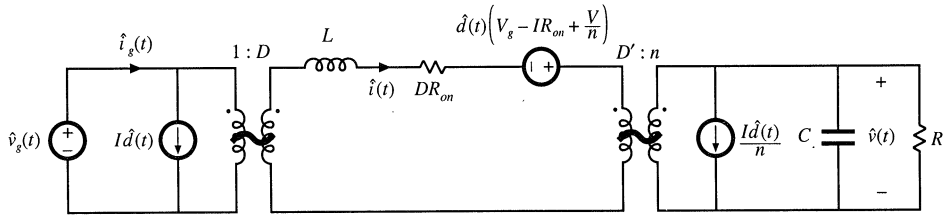

Fig. 7.27 Small-signal ac equivalent circuit model of the flyback converter.

7.3 STATE-SPACE AVERAGING

A number of ac converter modeling techniques have appeared in the literature, including the current-injected approach, circuit averaging, and the state-space averaging method. Although the proponents of a given method may prefer to express the end result in a specific form, the end results of nearly all methods are equivalent. And everybody will agree that averaging and small-signal linearization are the key steps in modeling PWM converters.

The state-space averaging approach [1, 2] is described in this section. The state-space description of dynamical systems is a mainstay of modern control theory; the state-space averaging method makes use of this description to derive the small-signal averaged equations of PWM switching converters. The state-space averaging method is otherwise identical to the procedure derived in Section 7.2. Indeed, the procedure of Section 7.2 amounts to state-space averaging, but without the formality of writing the equations in matrix form. A benefit of the state-space averaging procedure is the generality of its result: a small-signal averaged model can always be obtained, provided that the state equations of the original converter can be written.

Section 7.3.1 summarizes how to write the state equations of a network. The basic results of state-space averaging are described in Section 7.3.2, and a short derivation is given in Section 7.3.3. Section 7.3.4 contains an example, in which the state-space averaging method is used to derive the quiescent dc and small-signal ac equations of a buck-boost converter.

7.3.1 The State Equations of a Network

The state-space description is a canonical form for writing the differential equations that describe a system. For a linear network, the derivatives of the *state variables* are expressed as linear combinations of the system independent inputs and the state variables themselves. The physical state variables of a system are usually associated with the storage of energy, and for a typical converter circuit, the physical state variables are the independent inductor currents and capacitor voltages. Other typical state variables include the position and velocity of a motor shaft. At a given point in time, the values of the state variables depend on the previous history of the system, rather than on the present values of the system inputs. To solve the differential equations of the system, the initial values of the state variables must be specified. So if we know the *state* of a system, that is, the values of all of the state variables, at a given time t_0, and if we additionally know the system inputs, then we can in principle solve the system state equations to find the system waveforms at any future time.

The state equations of a system can be written in the compact matrix form of Eq. (7.77):

$$\mathbf{K}\frac{d\mathbf{x}(t)}{dt} = \mathbf{A}\mathbf{x}(t) + \mathbf{B}\mathbf{u}(t)$$
$$\mathbf{y}(t) = \mathbf{C}\mathbf{x}(t) + \mathbf{E}\mathbf{u}(t) \tag{7.77}$$

Here, the state vector $\mathbf{x}(t)$ is a vector containing all of the state variables, that is, the inductor currents, capacitor voltages, etc. The input vector $\mathbf{u}(t)$ contains the independent inputs to the system, such as the input voltage source $v_g(t)$. The derivative of the state vector is a vector whose elements are equal to the derivatives of the corresponding elements of the state vector:

$$\mathbf{x}(t) = \begin{bmatrix} x_1(t) \\ x_2(t) \\ \vdots \end{bmatrix}, \qquad \frac{d\mathbf{x}(t)}{dt} = \begin{bmatrix} \frac{dx_1(t)}{dt} \\ \frac{dx_2(t)}{dt} \\ \vdots \end{bmatrix} \tag{7.78}$$

In the standard form of Eq. (7.77), $\mathbf{K}$ is a matrix containing the values of capacitance, inductance, and mutual inductance (if any), such that $\mathbf{K}d\mathbf{x}(t)/dt$ is a vector containing the inductor winding voltages and capacitor currents. In other physical systems, $\mathbf{K}$ may contain other quantities such as moment of inertia or mass. Equation (7.77) states that the inductor voltages and capacitor currents of the system can be expressed as linear combinations of the state variables and the independent inputs. The matrices $\mathbf{A}$ and $\mathbf{B}$ contain constants of proportionality.

It may also be desired to compute other circuit waveforms that do not coincide with the elements of the state vector $\mathbf{x}(t)$ or the input vector $\mathbf{u}(t)$. These other signals are, in general, dependent waveforms that can be expressed as linear combinations of the elements of the state vector and input vector. The vector $\mathbf{y}(t)$ is usually called the *output vector*. We are free to place any dependent signal in this vector, regardless of whether the signal is actually a physical output. The converter input current $i_g(t)$ is often chosen to be an element of $\mathbf{y}(t)$. In the state equations (7.77), the elements of $\mathbf{y}(t)$ are expressed as a linear combination of the elements of the $\mathbf{x}(t)$ and $\mathbf{u}(t)$ vectors. The matrices $\mathbf{C}$ and $\mathbf{E}$ contain constants of proportionality.

As an example, let us write the state equations of the circuit of Fig. 7.28. This circuit contains two capacitors and an inductor, and hence the physical state variables are the independent capacitor voltages $v_1(t)$ and $v_2(t)$, as well as the inductor current $i(t)$. So we can define the state vector as

$$\mathbf{x}(t) = \begin{bmatrix} v_1(t) \\ v_2(t) \\ i(t) \end{bmatrix} \tag{7.79}$$

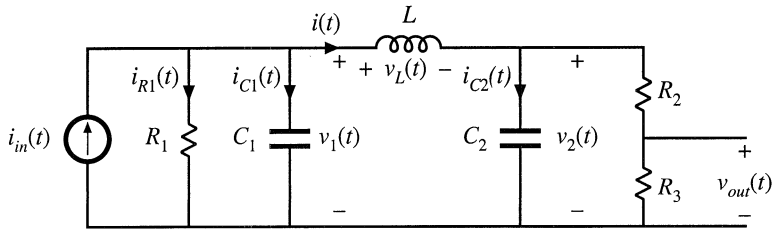

Fig. 7.28 Circuit example.

Since there are no coupled inductors, the matrix **K** is diagonal, and simply contains the values of capacitance and inductance:

$$\mathbf{K} = \begin{bmatrix} C_1 & 0 & 0 \\ 0 & C_2 & 0 \\ 0 & 0 & L \end{bmatrix} \tag{7.80}$$

The circuit has one independent input, the current source $i_{in}(t)$. Hence we should define the input vector as

$$\mathbf{u}(t) = \begin{bmatrix} i_{in}(t) \end{bmatrix} \tag{7.81}$$

We are free to place any dependent signal in vector $\mathbf{y}(t)$. Suppose that we are interested in also computing the voltage $v_{out}(t)$ and the current $i_{R1}(t)$. We can therefore define $\mathbf{y}(t)$ as

$$\mathbf{y}(t) = \begin{bmatrix} v_{out}(t) \\ i_{R1}(t) \end{bmatrix} \tag{7.82}$$

To write the state equations in the canonical form of Eq. (7.77), we need to express the inductor voltages and capacitor currents as linear combinations of the elements of $\mathbf{x}(t)$ and $\mathbf{u}(t)$, that is, as linear combinations of $v_1(t)$, $v_2(t)$, $i(t)$, and $i_{in}(t)$.

The capacitor current $i_{C1}(t)$ is given by the node equation

$$i_{C1}(t) = C_1 \frac{dv_1(t)}{dt} = i_{in}(t) - \frac{v_1(t)}{R_1} - i(t) \tag{7.83}$$

This equation will become the top row of the matrix equation (7.77). The capacitor current $i_{C2}(t)$ is given by the node equation,

$$i_{C2}(t) = C_2 \frac{dv_2(t)}{dt} = i(t) - \frac{v_2(t)}{R_2 + R_3} \tag{7.84}$$

Note that we have been careful to express this current as a linear combination of the elements of $\mathbf{x}(t)$ and $\mathbf{u}(t)$ alone. The inductor voltage is given by the loop equation,

$$v_L(t) = L \frac{di(t)}{dt} = v_1(t) - v_2(t) \tag{7.85}$$

Equations (7.83) to (7.85) can be written in the following matrix form:

$$\underbrace{\begin{bmatrix} C_1 & 0 & 0 \\ 0 & C_2 & 0 \\ 0 & 0 & L \end{bmatrix}}_{\mathbf{K}} \underbrace{\begin{bmatrix} \frac{dv_1(t)}{dt} \\ \frac{dv_2(t)}{dt} \\ \frac{di(t)}{dt} \end{bmatrix}}_{\frac{d\mathbf{x}(t)}{dt}} = \underbrace{\begin{bmatrix} -\frac{1}{R_1} & 0 & -1 \\ 0 & -\frac{1}{R_2 + R_3} & 1 \\ 1 & -1 & 0 \end{bmatrix}}_{\mathbf{A}} \underbrace{\begin{bmatrix} v_1(t) \\ v_2(t) \\ i(t) \end{bmatrix}}_{\mathbf{x}(t)} + \underbrace{\begin{bmatrix} 1 \\ 0 \\ 0 \end{bmatrix}}_{\mathbf{B}} \underbrace{\begin{bmatrix} i_{in}(t) \end{bmatrix}}_{\mathbf{u}(t)} \tag{7.86}$$

Matrices **A** and **B** are now known.

It is also necessary to express the elements of $\mathbf{y}(t)$ as linear combinations of the elements of $\mathbf{x}(t)$ and $\mathbf{u}(t)$. By solution of the circuit of Fig. 7.28, $v_{out}(t)$ can be written in terms of $v_2(t)$ as

$$v_{out}(t) = v_2(t) \frac{R_3}{R_2 + R_3} \tag{7.87}$$

Also, $i_{R1}(t)$ can be expressed in terms of $v_1(t)$ as

$$i_{R1}(t) = \frac{v_1(t)}{R_1} \tag{7.88}$$

By collecting Eqs. (7.87) and (7.88) into the standard matrix form of Eq. (7.77), we obtain

$$\underbrace{\begin{bmatrix} v_{out}(t) \\ i_{R1}(t) \end{bmatrix}}_{\mathbf{y}(t)} = \underbrace{\begin{bmatrix} 0 & \frac{R_3}{R_2 + R_3} & 0 \\ \frac{1}{R_1} & 0 & 0 \end{bmatrix}}_{\mathbf{C}} \underbrace{\begin{bmatrix} v_1(t) \\ v_2(t) \\ i(t) \end{bmatrix}}_{\mathbf{x}(t)} + \underbrace{\begin{bmatrix} 0 \\ 0 \end{bmatrix}}_{\mathbf{E}} \underbrace{\left[i_{in}(t) \right]}_{\mathbf{u}(t)} \tag{7.89}$$

We can now identify the matrices **C** and **E** as shown above.

It should be recognized that, starting in Chapter 2, we have always begun the analysis of converters by writing their state equations. We are now simply writing these equations in matrix form.

7.3.2 The Basic State-Space Averaged Model

Consider now that we are given a PWM converter, operating in the continuous conduction mode. The converter circuit contains independent states that form the state vector $\mathbf{x}(t)$, and the converter is driven by independent sources that form the input vector $\mathbf{u}(t)$. During the first subinterval, when the switches are in position 1, the converter reduces to a linear circuit that can be described by the following state equations:

$$\begin{aligned} \mathbf{K} \frac{d\mathbf{x}(t)}{dt} &= \mathbf{A}_1 \mathbf{x}(t) + \mathbf{B}_1 \mathbf{u}(t) \\ \mathbf{y}(t) &= \mathbf{C}_1 \mathbf{x}(t) + \mathbf{E}_1 \mathbf{u}(t) \end{aligned} \tag{7.90}$$

During the second subinterval, with the switches in position 2, the converter reduces to another linear circuit whose state equations are

$$\begin{aligned} \mathbf{K} \frac{d\mathbf{x}(t)}{dt} &= \mathbf{A}_2 \mathbf{x}(t) + \mathbf{B}_2 \mathbf{u}(t) \\ \mathbf{y}(t) &= \mathbf{C}_2 \mathbf{x}(t) + \mathbf{E}_2 \mathbf{u}(t) \end{aligned} \tag{7.91}$$

During the two subintervals, the circuit elements are connected differently; therefore, the respective state equation matrices $\mathbf{A}_1$, $\mathbf{B}_1$, $\mathbf{C}_1$, $\mathbf{E}_1$ and $\mathbf{A}_2$, $\mathbf{B}_2$, $\mathbf{C}_2$, $\mathbf{E}_2$ may also differ. Given these state equations, the result of state-space averaging is the state equations of the equilibrium and small-signal ac models.

Provided that the natural frequencies of the converter, as well as the frequencies of variations of the converter inputs, are much slower than the switching frequency, then the state-space averaged model

that describes the converter in equilibrium is

$$\begin{aligned} \mathbf{0} &= \mathbf{AX} + \mathbf{BU} \\ \mathbf{Y} &= \mathbf{CX} + \mathbf{EU} \end{aligned} \tag{7.92}$$

where the averaged matrices are

$$\begin{aligned} \mathbf{A} &= D\mathbf{A}_1 + D'\mathbf{A}_2 \\ \mathbf{B} &= D\mathbf{B}_1 + D'\mathbf{B}_2 \\ \mathbf{C} &= D\mathbf{C}_1 + D'\mathbf{C}_2 \\ \mathbf{E} &= D\mathbf{E}_1 + D'\mathbf{E}_2 \end{aligned} \tag{7.93}$$

The equilibrium dc components are

$$\begin{aligned} \mathbf{X} &= \text{equilibrium (dc) state vector} \\ \mathbf{U} &= \text{equilibrium (dc) input vector} \\ \mathbf{Y} &= \text{equilibrium (dc) output vector} \\ D &= \text{equilibrium (dc) duty cycle} \end{aligned} \tag{7.94}$$

Quantities defined in Eq. (7.94) represent the equilibrium values of the averaged vectors. Equation (7.92) can be solved to find the equilibrium state and output vectors:

$$\begin{aligned} \mathbf{X} &= -\mathbf{A}^{-1}\mathbf{BU} \\ \mathbf{Y} &= \left(-\mathbf{CA}^{-1}\mathbf{B} + \mathbf{E}\right)\mathbf{U} \end{aligned} \tag{7.95}$$

The state equations of the small-signal ac model are

$$\begin{aligned} \mathbf{K}\frac{d\hat{\mathbf{x}}(t)}{dt} &= \mathbf{A}\hat{\mathbf{x}}(t) + \mathbf{B}\hat{\mathbf{u}}(t) + \left\{\left(\mathbf{A}_1 - \mathbf{A}_2\right)\mathbf{X} + \left(\mathbf{B}_1 - \mathbf{B}_2\right)\mathbf{U}\right\}\hat{d}(t) \\ \hat{\mathbf{y}}(t) &= \mathbf{C}\hat{\mathbf{x}}(t) + \mathbf{E}\hat{\mathbf{u}}(t) + \left\{\left(\mathbf{C}_1 - \mathbf{C}_2\right)\mathbf{X} + \left(\mathbf{E}_1 - \mathbf{E}_2\right)\mathbf{U}\right\}\hat{d}(t) \end{aligned} \tag{7.96}$$

The quantities $\hat{\mathbf{x}}(t)$, $\hat{\mathbf{u}}(t)$, $\hat{\mathbf{y}}(t)$, and $\hat{d}(t)$ in Eq. (7.96) are small ac variations about the equilibrium solution, or quiescent operating point, defined by Eqs. (7.92) to (7.95).

So if we can write the converter state equations, Eqs. (7.90) and (7.91), then we can always find the averaged dc and small-signal ac models, by evaluation of Eqs. (7.92) to (7.96).

7.3.3 Discussion of the State-Space Averaging Result

As in Sections 7.1 and 7.2, the low-frequency components of the inductor currents and capacitor voltages are modeled by averaging over an interval of length T_s. Hence, we can define the average of the state vector $\mathbf{x}(t)$ as

$$\left\langle \mathbf{x}(t) \right\rangle_{T_s} = \frac{1}{T_s}\int_t^{t+T_s} \mathbf{x}(\tau)\,d\tau \tag{7.97}$$

The low-frequency components of the input and output vectors are modeled in a similar manner. By averaging the inductor voltages and capacitor currents, one then obtains the following low-frequency state equation:

$$\mathbf{K}\frac{d\langle \mathbf{x}(t)\rangle_{T_s}}{dt} = \left(d(t)\,\mathbf{A}_1 + d'(t)\,\mathbf{A}_2\right)\langle \mathbf{x}(t)\rangle_{T_s} + \left(d(t)\,\mathbf{B}_1 + d'(t)\,\mathbf{B}_2\right)\langle \mathbf{u}(t)\rangle_{T_s} \tag{7.98}$$

This result is equivalent to Eq. (7.2).

For example, let us consider how the elements of the state vector $\mathbf{x}(t)$ change over one switching period. During the first subinterval, with the switches in position 1, the converter state equations are given by Eq. (7.90). Therefore, the elements of $\mathbf{x}(t)$ change with the slopes $\mathbf{K}^{-1}(\mathbf{A}_1\mathbf{x}(t) + \mathbf{B}_1\mathbf{u}(t))$. If we make the small ripple approximation, that $\mathbf{x}(t)$ and $\mathbf{u}(t)$ do not change much over one switching period, then the slopes are essentially constant and are approximately equal to

$$\frac{d\mathbf{x}(t)}{dt} = \mathbf{K}^{-1}\left(\mathbf{A}_1\langle \mathbf{x}(t)\rangle_{T_s} + \mathbf{B}_1\langle \mathbf{u}(t)\rangle_{T_s}\right) \tag{7.99}$$

This assumption coincides with the requirements for small switching ripple in all elements of $\mathbf{x}(t)$ and that variations in $\mathbf{u}(t)$ be slow compared to the switching frequency. If we assume that the state vector is initially equal to $\mathbf{x}(0)$, then we can write

$$\underbrace{\mathbf{x}(dT_s)}_{\substack{\text{final}\\\text{value}}} = \underbrace{\mathbf{x}(0)}_{\substack{\text{initial}\\\text{value}}} + \underbrace{(dT_s)}_{\substack{\text{interval}\\\text{length}}}\ \underbrace{\mathbf{K}^{-1}\left(\mathbf{A}_1\langle \mathbf{x}(t)\rangle_{T_s} + \mathbf{B}_1\langle \mathbf{u}(t)\rangle_{T_s}\right)}_{\text{slope}} \tag{7.100}$$

Similar arguments apply during the second subinterval. With the switch in position 2, the state equations are given by Eq. (7.91). With the assumption of small ripple during this subinterval, the state vector now changes with slope

$$\frac{d\mathbf{x}(t)}{dt} = \mathbf{K}^{-1}\left(\mathbf{A}_2\langle \mathbf{x}(t)\rangle_{T_s} + \mathbf{B}_2\langle \mathbf{u}(t)\rangle_{T_s}\right) \tag{7.101}$$

The state vector at the end of the switching period is

$$\underbrace{\mathbf{x}(T_s)}_{\substack{\text{final}\\\text{value}}} = \underbrace{\mathbf{x}(dT_s)}_{\substack{\text{initial}\\\text{value}}} + \underbrace{(d'T_s)}_{\substack{\text{interval}\\\text{length}}}\ \underbrace{\mathbf{K}^{-1}\left(\mathbf{A}_2\langle \mathbf{x}(t)\rangle_{T_s} + \mathbf{B}_2\langle \mathbf{u}(t)\rangle_{T_s}\right)}_{\text{slope}} \tag{7.102}$$

Substitution of Eq. (7.100) into Eq. (7.102) allows us to determine $\mathbf{x}(T_s)$ in terms of $\mathbf{x}(0)$:

$$\mathbf{x}(T_s) = \mathbf{x}(0) + dT_s\mathbf{K}^{-1}\left(\mathbf{A}_1\langle \mathbf{x}(t)\rangle_{T_s} + \mathbf{B}_1\langle \mathbf{u}(t)\rangle_{T_s}\right) + d'T_s\mathbf{K}^{-1}\left(\mathbf{A}_2\langle \mathbf{x}(t)\rangle_{T_s} + \mathbf{B}_2\langle \mathbf{u}(t)\rangle_{T_s}\right) \tag{7.103}$$

Upon collecting terms, one obtains

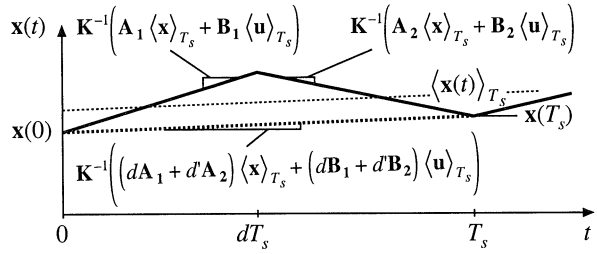

Fig. 7.29 How an element of the state vector, and its average, evolve over one switching period.

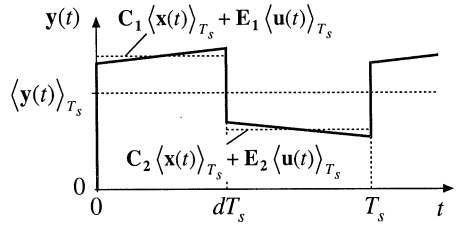

Fig. 7.30 Averaging an element of the output vector $\mathbf{y}(t)$.

$$\mathbf{x}(T_s)=\mathbf{x}(0)+T_s\mathbf{K}^{-1}\left(d(t)\mathbf{A}_1+d'(t)\mathbf{A}_2\right)\langle\mathbf{x}(t)\rangle_{T_s}+T_s\mathbf{K}^{-1}\left(d(t)\mathbf{B}_1+d'(t)\mathbf{B}_2\right)\langle\mathbf{u}(t)\rangle_{T_s} \tag{7.104}$$

Next, we approximate the derivative of $\langle\mathbf{x}(t)\rangle_{T_s}$ using the net change over one switching period:

$$\frac{d\langle\mathbf{x}(t)\rangle_{T_s}}{dt}\approx\frac{\mathbf{x}(T_s)-\mathbf{x}(0)}{T_s} \tag{7.105}$$

Substitution of Eq. (7.104) into (7.105) leads to

$$\mathbf{K}\frac{d\langle\mathbf{x}(t)\rangle_{T_s}}{dt}=\left(d(t)\,\mathbf{A}_1+d'(t)\,\mathbf{A}_2\right)\langle\mathbf{x}(t)\rangle_{T_s}+\left(d(t)\,\mathbf{B}_1+d'(t)\,\mathbf{B}_2\right)\langle\mathbf{u}(t)\rangle_{T_s} \tag{7.106}$$

which is identical to Eq. (7.99). This is the basic averaged model which describes the converter dynamics. It is nonlinear because the control input $d(t)$ is multiplied by $\langle\mathbf{x}(t)\rangle_{T_s}$ and $\langle\mathbf{u}(t)\rangle_{T_s}$. Variation of a typical element of $\mathbf{x}(t)$ and its average are illustrated in Fig. 7.29.

It is also desired to find the low-frequency components of the output vector $\mathbf{y}(t)$ by averaging. The vector $\mathbf{y}(t)$ is described by Eq. (7.90) for the first subinterval, and by Eq. (7.91) for the second subinterval. Hence, the elements of $\mathbf{y}(t)$ may be discontinuous at the switching transitions, as illustrated in Fig. 7.30. We can again remove the switching harmonics by averaging over one switching period; the

result is

$$\langle \mathbf{y}(t) \rangle_{T_s} = d(t) \left(\mathbf{C}_1 \langle \mathbf{x}(t) \rangle_{T_s} + \mathbf{E}_1 \langle \mathbf{u}(t) \rangle_{T_s} \right) + d'(t) \left(\mathbf{C}_2 \langle \mathbf{x}(t) \rangle_{T_s} + \mathbf{E}_2 \langle \mathbf{u}(t) \rangle_{T_s} \right) \tag{7.107}$$

Rearrangement of terms yields

$$\langle \mathbf{y}(t) \rangle_{T_s} = \left(d(t)\, \mathbf{C}_1 + d'(t)\, \mathbf{C}_2 \right) \langle \mathbf{x}(t) \rangle_{T_s} + \left(d(t)\, \mathbf{E}_1 + d'(t)\, \mathbf{E}_2 \right) \langle \mathbf{u}(t) \rangle_{T_s} \tag{7.108}$$

This is again a nonlinear equation.

The averaged state equations, (7.106) and (7.108), are collected below:

$$\begin{aligned} \mathbf{K} \frac{d \langle \mathbf{x}(t) \rangle_{T_s}}{dt} &= \left(d(t)\, \mathbf{A}_1 + d'(t)\, \mathbf{A}_2 \right) \langle \mathbf{x}(t) \rangle_{T_s} + \left(d(t)\, \mathbf{B}_1 + d'(t)\, \mathbf{B}_2 \right) \langle \mathbf{u}(t) \rangle_{T_s} \\ \langle \mathbf{y}(t) \rangle_{T_s} &= \left(d(t)\, \mathbf{C}_1 + d'(t)\, \mathbf{C}_2 \right) \langle \mathbf{x}(t) \rangle_{T_s} + \left(d(t)\, \mathbf{E}_1 + d'(t)\, \mathbf{E}_2 \right) \langle \mathbf{u}(t) \rangle_{T_s} \end{aligned} \tag{7.109}$$

The next step is the linearization of these equations about a quiescent operating point, to construct a small-signal ac model. When dc inputs $d(t) = D$ and $\mathbf{u}(t) = \mathbf{U}$ are applied, converter operates in equilibrium when the derivatives of all of the elements of $\langle \mathbf{x}(t) \rangle_{T_s}$ are zero. Hence, by setting the derivative of $\langle \mathbf{x}(t) \rangle_{T_s}$ to zero in Eq. (7.109), we can define the converter quiescent operating point as the solution of

$$\begin{aligned} \mathbf{0} &= \mathbf{AX} + \mathbf{BU} \\ \mathbf{Y} &= \mathbf{CX} + \mathbf{EU} \end{aligned} \tag{7.110}$$

where definitions (7.93) and (7.94) have been used. We now perturb and linearize the converter waveforms about this quiescent operating point:

$$\begin{aligned} \langle \mathbf{x}(t) \rangle_{T_s} &= \mathbf{X} + \hat{\mathbf{x}}(t) \\ \langle \mathbf{u}(t) \rangle_{T_s} &= \mathbf{U} + \hat{\mathbf{u}}(t) \\ \langle \mathbf{y}(t) \rangle_{T_s} &= \mathbf{Y} + \hat{\mathbf{y}}(t) \\ d(t) &= D + \hat{d}(t) \quad \Rightarrow \quad d'(t) = D' - \hat{d}(t) \end{aligned} \tag{7.111}$$

Here, $\hat{\mathbf{u}}(t)$ and $\hat{d}(t)$ are small ac variations in the input vector and duty ratio. The vectors $\hat{\mathbf{x}}(t)$ and $\hat{\mathbf{y}}(t)$ are the resulting small ac variations in the state and output vectors. We must assume that these ac variations are much smaller than the quiescent values. In other words,

$$\begin{aligned} \| \mathbf{U} \| &\gg \| \hat{\mathbf{u}}(t) \| \\ D &\gg | \hat{d}(t) | \\ \| \mathbf{X} \| &\gg \| \hat{\mathbf{x}}(t) \| \\ \| \mathbf{Y} \| &\gg \| \hat{\mathbf{y}}(t) \| \end{aligned} \tag{7.112}$$

Here, $\| \mathbf{x} \|$ denotes a norm of the vector $\mathbf{x}$.

Substitution of Eq. (7.111) into Eq. (7.109) yields

$$\mathbf{K}\frac{d\left(\mathbf{X}+\hat{\mathbf{x}}(t)\right)}{dt}=\left(\left(D+\hat{d}(t)\right)\mathbf{A}_1+\left(D'-\hat{d}(t)\right)\mathbf{A}_2\right)\left(\mathbf{X}+\hat{\mathbf{x}}(t)\right)$$
$$+\left(\left(D+\hat{d}(t)\right)\mathbf{B}_1+\left(D'-\hat{d}(t)\right)\mathbf{B}_2\right)\left(\mathbf{U}+\hat{\mathbf{u}}(t)\right)$$
$$\left(\mathbf{Y}+\hat{\mathbf{y}}(t)\right)=\left(\left(D+\hat{d}(t)\right)\mathbf{C}_1+\left(D'-\hat{d}(t)\right)\mathbf{C}_2\right)\left(\mathbf{X}+\hat{\mathbf{x}}(t)\right)$$
$$+\left(\left(D+\hat{d}(t)\right)\mathbf{E}_1+\left(D'-\hat{d}(t)\right)\mathbf{E}_2\right)\left(\mathbf{U}+\hat{\mathbf{u}}(t)\right) \tag{7.113}$$

The derivative $d\mathbf{X}/dt$ is zero. By collecting terms, one obtains

$$\underbrace{\mathbf{K}\frac{d\hat{\mathbf{x}}(t)}{dt}}_{\text{first-order ac}}=\underbrace{\left(\mathbf{AX}+\mathbf{BU}\right)}_{\text{dc terms}}+\underbrace{\mathbf{A}\hat{\mathbf{x}}(t)+\mathbf{B}\hat{\mathbf{u}}(t)+\left\{\left(\mathbf{A}_1-\mathbf{A}_2\right)\mathbf{X}+\left(\mathbf{B}_1-\mathbf{B}_2\right)\mathbf{U}\right\}\hat{d}(t)}_{\text{first-order ac terms}}$$
$$+\underbrace{\left(\mathbf{A}_1-\mathbf{A}_2\right)\hat{\mathbf{x}}(t)\hat{d}(t)+\left(\mathbf{B}_1-\mathbf{B}_2\right)\hat{\mathbf{u}}(t)\hat{d}(t)}_{\text{second-order nonlinear terms}}$$
$$\underbrace{\left(\mathbf{Y}+\hat{\mathbf{y}}(t)\right)}_{\text{dc + 1}^{st}\text{ order ac}}=\underbrace{\left(\mathbf{CX}+\mathbf{EU}\right)}_{\text{dc terms}}+\underbrace{\mathbf{C}\hat{\mathbf{x}}(t)+\mathbf{E}\hat{\mathbf{u}}(t)+\left\{\left(\mathbf{C}_1-\mathbf{C}_2\right)\mathbf{X}+\left(\mathbf{E}_1-\mathbf{E}_2\right)\mathbf{U}\right\}\hat{d}(t)}_{\text{first-order ac terms}}$$
$$+\underbrace{\left(\mathbf{C}_1-\mathbf{C}_2\right)\hat{\mathbf{x}}(t)\hat{d}(t)+\left(\mathbf{E}_1-\mathbf{E}_2\right)\hat{\mathbf{u}}(t)\hat{d}(t)}_{\text{second-order nonlinear terms}} \tag{7.114}$$

Since the dc terms satisfy Eq. (7.110), they drop out of Eq. (7.114). Also, if the small-signal assumption (7.112) is satisfied, then the second-order nonlinear terms of Eq. (7.114) are small in magnitude compared to the first-order ac terms. We can therefore neglect the nonlinear terms, to obtain the following linearized ac model:

$$\mathbf{K}\frac{d\hat{\mathbf{x}}(t)}{dt}=\mathbf{A}\hat{\mathbf{x}}(t)+\mathbf{B}\hat{\mathbf{u}}(t)+\left\{\left(\mathbf{A}_1-\mathbf{A}_2\right)\mathbf{X}+\left(\mathbf{B}_1-\mathbf{B}_2\right)\mathbf{U}\right\}\hat{d}(t)$$
$$\hat{\mathbf{y}}(t)=\mathbf{C}\hat{\mathbf{x}}(t)+\mathbf{E}\hat{\mathbf{u}}(t)+\left\{\left(\mathbf{C}_1-\mathbf{C}_2\right)\mathbf{X}+\left(\mathbf{E}_1-\mathbf{E}_2\right)\mathbf{U}\right\}\hat{d}(t) \tag{7.115}$$

This is the desired result, which coincides with Eq. (7.95).

7.3.4 Example: State-Space Averaging of a Nonideal Buck-Boost Converter

Let us apply the state-space averaging method to model the buck-boost converter of Fig. 7.31. We will model the conduction loss of MOSFET Q_1 by on-resistance R_{on}, and the forward voltage drop of diode

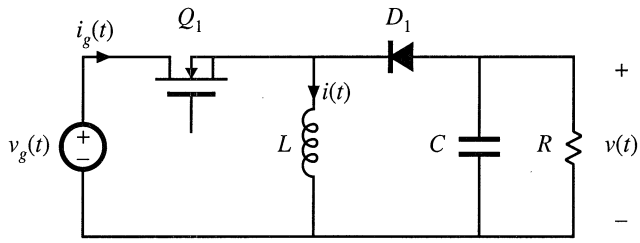

Fig. 7.31 Buck-boost converter example.

D_1 by an independent voltage source of value V_D. It is desired to obtain a complete equivalent circuit, which models both the input port and the output port of the converter.

The independent states of the converter are the inductor current $i(t)$ and the capacitor voltage $v(t)$. Therefore, we should define the state vector $\mathbf{x}(t)$ as

$$\mathbf{x}(t) = \begin{bmatrix} i(t) \\ v(t) \end{bmatrix} \tag{7.116}$$

The input voltage $v_g(t)$ is an independent source which should be placed in the input vector $\mathbf{u}(t)$. In addition, we have chosen to model the diode forward voltage drop with an independent voltage source of value V_D. So this voltage source should also be included in the input vector $\mathbf{u}(t)$. Therefore, let us define the input vector as

$$\mathbf{u}(t) = \begin{bmatrix} v_g(t) \\ V_D \end{bmatrix} \tag{7.117}$$

To model the converter input port, we need to find the converter input current $i_g(t)$. To calculate this dependent current, it should be included in the output vector $\mathbf{y}(t)$. Therefore, let us choose to define $\mathbf{y}(t)$ as

$$\mathbf{y}(t) = \begin{bmatrix} i_g(t) \end{bmatrix} \tag{7.118}$$

Note that it isn't necessary to include the output voltage $v(t)$ in the output vector $\mathbf{y}(t)$, since $v(t)$ is already included in the state vector $\mathbf{x}(t)$.

Next, let us write the state equations for each subinterval. When the switch is in position 1, the converter circuit of Fig. 7.32(a) is obtained. The inductor voltage, capacitor current, and converter input current are

$$\begin{aligned} L\frac{di(t)}{dt} &= v_g(t) - i(t)\,R_{on} \\ C\frac{dv(t)}{dt} &= -\frac{v(t)}{R} \\ i_g(t) &= i(t) \end{aligned} \tag{7.119}$$

These equations can be written in the following state-space form:

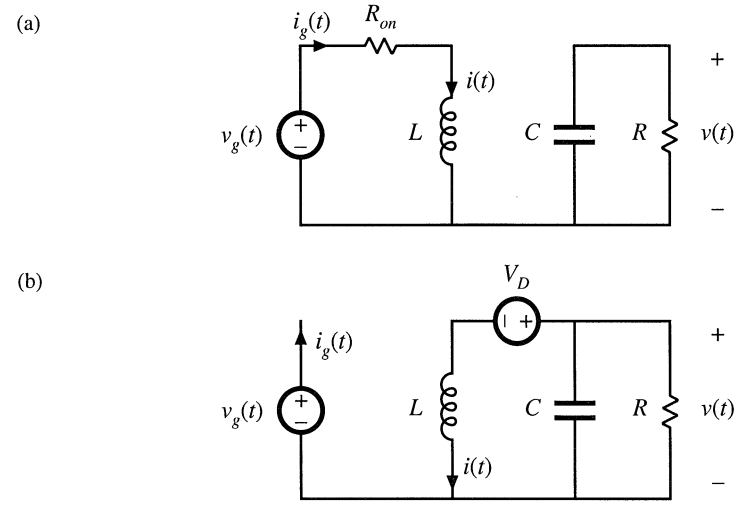

Fig. 7.32 Buck-boost converter circuit: (a) during subinterval 1, (b) during subinterval 2.

$$\underbrace{\begin{bmatrix} L & 0 \\ 0 & C \end{bmatrix}}_{\mathbf{K}} \underbrace{\frac{d}{dt}\begin{bmatrix} i(t) \\ v(t) \end{bmatrix}}_{\frac{d\mathbf{x}(t)}{dt}} = \underbrace{\begin{bmatrix} -R_{on} & 0 \\ 0 & -\frac{1}{R} \end{bmatrix}}_{\mathbf{A}_1} \underbrace{\begin{bmatrix} i(t) \\ v(t) \end{bmatrix}}_{\mathbf{x}(t)} + \underbrace{\begin{bmatrix} 1 & 0 \\ 0 & 0 \end{bmatrix}}_{\mathbf{B}_1} \underbrace{\begin{bmatrix} v_g(t) \\ V_D \end{bmatrix}}_{\mathbf{u}(t)}$$

$$\underbrace{\begin{bmatrix} i_g(t) \end{bmatrix}}_{\mathbf{y}(t)} = \underbrace{\begin{bmatrix} 1 & 0 \end{bmatrix}}_{\mathbf{C}_1} \underbrace{\begin{bmatrix} i(t) \\ v(t) \end{bmatrix}}_{\mathbf{x}(t)} + \underbrace{\begin{bmatrix} 0 & 0 \end{bmatrix}}_{\mathbf{E}_1} \underbrace{\begin{bmatrix} v_g(t) \\ V_D \end{bmatrix}}_{\mathbf{u}(t)} \tag{7.120}$$

So we have identified the state equation matrices $\mathbf{A}_1$, $\mathbf{B}_1$, $\mathbf{C}_1$, and $\mathbf{E}_1$.

With the switch in position 2, the converter circuit of Fig. 7.32(b) is obtained. For this subinterval, the inductor voltage, capacitor current, and converter input current are given by

$$\begin{aligned} L\frac{di(t)}{dt} &= v(t) - V_D \\ C\frac{dv(t)}{dt} &= -\frac{v(t)}{R} - i(t) \\ i_g(t) &= 0 \end{aligned} \tag{7.121}$$

When written in state-space form, these equations become

$$\underbrace{\begin{bmatrix} L & 0 \\ 0 & C \end{bmatrix}}_{\mathbf{K}} \underbrace{\frac{d}{dt}\begin{bmatrix} i(t) \\ v(t) \end{bmatrix}}_{\frac{d\mathbf{x}(t)}{dt}} = \underbrace{\begin{bmatrix} 0 & 1 \\ -1 & -\frac{1}{R} \end{bmatrix}}_{\mathbf{A}_2} \underbrace{\begin{bmatrix} i(t) \\ v(t) \end{bmatrix}}_{\mathbf{x}(t)} + \underbrace{\begin{bmatrix} 0 & -1 \\ 0 & 0 \end{bmatrix}}_{\mathbf{B}_2} \underbrace{\begin{bmatrix} v_g(t) \\ V_D \end{bmatrix}}_{\mathbf{u}(t)}$$

$$\underbrace{\begin{bmatrix} i_g(t) \end{bmatrix}}_{\mathbf{y}(t)} = \underbrace{\begin{bmatrix} 0 & 0 \end{bmatrix}}_{\mathbf{C}_2} \underbrace{\begin{bmatrix} i(t) \\ v(t) \end{bmatrix}}_{\mathbf{x}(t)} + \underbrace{\begin{bmatrix} 0 & 0 \end{bmatrix}}_{\mathbf{E}_2} \underbrace{\begin{bmatrix} v_g(t) \\ V_D \end{bmatrix}}_{\mathbf{u}(t)} \tag{7.122}$$

So we have also identified the subinterval 2 matrices $\mathbf{A}_2$, $\mathbf{B}_2$, $\mathbf{C}_2$, and $\mathbf{E}_2$.

The next step is to evaluate the state-space averaged equilibrium equations (7.92) to (7.94). The averaged matrix $\mathbf{A}$ is

$$\mathbf{A} = D\mathbf{A}_1 + D'\mathbf{A}_2 = D\begin{bmatrix} -R_{on} & 0 \\ 0 & -\frac{1}{R} \end{bmatrix} + D'\begin{bmatrix} 0 & 1 \\ -1 & -\frac{1}{R} \end{bmatrix} = \begin{bmatrix} -DR_{on} & D' \\ -D' & -\frac{1}{R} \end{bmatrix} \tag{7.123}$$

In a similar manner, the averaged matrices $\mathbf{B}$, $\mathbf{C}$, and $\mathbf{E}$ are evaluated, with the following results:

$$\begin{aligned} \mathbf{B} &= D\mathbf{B}_1 + D'\mathbf{B}_2 = \begin{bmatrix} D & -D' \\ 0 & 0 \end{bmatrix} \\ \mathbf{C} &= D\mathbf{C}_1 + D'\mathbf{C}_2 = \begin{bmatrix} D & 0 \end{bmatrix} \\ \mathbf{E} &= D\mathbf{E}_1 + D'\mathbf{E}_2 = \begin{bmatrix} 0 & 0 \end{bmatrix} \end{aligned} \tag{7.124}$$

The dc state equations (7.92) therefore become

$$\begin{aligned} \begin{bmatrix} 0 \\ 0 \end{bmatrix} &= \begin{bmatrix} -DR_{on} & D' \\ -D' & -\frac{1}{R} \end{bmatrix} \begin{bmatrix} I \\ V \end{bmatrix} + \begin{bmatrix} D & -D' \\ 0 & 0 \end{bmatrix} \begin{bmatrix} V_g \\ V_D \end{bmatrix} \\ \begin{bmatrix} I_g \end{bmatrix} &= \begin{bmatrix} D & 0 \end{bmatrix} \begin{bmatrix} I \\ V \end{bmatrix} + \begin{bmatrix} 0 & 0 \end{bmatrix} \begin{bmatrix} V_g \\ V_D \end{bmatrix} \end{aligned} \tag{7.125}$$

Evaluation of Eq. (7.95) leads to the following solution for the equilibrium state and output vectors:

$$\begin{aligned} \begin{bmatrix} I \\ V \end{bmatrix} &= \left(\frac{1}{1 + \frac{D}{D'^2}\frac{R_{on}}{R}}\right) \begin{bmatrix} \frac{D}{D'^2R} & \frac{1}{D'R} \\ -\frac{D}{D'} & 1 \end{bmatrix} \begin{bmatrix} V_g \\ V_D \end{bmatrix} \\ \begin{bmatrix} I_g \end{bmatrix} &= \left(\frac{1}{1 + \frac{D}{D'^2}\frac{R_{on}}{R}}\right) \begin{bmatrix} \frac{D^2}{D'^2R} & \frac{D}{D'R} \end{bmatrix} \begin{bmatrix} V_g \\ V_D \end{bmatrix} \end{aligned} \tag{7.126}$$

Alternatively, the steady-state equivalent circuit of Fig. 7.33 can be constructed as usual from

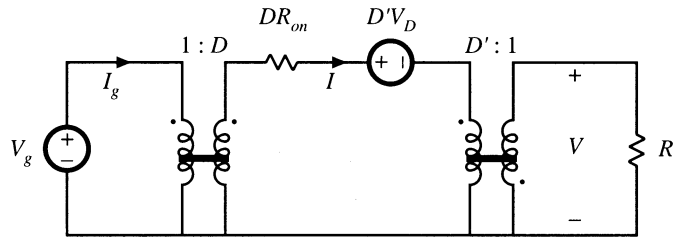

Fig. 7.33 Dc circuit model for the buck-boost converter example, equivalent to Eq. (7.125).

Eq. (7.125). The top row of Eq. (7.125) could have been obtained by application of the principle of inductor volt-second balance to the inductor voltage waveform. The second row of Eq. (7.125) could have been obtained by application of the principle of capacitor charge balance to the capacitor current waveform. The $i_g(t)$ equation expresses the dc component of the converter input current. By reconstructing circuits that are equivalent to these three equations, the dc model of Fig. 7.33 is obtained.

The small-signal model is found by evaluation of Eq. (7.95). The vector coefficients of $\hat{d}(t)$ in Eq. (7.95) are

$$\begin{aligned}
\left(\mathbf{A}_1 - \mathbf{A}_2\right)\mathbf{X} + \left(\mathbf{B}_1 - \mathbf{B}_2\right)\mathbf{U} &= \begin{bmatrix} -V - IR_{on} \\ I \end{bmatrix} + \begin{bmatrix} V_g + V_D \\ 0 \end{bmatrix} = \begin{bmatrix} V_g - V - IR_{on} + V_D \\ I \end{bmatrix} \\
\left(\mathbf{C}_1 - \mathbf{C}_2\right)\mathbf{X} + \left(\mathbf{E}_1 - \mathbf{E}_2\right)\mathbf{U} &= \begin{bmatrix} I \end{bmatrix}
\end{aligned} \tag{7.127}$$

The small-signal ac state equations (7.95) therefore become

$$\begin{aligned}
\begin{bmatrix} L & 0 \\ 0 & C \end{bmatrix} \frac{d}{dt} \begin{bmatrix} \hat{i}(t) \\ \hat{v}(t) \end{bmatrix} &= \begin{bmatrix} -DR_{on} & D' \\ -D' & -\frac{1}{R} \end{bmatrix} \begin{bmatrix} \hat{i}(t) \\ \hat{v}(t) \end{bmatrix} + \begin{bmatrix} D & -D' \\ 0 & 0 \end{bmatrix} \begin{bmatrix} \hat{v}_g(t) \\ 0 \end{bmatrix} + \begin{bmatrix} V_g - V - IR_{on} + V_D \\ I \end{bmatrix} \hat{d}(t) \\
\begin{bmatrix} \hat{i}_g(t) \end{bmatrix} &= \begin{bmatrix} D & 0 \end{bmatrix} \begin{bmatrix} \hat{i}(t) \\ \hat{v}(t) \end{bmatrix} + \begin{bmatrix} 0 & 0 \end{bmatrix} \begin{bmatrix} \hat{v}_g(t) \\ 0 \end{bmatrix} + \begin{bmatrix} I \end{bmatrix} \hat{d}(t)
\end{aligned} \tag{7.128}$$

Note that, since the diode forward voltage drop is modeled as the constant value V_D, there are no ac variations in this source, and $\hat{v}_D(t)$ equals zero. Again, a circuit model equivalent to Eq. (7.128) can be constructed, in the usual manner. When written in scalar form, Eq. (7.128) becomes

$$\begin{aligned}
L \frac{d\hat{i}(t)}{dt} &= D' \hat{v}(t) - DR_{on} \hat{i}(t) + D \hat{v}_g(t) + \left(V_g - V - IR_{on} + V_D\right) \hat{d}(t) \\
C \frac{d\hat{v}(t)}{dt} &= -D' \hat{i}(t) - \frac{\hat{v}(t)}{R} + I \hat{d}(t) \\
\hat{i}_g(t) &= D \hat{i}(t) + I \hat{d}(t)
\end{aligned} \tag{7.129}$$

Circuits corresponding to these equations are listed in Fig. 7.34. These circuits can be combined into the complete small-signal ac equivalent circuit model of Fig. 7.35.

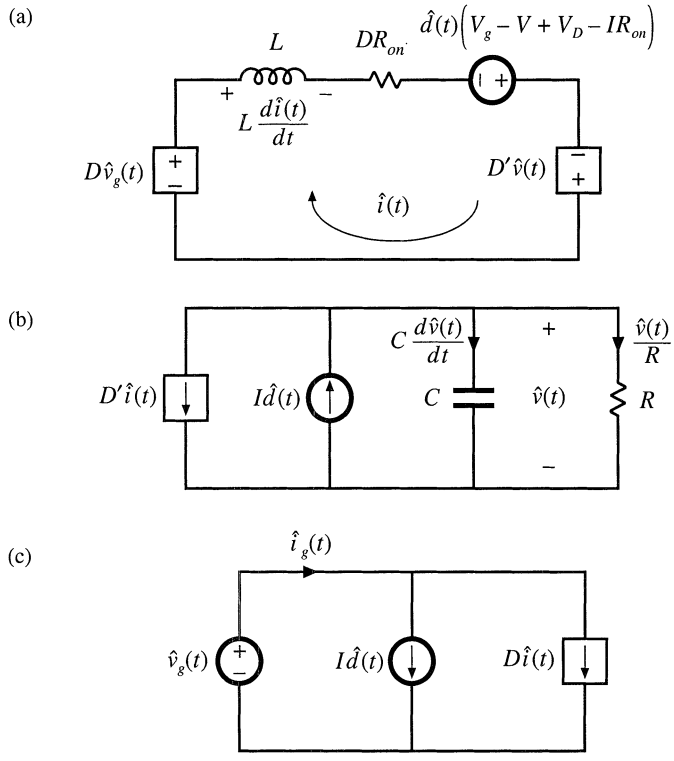

Fig. 7.34 Circuits equivalent to the small-signal converter equations: (a) inductor loop, (b) capacitor node, (c) input port.

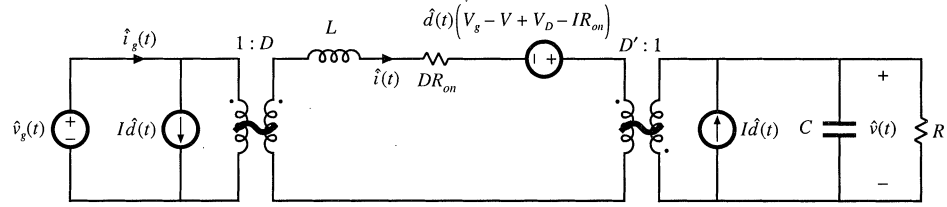

Fig. 7.35 Complete small-signal ac equivalent circuit model, nonideal buck-boost converter example.

7.4 CIRCUIT AVERAGING AND AVERAGED SWITCH MODELING

Circuit averaging is another well-known technique for derivation of converter equivalent circuits. Rather than averaging the converter state equations, with the circuit averaging technique we average the converter waveforms directly. All manipulations are performed on the circuit diagram, instead of on its equa-

tions, and hence the circuit averaging technique gives a more physical interpretation to the model. Since circuit averaging involves averaging and small-signal linearization, it is equivalent to state-space averaging. However, in many cases circuit averaging is easier to apply, and allows the small-signal ac model to be written almost by inspection. The circuit averaging technique can also be applied directly to a number of different types of converters and switch elements, including phase-controlled rectifiers, PWM converters operated in discontinuous conduction mode or with current programming, and quasi-resonant converters—these are described in later chapters. However, in other cases it may lead to involuted models that are less easy to analyze and understand. To overcome this problem, the circuit averaging and state-space averaging approaches can be combined. Circuit averaging was developed before state-space averaging, and is described in [4]. Because of its generality, there has been a recent resurgence of interest in circuit averaging of switch networks [13–20].

The key step in circuit averaging is to replace the converter switches with voltage and current sources, to obtain a time-invariant circuit topology. The waveforms of the voltage and current generators are defined to be identical to the switch waveforms of the original converter. Once a time-invariant circuit network is obtained, then the converter waveforms can be averaged over one switching period to remove the switching harmonics. Any nonlinear elements in the averaged circuit model can then be perturbed and linearized, leading to the small-signal ac model.

In Fig. 7.36, the switching elements are separated from the remainder of the converter. The converter therefore consists of a switch network containing the converter switching elements, and a time-invariant network, containing the reactive and other remaining elements. Figure 7.36 illustrates the simple case in which there are two single-pole single-throw (SPST) switches; the switches can then be represented using a two-port network. In more complicated systems containing multiple transistors or diodes, such as in polyphase converters, the switch network may contain more than two ports.

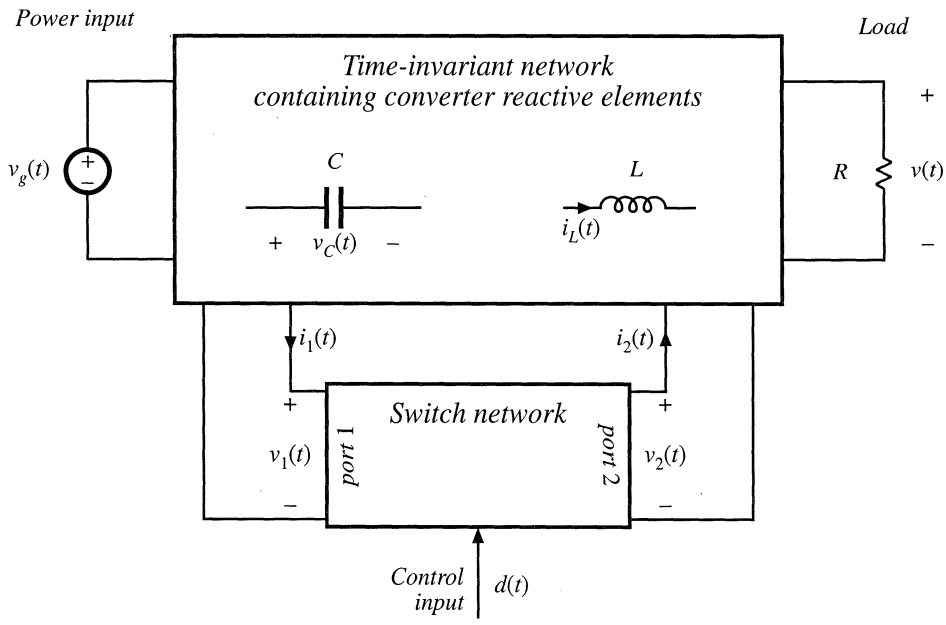

Fig. 7.36 A switching converter can be viewed as a switch network connected to a time-invariant network.

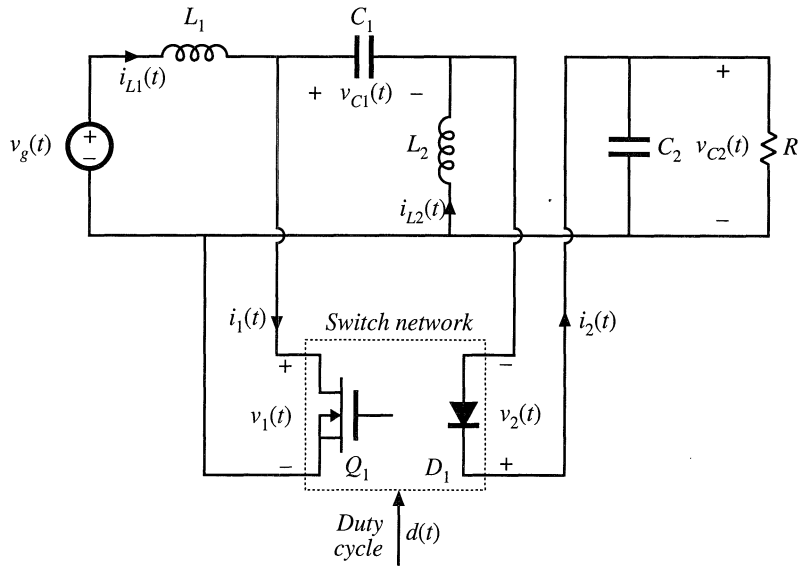

Fig. 7.37 Schematic of the SEPIC, arranged in the form of Fig. 7.36.

The central idea of the *averaged switch modeling* approach is to find an averaged circuit model for the switch network. The resulting averaged switch model can then be inserted into the converter circuit to obtain a complete averaged circuit model of the converter. An important advantage of the averaged switch modeling approach is that the same model can be used in many different converter configurations. It is not necessary to rederive an averaged circuit model for each particular converter. Furthermore, in many cases, the averaged switch model simplifies converter analysis and yields good intuitive understanding of the converter steady-state and dynamic properties.

The first step in the process of finding an averaged switch model for a switch network is to sketch the converter in the form of Fig. 7.36, in which a switch network containing only the converter switching elements is explicitly defined. The CCM SEPIC example shown in Fig. 7.37 is used to illustrate the process. There is usually more than one way to define the two ports of the switch network; a natural way to define the two-port switch network of the SEPIC is illustrated in Fig. 7.37. The switch network terminal quantities $v_1(t)$, $i_1(t)$, $v_2(t)$, and $i_2(t)$ are illustrated in Fig. 7.38 for CCM operation. Note that it is not necessary that the ports of the switch network be electrically connected within the switch network itself. Furthermore, there is no requirement that any of the terminal voltage or current waveforms of the switch network be nonpulsating.

7.4.1 Obtaining a Time-Invariant Circuit

The first step in the circuit averaging technique is to replace the switch network with voltage and current sources, such that the circuit connections do not vary in time. The switch network defined in the SEPIC is shown in Fig. 7.39(a). As with any two-port network, two of the four terminal voltages and

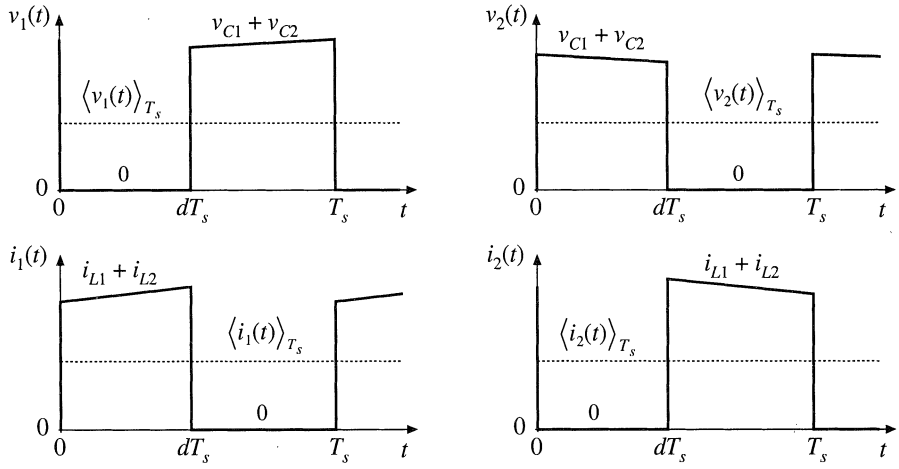

Fig. 7.38 Terminal switch network waveforms in the CCM SEPIC.

currents can be taken as independent inputs to the switch network. The remaining two voltages and/or currents are viewed as dependent outputs of the switch network. In general, the choice of independent inputs is arbitrary, as long as the inputs can indeed be independent in the given converter circuit. For CCM operation, one can choose one terminal current and one terminal voltage as the independent inputs. Let us select $i_1(t)$ and $v_2(t)$ as the switch network independent inputs. In addition, the duty cycle $d(t)$ is the independent control input.

In Fig. 7.39(b), the ports of the switch network are replaced by dependent voltage and current sources. The waveforms of these dependent sources are defined to be identical to the actual dependent outputs $v_1(t)$ and $i_2(t)$ given in Fig. 7.38. Since all waveforms in Fig. 7.39(b) match the waveforms of Figs. 7.39(a) and 7.38, the circuits are electrically equivalent. So far, no approximations have been made.

7.4.2 Circuit Averaging

The next step is determination of the average values of the switch network terminal waveforms in terms of the converter state variables (inductor currents and capacitor voltages) and the converter independent inputs (such as the input voltage and the transistor duty cycle). The basic assumption is made that the natural time constants of the converter network are much longer that the switching period T_s. This assumption coincides with the requirement for small switching ripple. One may average the waveforms over a time interval which is short compared to the system natural time constants, without significantly altering the system response. Hence, when the basic assumption is satisfied, it is a good approximation to average the converter waveforms over the switching period T_s. The resulting averaged model predicts the low-frequency behavior of the system, while neglecting the high-frequency switching harmonics. In the SEPIC example, by use of the usual small ripple approximation, the average values of the switch network terminal waveforms of Fig. 7.38 can be expressed in terms of the independent inputs and the state variables as follows:

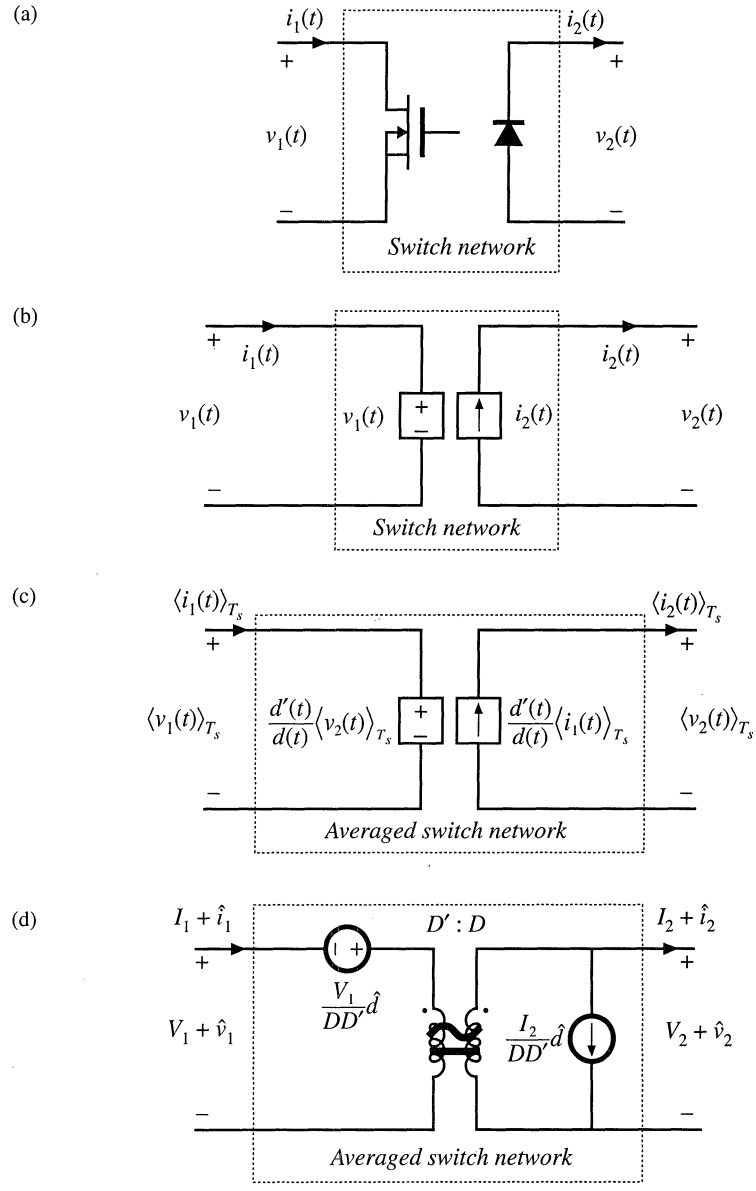

Fig. 7.39 Derivation of the averaged switch model for the CCM SEPIC: (a) switch network; (b) switch network where the switches are replaced with dependent sources whose waveforms match the switch terminal dependent waveforms; (c) large-signal, nonlinear averaged switch model obtained by averaging the switch network terminal waveforms in (b); (d) dc and ac small-signal averaged switch model.

$$\langle v_1(t)\rangle_{T_s} = d'(t)\left(\langle v_{C1}(t)\rangle_{T_s} + \langle v_{C2}(t)\rangle_{T_s}\right) \tag{7.130}$$

$$\langle i_1(t)\rangle_{T_s} = d(t)\left(\langle i_{L1}(t)\rangle_{T_s} + \langle i_{L2}(t)\rangle_{T_s}\right) \tag{7.131}$$

$$\langle v_2(t)\rangle_{T_s} = d(t)\left(\langle v_{C1}(t)\rangle_{T_s} + \langle v_{C2}(t)\rangle_{T_s}\right) \tag{7.132}$$

$$\langle i_2(t)\rangle_{T_s} = d'(t)\left(\langle i_{L1}(t)\rangle_{T_s} + \langle i_{L2}(t)\rangle_{T_s}\right) \tag{7.133}$$

We have selected $\langle i_1(t)\rangle_{T_s}$ and $\langle v_2(t)\rangle_{T_s}$ as the switch network independent inputs. The dependent outputs of the averaged switch network are then $\langle i_2(t)\rangle_{T_s}$ and $\langle v_1(t)\rangle_{T_s}$. The next step is to express, if possible, the switch network dependent outputs $\langle i_2(t)\rangle_{T_s}$ and $\langle v_1(t)\rangle_{T_s}$ as functions *solely* of the switch network independent inputs $\langle i_1(t)\rangle_{T_s}$, $\langle v_2(t)\rangle_{T_s}$, and the control input $d(t)$. In this step, the averaged switch outputs should not be written as functions of other converter signals such as $\langle v_g(t)\rangle_{T_s}$, $\langle v_{C1}(t)\rangle_{T_s}$, $\langle v_{C2}(t)\rangle_{T_s}$, $\langle i_{L1}(t)\rangle_{T_s}$, $\langle i_{L2}(t)\rangle_{T_s}$, etc.

We can use Eqs. (7.131) and (7.132) to write

$$\langle i_{L1}(t)\rangle_{T_s} + \langle i_{L2}(t)\rangle_{T_s} = \frac{\langle i_1(t)\rangle_{T_s}}{d(t)} \tag{7.134}$$

$$\langle v_{C1}(t)\rangle_{T_s} + \langle v_{C2}(t)\rangle_{T_s} = \frac{\langle v_2(t)\rangle_{T_s}}{d(t)} \tag{7.135}$$

Substitution of these expressions into Eqs. (7.130) and (7.133) leads to

$$\langle v_1(t)\rangle_{T_s} = \frac{d'(t)}{d(t)}\langle v_2(t)\rangle_{T_s} \tag{7.136}$$

$$\langle i_2(t)\rangle_{T_s} = \frac{d'(t)}{d(t)}\langle i_1(t)\rangle_{T_s} \tag{7.137}$$

The averaged equivalent circuit for the switch network, that corresponds to Eqs. (7.136) and (7.137), is illustrated in Fig. 7.39(c). Upon completing the averaging step, the switching harmonics have been removed from all converter waveforms, leaving only the dc and low-frequency ac components. This large-signal, nonlinear, time-invariant model is valid for frequencies sufficiently less than the switching frequency. Averaging the waveforms of Fig. 7.38 modifies only the switch network; the remainder of the converter circuit is unchanged. Therefore, the averaged circuit model of the converter is obtained simply by replacing the switch network with the averaged switch model. The switch network of Fig. 7.39(a) can be identified in any two-switch converter, such as buck, boost, buck-boost, SEPIC, or Ćuk. If the converter operates in continuous conduction mode, the derivation of the averaged switch model follows the same steps, and the result shown in Fig. 7.39(c) is the same as in the SEPIC example. This means that the model of Fig. 7.39(c) can be used as a general large-signal averaged switch model for all two-switch converters operating in CCM.

7.4.3 Perturbation and Linearization

The model of Fig. 7.39(c) is nonlinear, because the dependent generators given by Eqs. (7.136) and (7.137) are nonlinear functions of $d(t)$, $\langle i_2(t)\rangle_{T_s}$ and $\langle v_1(t)\rangle_{T_s}$. To construct a small-signal ac model, we perturb and linearize Eqs. (7.136) and (7.137) in the usual fashion. Let

$$\begin{aligned} d(t) &= D + \hat{d}(t) \\ \langle v_1(t)\rangle_{T_s} &= V_1 + \hat{v}_1(t) \\ \langle i_1(t)\rangle_{T_s} &= I_1 + \hat{i}_1(t) \\ \langle v_2(t)\rangle_{T_s} &= V_2 + \hat{v}_2(t) \\ \langle i_2(t)\rangle_{T_s} &= I_2 + \hat{i}_2(t) \end{aligned} \tag{7.138}$$

With these substitutions, Eq. (7.136) becomes

$$\left(D + \hat{d}\right)\left(V_1 + \hat{v}_1\right) = \left(D' - \hat{d}\right)\left(V_2 + \hat{v}_2\right) \tag{7.139}$$

It is desired to solve for the dependent quantity $V_1 + \hat{v}_1$. Equation (7.139) can be manipulated as follows:

$$D\left(V_1 + \hat{v}_1\right) = D'\left(V_2 + \hat{v}_2\right) - \hat{d}\left(V_1 + V_2\right) - \hat{d}\hat{v}_1 - \hat{d}\hat{v}_2 \tag{7.140}$$

The terms $\hat{d}(t)\hat{v}_1(t)$ and $\hat{d}(t)\hat{v}_2(t)$ are nonlinear, and are small in magnitude provided that the ac variations are much smaller than the quiescent values [as in Eq. (7.32)]. When the small-signal assumption is satisfied, these terms can be neglected. Upon eliminating the nonlinear terms and solving for the switch network dependent output $V_1 + \hat{v}_1$, we obtain

$$\begin{aligned} \left(V_1 + \hat{v}_1\right) &= \frac{D'}{D}\left(V_2 + \hat{v}_2\right) - \hat{d}\left(\frac{V_1 + V_2}{D}\right) \\ &= \frac{D'}{D}\left(V_2 + \hat{v}_2\right) - \hat{d}\left(\frac{V_1}{DD'}\right) \end{aligned} \tag{7.141}$$

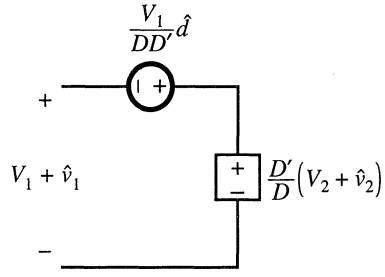

Fig. 7.40 Linearization of the dependent voltage source.

The term $(V_1/DD')\hat{d}(t)$ is driven by the control input $\hat{d}$, and hence can be represented by an independent voltage source as in Fig. 7.40. The term $(D'/D)(V_2 + \hat{v}_2(t))$ is equal to the constant value (D'/D) multiplied by the port 2 independent voltage $(V_2 + \hat{v}_2(t))$. This term is represented by a dependent voltage source in Fig. 7.40. This dependent source will become the primary winding of an ideal transformer.

In a similar manner, substitution of the relationships (7.138) into Eq. (7.137) leads to:

$$\left(D + \hat{d}\right)\left(I_2 + \hat{i}_2\right) = \left(D' - \hat{d}\right)\left(I_1 + \hat{i}_1\right) \tag{7.142}$$

The terms $\hat{i}_1(t)\hat{d}(t)$ and $\hat{i}_2(t)\hat{d}(t)$ are nonlinear, and can be neglected when the small-signal assumption is satisfied. Elimination of the nonlinear terms, and solution for $I_2 + \hat{i}_2$, yields:

$$\begin{aligned}\left(I_2+\hat{i}_2\right) &= \frac{D'}{D}\left(I_1+\hat{i}_1\right)-\hat{d}\left(\frac{I_1+I_2}{D}\right) \\ &= \frac{D'}{D}\left(I_1+\hat{i}_1\right)-\hat{d}\left(\frac{I_2}{DD'}\right)\end{aligned} \tag{7.143}$$

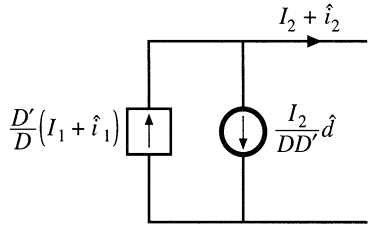

Fig. 7.41 Linearization of the dependent current source.

The term $(I_2/DD')\hat{d}(t)$ is driven by the control input $\hat{d}(t)$, and is represented by an independent current source in Fig. 7.41. The term $(D'/D)(I_1 + \hat{i}_1(t))$ is dependent on the port 1 current $(I_1 + \hat{i}_1(t))$. This term is modeled by a dependent current source in Fig. 7.41; this source will become the secondary winding of an ideal transformer. Equations (7.141) and (7.143) describe the averaged switch network model of Fig. 7.39(d). Note that the model contains both dc and small-signal ac terms: one equivalent circuit is used for both the dc and the small-signal ac models. The transformer symbol contains both a solid line (indicating that it is an ideal transformer capable of passing dc voltages and currents) and a sinusoidal line (which indicates that small-signal ac variations are modeled). The averaged switch model of Fig. 7.39(d) reveals that the switch network performs the functions of: (i) transformation of dc and small-signal ac voltage and current levels according to the D':D conversion ratio, and (ii) introduction of ac voltage and current variations into the converter circuit, driven by the control input $d(t)$. When this model is inserted into Fig. 7.37, the dc and small-signal ac SEPIC model of Fig. 7.42 is obtained. This model can now be solved to determine the steady-state voltages and currents as well as the small-signal converter transfer functions.

The switch network of Fig. 7.39(a) can be identified in all two-switch converters, including buck, boost, SEPIC, Ćuk, etc. As illustrated Fig. 7.43, a complete averaged circuit model of the converter can be constructed simply by replacing the switch network with the averaged switch model. For exam-

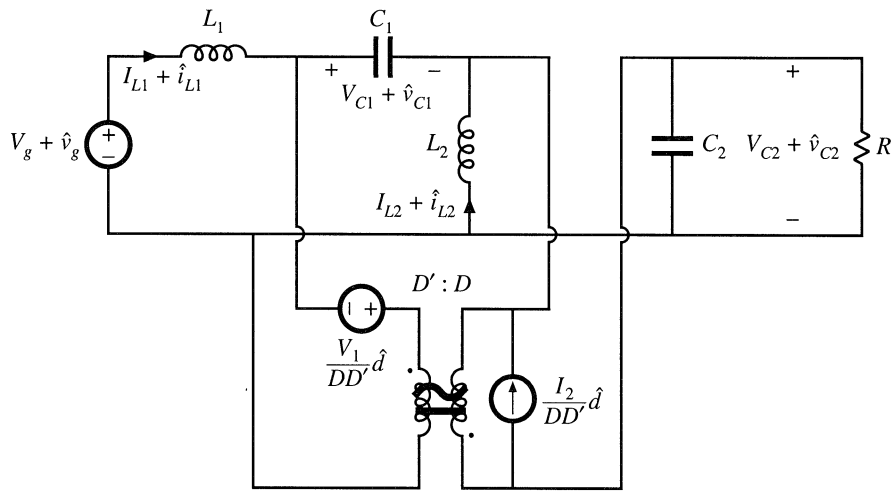

Fig. 7.42 A dc and small-signal ac averaged circuit model of the CCM SEPIC.

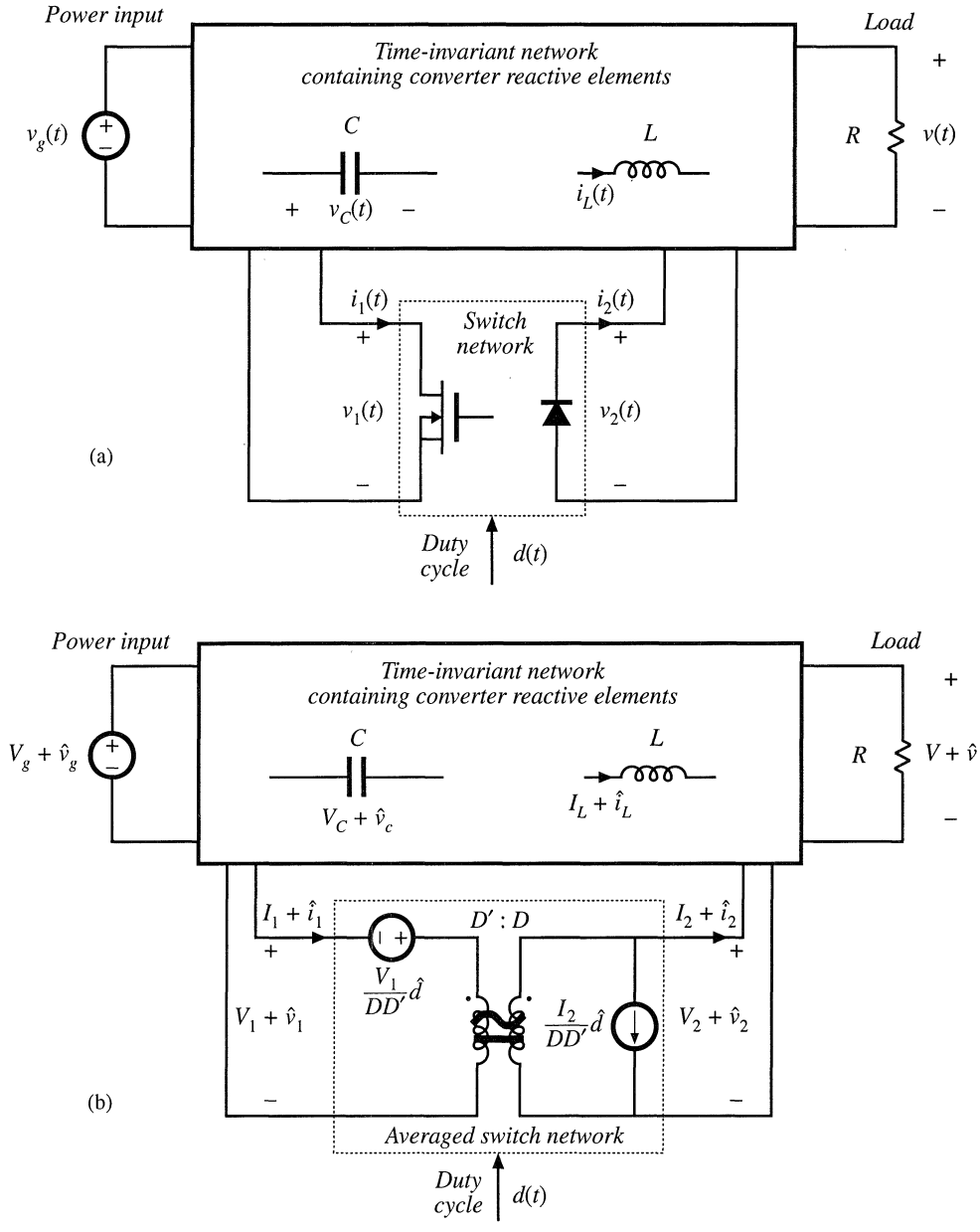

Fig. 7.43 Construction of an averaged circuit model for a two-switch converter operating in CCM: (a) the converter circuit with the general two-switch network identified; (b) dc and ac small-signal averaged circuit model obtained by replacing the switch network with the averaged model.

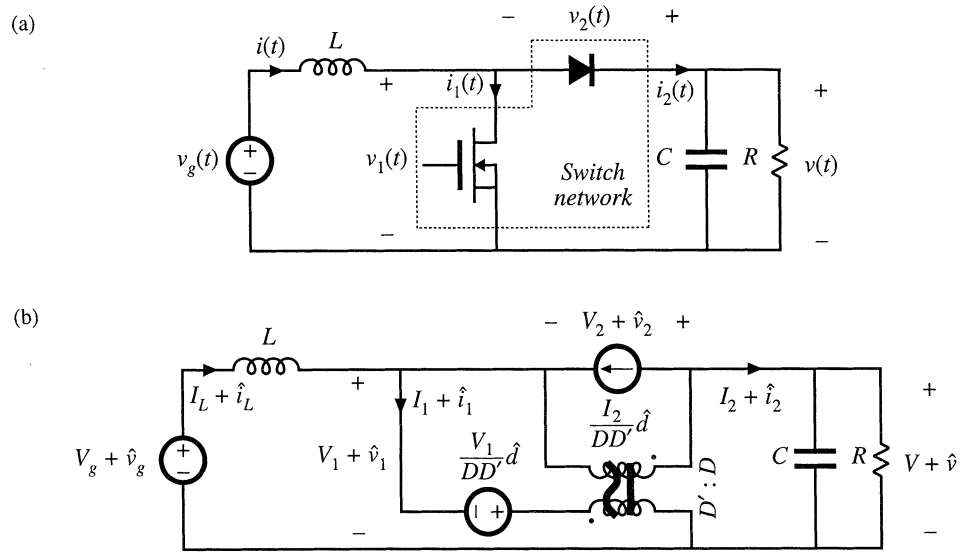

Fig. 7.44 Construction of an averaged circuit model for an ideal boost converter example: (a) converter circuit with the switch network of Fig. 7.39(a) identified; (b) a dc and small-signal ac averaged circuit model obtained by replacing the switch network with the model of Fig. 7.39(d).

ple, Fig. 7.44 shows an averaged circuit model of the boost converter obtained by identifying the switch network of Fig. 7.39(a) and replacing the switch network with the model of Fig. 7.39(d).

In summary, the circuit averaging method involves replacing the switch network with equivalent voltage and current sources, such that a time-invariant network is obtained. The converter waveforms are then averaged over one switching period to remove the switching harmonics. The large-signal model is perturbed and linearized about a quiescent operating point, to obtain a dc and a small-signal averaged switch model. Replacement of the switch network with the averaged switch model yields a complete averaged circuit model of the converter.

7.4.4 Switch Networks

So far, we have described derivation of the averaged switch model for the general two-switch network where the ports of the switch network coincide with the switch ports. No connections are assumed between the switches within the switch network itself. As a result, this switch network and its averaged model can be used to easily construct averaged circuit models of many two-switch converters, as illustrated in Fig. 7.43. It is important to note, however, that the definition of the switch network ports is not unique. Different definitions of the switch network lead to equivalent, but not identical, averaged switch models. The alternative forms of the averaged switch model may result in simpler circuit models, or models that provide better physical insight. Two alternative averaged switch models, better suited for analyses of boost and buck converters, are described in this section.

Consider the ideal boost converter of Fig. 7.45(a). The switch network contains the transistor

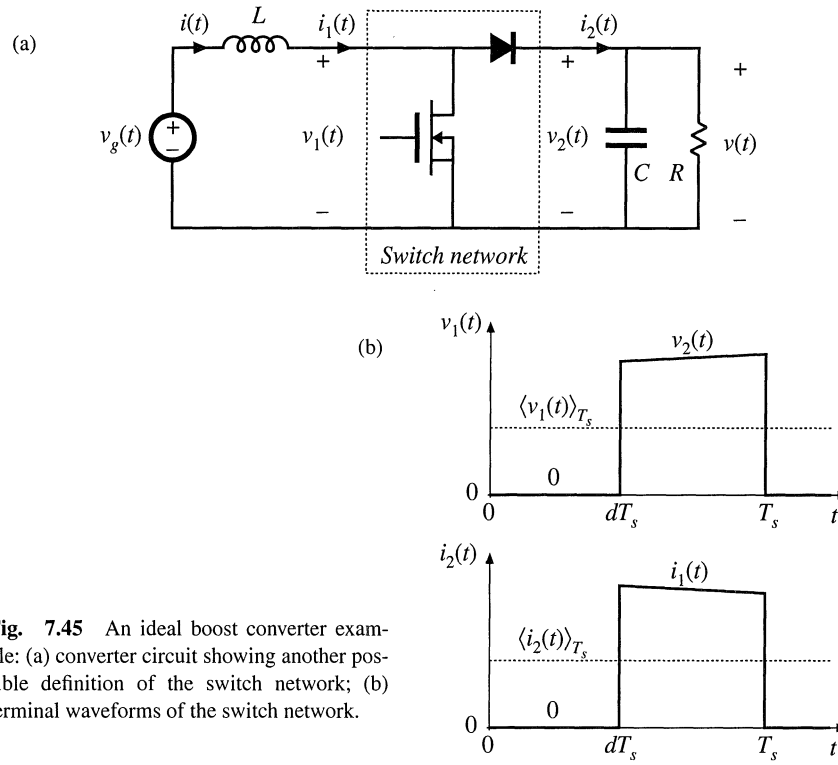

Fig. 7.45 An ideal boost converter example: (a) converter circuit showing another possible definition of the switch network; (b) terminal waveforms of the switch network.

and the diode, as in Fig. 7.44(a), but the switch network ports are defined differently. Let us proceed with the derivation of the corresponding averaged switch model. The switch network terminal waveforms are shown in Fig. 7.45(b). Since $i_1(t)$ and $v_2(t)$ coincide with the converter inductor current and capacitor voltage, it is convenient to choose these waveforms as the independent inputs to the switch network. The steps in the derivation of the averaged switch model are illustrated in Fig. 7.46.

First, we replace the switch network with dependent voltage and current generators as illustrated in Fig. 7.46(b). The voltage generator $v_1(t)$ models the dependent voltage waveform at the input port of the switch network, i.e., the transistor voltage. As illustrated in Fig. 7.45(b), $v_1(t)$ is zero when the transistor conducts, and is equal to $v_2(t)$ when the diode conducts:

$$v_1(t) = \begin{cases} 0, & 0 < t < dT_s \\ v_2(t), & dT_s < t < T_s \end{cases} \tag{7.144}$$

When $v_1(t)$ is defined in this manner, the inductor voltage waveform is unchanged. Likewise, $i_2(t)$ models the dependent current waveform at port 2 of the network, i.e., the diode current. As illustrated in Fig. 7.45(b), $i_2(t)$ is equal to zero when the transistor conducts, and is equal to $i_1(t)$ when the diode conducts:

$$i_2(t) = \begin{cases} 0, & 0 < t < dT_s \\ i_1(t), & dT_s < t < T_s \end{cases} \tag{7.145}$$

With $i_2(t)$ defined in this manner, the capacitor current waveform is unchanged. Therefore, the original converter circuit shown in Fig. 7.45(a), and the circuit obtained by replacing the switch network of Fig. 7.46(a) with the switch network of Fig. 7.46(b), are electrically identical. So far, no approximations have been made. Next, we remove the switching harmonics by averaging all signals over one switching period, as in Eq. (7.3). The results are

$$\begin{aligned} \left\langle v_1(t) \right\rangle_{T_s} &= d'(t) \left\langle v_2(t) \right\rangle_{T_s} \\ \left\langle i_2(t) \right\rangle_{T_s} &= d'(t) \left\langle i_1(t) \right\rangle_{T_s} \end{aligned} \tag{7.146}$$

Here we have assumed that the switching ripples of the inductor current and capacitor voltage are small, or at least linear functions of time. The averaged switch model of Fig. 7.46(c) is now obtained. This is a large-signal, nonlinear model, which can replace the switch network in the original converter circuit, for construction of a large-signal nonlinear circuit model of the converter. The switching harmonics have been removed from all converter waveforms, leaving only the dc and low-frequency ac components.

The model can be linearized by perturbing and linearizing the converter waveforms about a quiescent operating point, in the usual manner. Let

$$\begin{aligned} \left\langle v_g(t) \right\rangle_{T_s} &= V_g + \hat{v}_g(t) \\ d(t) &= D + \hat{d}(t) \quad \Rightarrow d'(t) = D' - \hat{d}(t) \\ \left\langle i(t) \right\rangle_{T_s} &= \left\langle i_1(t) \right\rangle_{T_s} = I + \hat{i}(t) \\ \left\langle v(t) \right\rangle_{T_s} &= \left\langle v_2(t) \right\rangle_{T_s} = V + \hat{v}(t) \\ \left\langle v_1(t) \right\rangle_{T_s} &= V_1 + \hat{v}_1(t) \\ \left\langle i_2(t) \right\rangle_{T_s} &= I_2 + \hat{i}_2(t) \end{aligned} \tag{7.147}$$

The nonlinear voltage generator at port 1 of the averaged switch network has value

$$\left(D' - \hat{d}(t)\right)\left(V + \hat{v}(t)\right) = D'\left(V + \hat{v}(t)\right) - V\hat{d}(t) - \hat{v}(t)\hat{d}(t) \tag{7.148}$$

The term $\hat{v}(t)\hat{d}(t)$ is nonlinear, and is small in magnitude provided that the ac variations are much smaller than the quiescent values [as in Eq. (7.32)]. When the small-signal assumption is satisfied, this term can be neglected. The term $V\hat{d}(t)$ is driven by the control input, and hence can be represented by an independent voltage source. The term $D'(V + \hat{v}(t))$ is equal to the constant value D' multiplied by the output voltage $(V + \hat{v}(t))$. This term is dependent on the output capacitor voltage; it is represented by a dependent voltage source. This dependent source will become the primary winding of an ideal transformer.

The nonlinear current generator at the port 2 of the averaged switch network is treated in a similar manner. Its current is

$$\left(D' - \hat{d}(t)\right)\left(I + \hat{i}(t)\right) = D'\left(I + \hat{i}(t)\right) - I\hat{d}(t) - \hat{i}(t)\hat{d}(t) \tag{7.149}$$

The term $\hat{i}(t)\hat{d}(t)$ is nonlinear, and can be neglected provided that the small-signal assumption is satisfied.

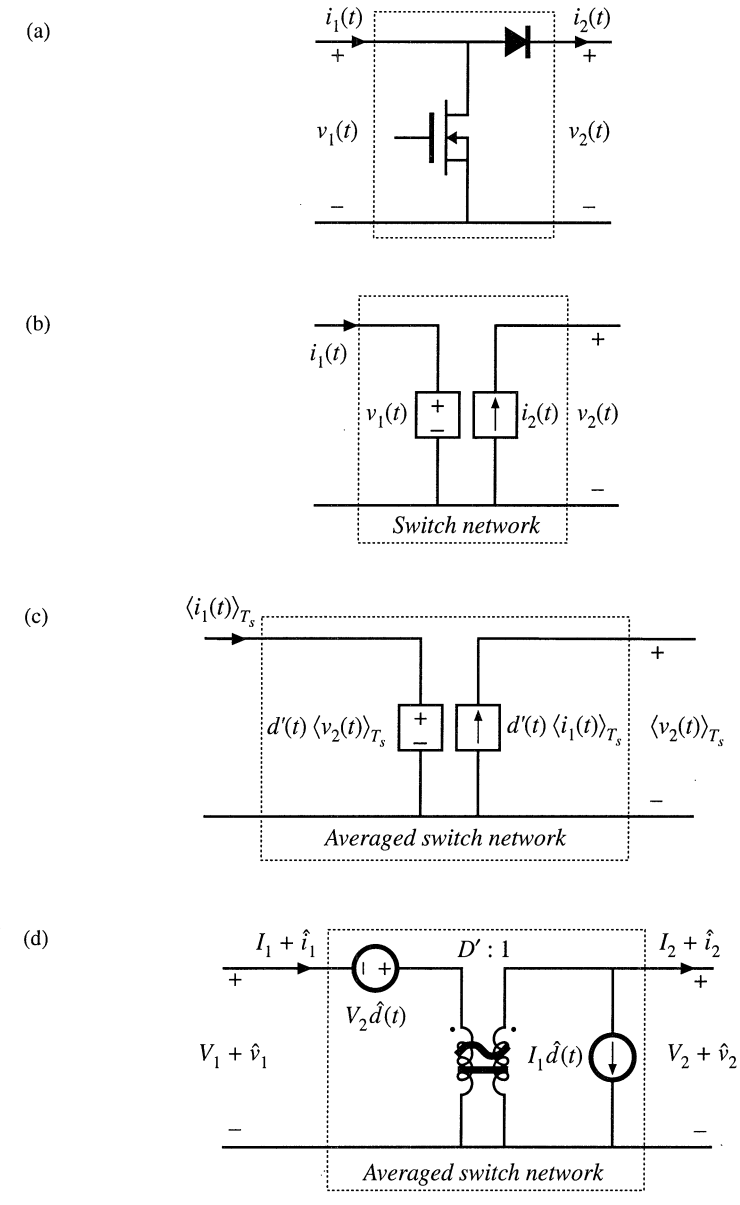

Fig. 7.46 Derivation of the averaged switch model for the CCM boost of Fig. 7.45: (a) switch network; (b) switch network where the switches are replaced by dependent sources whose waveforms match the switch terminal waveforms; (c) large-signal, nonlinear averaged switch model obtained by averaging the switch network terminal waveforms; (d) dc and ac small-signal averaged switch network model.

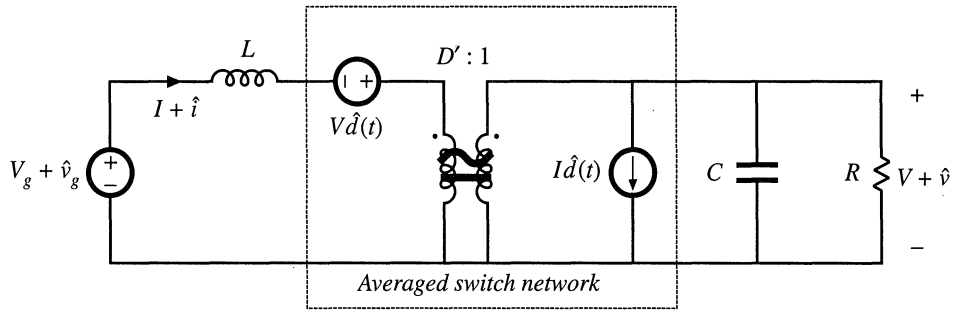

Fig. 7.47 Dc and small-signal ac averaged circuit model of the boost converter.

The term $I\hat{d}(t)$ is driven by the control input $\hat{d}(t)$, and is represented by an independent current source. The term $D'(I + \hat{i}(t))$ is dependent on the inductor current $(I + \hat{i}(t))$. This term is modeled by a dependent current source; this source will become the secondary winding of an ideal transformer.

Upon elimination of the nonlinear terms, and replacement of the dependent generators with an ideal D':1 transformer, the combined dc and small-signal ac averaged switch model of Fig. 7.46(d) is obtained. Figure 7.47 shows the complete averaged circuit model of the boost converter.

It is interesting to compare the models of Fig. 7.44(b) and Fig. 7.47. The two averaged circuit models of the boost converter are equivalent—they result in the same steady-state solution, and the same converter transfer functions. However, since both ports of the switch network in Fig. 7.45(a) share the same reference ground, the resulting averaged circuit model in Fig. 7.47 is easier to solve, and gives better physical insight into steady-state operation and dynamics of the boost converter. The circuit model of Fig. 7.47 reveals that the switch network performs the functions of: (*i*) transformation of dc and small-signal ac voltage and current levels according to the D':1 conversion ratio, and (*ii*) introduction of ac voltage and current variations into the converter circuit, driven by the control input $d(t)$. The model of Fig. 7.47 obtained using the circuit averaging approach is identical to the model of Fig. 7.17(b) obtained using the basic ac modeling technique of Section 7.2.

Next, we consider the CCM buck converter of Fig. 7.48, where the switch network ports are defined to share a common ground terminal. The derivation of the corresponding averaged switch model follows the same steps as in the SEPIC and the boost examples. Let us select $v_1(t)$ and $i_2(t)$ as the independent terminal variables of the two-port switch network, since these quantities coincide with the applied converter input voltage $v_g(t)$ and the inductor current $i(t)$, respectively. We then need to express the averaged dependent terminal waveforms $\langle i_1(t)\rangle_{T_s}$ and $\langle v_2(t)\rangle_{T_s}$ as functions of the control input $d(t)$ and of $\langle v_1(t)\rangle_{T_s}$ and $\langle i_2(t)\rangle_{T_s}$. Upon averaging the waveforms of Fig. 7.48(b), one obtains

$$\begin{aligned} \langle i_1(t)\rangle_{T_s} &= d(t)\,\langle i_2(t)\rangle_{T_s} \\ \langle v_2(t)\rangle_{T_s} &= d(t)\,\langle v_1(t)\rangle_{T_s} \end{aligned} \tag{7.150}$$

Perturbation and linearization of Eq. (7.150) then leads to

$$\begin{aligned} I_1 + \hat{i}_1(t) &= D\left(I_2 + \hat{i}_2(t)\right) + I_2\,\hat{d}(t) \\ V_2 + \hat{v}_2(t) &= D\left(V_1 + \hat{v}_1(t)\right) + V_1\,\hat{d}(t) \end{aligned} \tag{7.151}$$

An equivalent circuit corresponding to Eq. (7.151) is illustrated in Fig. 7.49(a). Replacement of the

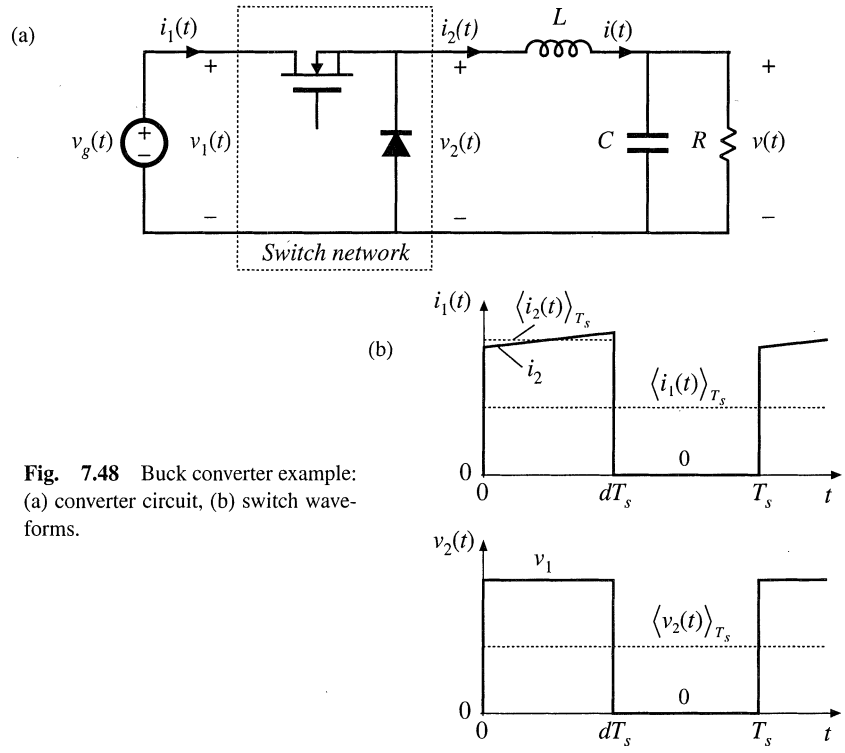

Fig. 7.48 Buck converter example: (a) converter circuit, (b) switch waveforms.

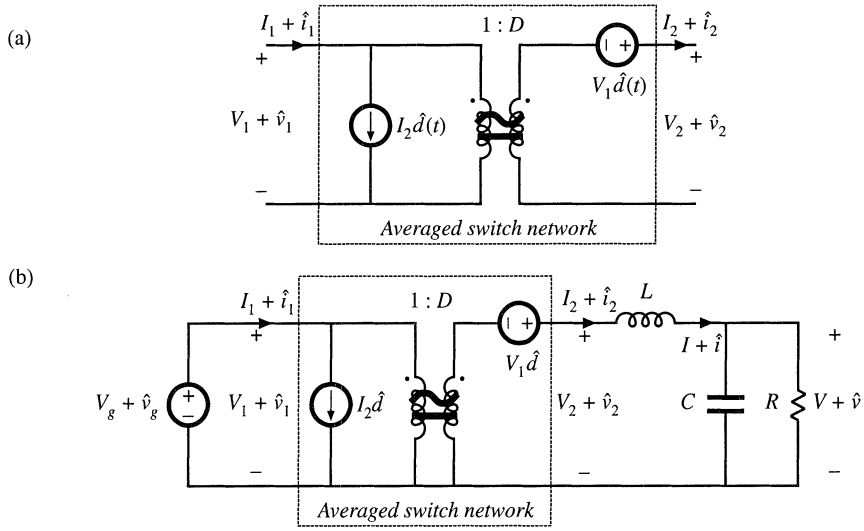

Fig. 7.49 Averaged switch modeling, buck converter example: (a) dc and small-signal ac averaged switch model; (b) Averaged circuit model of the buck converter obtained by replacement of the switch network by the averaged switch model.

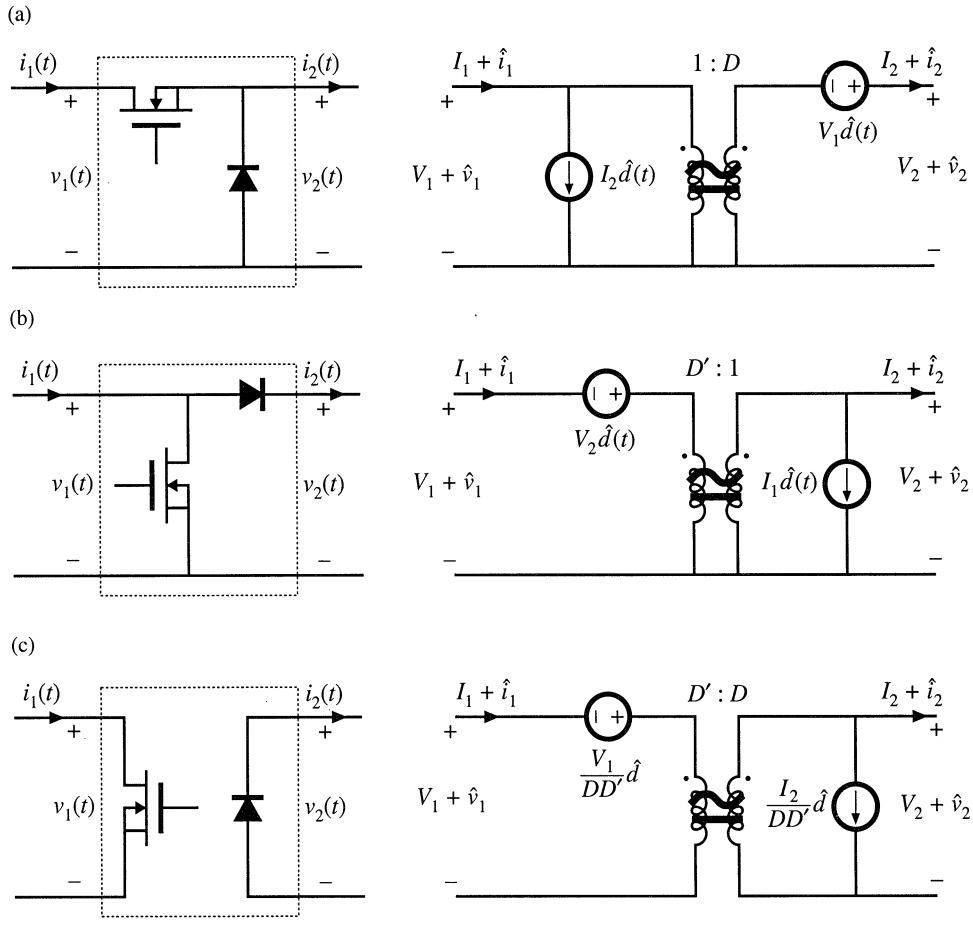

Fig. 7.50 Three basic switch networks, and their CCM dc and small-signal ac averaged switch models: (a) the buck switch network, (b) the boost switch network, and (c) the general two-switch network.

switch network in Fig. 7.48(a) with the averaged switch model of Fig. 7.49(a) leads to the converter averaged circuit model of Fig. 7.49(b). The circuit model of Fig. 7.49(b) reveals that the switch network performs the functions of: (*i*) transformation of dc and small-signal ac voltage and current levels according to the 1:*D* conversion ratio, and (*ii*) introduction of ac voltage and current variations into the converter circuit, driven by the control input $d(t)$. The model is easy to solve for both dc conversion ratio and small-signal frequency responses. It is identical to the model shown in Fig. 7.17(a).

The three basic switch networks—the buck switch network, the boost switch network, and the general two-switch network—together with the corresponding averaged switch models are shown in Fig. 7.50. Averaged switch models can be refined to include conduction and switching losses. These models can then be used to predict the voltages, currents, and efficiencies of nonideal converters. Two examples of averaged switch models that include losses are described in Sections 7.4.5 and 7.4.6.

7.4.5 Example: Averaged Switch Modeling of Conduction Losses

An averaged switch model can be refined to include switch conduction losses. Consider again the SEPIC of Fig. 7.37. Suppose that the transistor on-resistance is R_{on} and the diode forward voltage drop V_D are approximately constant. In this example, all other conduction or switching losses are neglected. Our objective is to derive an averaged switch model that includes conduction losses caused by the voltage drops across R_{on} and V_D. Let us define the switch network as in Fig. 7.39(a). The waveforms of the switch network terminal currents are the same as in Fig. 7.38, but the voltage waveforms are affected by the voltage drops across R_{on} and V_D as shown in Fig. 7.51. We select $i_1(t)$ and $v_2(t)$ as the switch network independent inputs, as in Section 7.4.1. The average values of $v_1(t)$ and $v_2(t)$ can be found as follows:

$$\langle v_1(t)\rangle_{T_s} = d(t)R_{on}\left(\langle i_{L1}(t)\rangle_{T_s} + \langle i_{L2}(t)\rangle_{T_s}\right) + d'(t)\left(\langle v_{C1}(t)\rangle_{T_s} + \langle v_{C2}(t)\rangle_{T_s} + V_D\right) \tag{7.152}$$

$$\langle v_2(t)\rangle_{T_s} = d(t)\left(\langle v_{C1}(t)\rangle_{T_s} + \langle v_{C2}(t)\rangle_{T_s} - R_{on}\left(\langle i_{L1}(t)\rangle_{T_s} + \langle i_{L2}(t)\rangle_{T_s}\right)\right) + d'(t)\left(-V_D\right) \tag{7.153}$$

Next, we proceed to eliminate $\langle i_{L1}(t)\rangle_{T_s}$, $\langle i_{L2}(t)\rangle_{T_s}$, $\langle v_{C1}(t)\rangle_{T_s}$, and $\langle v_{C2}(t)\rangle_{T_s}$, to write the above equations in terms of the averaged independent terminal currents and voltages of the switch network. By combining Eqs. (7.152) and (7.153), we obtain:

$$\langle v_{C1}(t)\rangle_{T_s} + \langle v_{C2}(t)\rangle_{T_s} = \langle v_1(t)\rangle_{T_s} + \langle v_2(t)\rangle_{T_s} \tag{7.154}$$

Since the current waveforms are the same as in Fig. 7.38, Eq. (7.134) can be used here:

$$\langle i_{L1}(t)\rangle_{T_s} + \langle i_{L2}(t)\rangle_{T_s} = \frac{\langle i_1(t)\rangle_{T_s}}{d(t)} \tag{7.155}$$

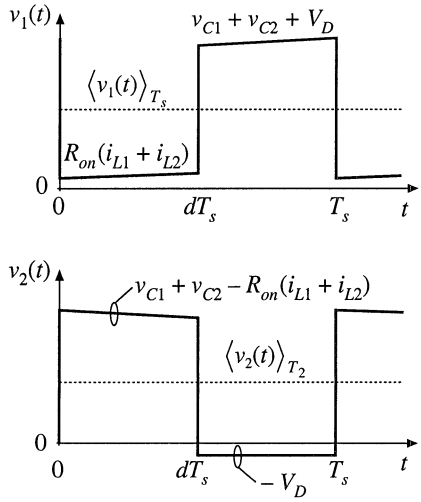

Fig. 7.51 The switch network terminal voltages $v_1(t)$ and $v_2(t)$ for the case when the transistor on-resistance is R_{on} and the diode forward voltage drop is V_D.

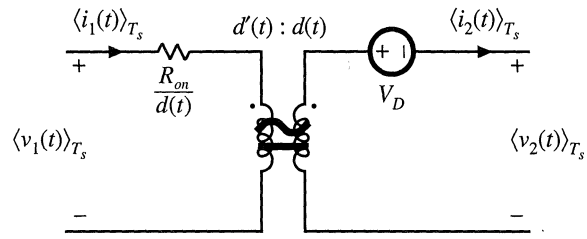

Fig. 7.52 Large-signal averaged switch model for the general two-switch network of Fig. 7.50. This model includes conduction losses due to the transistor on-resistance R_{on} and the diode forward voltage drop V_D.

Substitution of Eqs. (7.154) and (7.155) into Eq. (7.152) results in:

$$\langle v_1(t)\rangle_{T_s} = R_{on}\langle i_1(t)\rangle_{T_s} + d'(t)\left(\langle v_1(t)\rangle_{T_s} + \langle v_2(t)\rangle_{T_s} + V_D\right) \tag{7.156}$$

Equation (7.156) can be solved for the voltage $\langle v_1(t)\rangle_{T_s}$:

$$\langle v_1(t)\rangle_{T_s} = \frac{R_{on}}{d(t)}\langle i_1(t)\rangle_{T_s} + \frac{d'(t)}{d(t)}\left(\langle v_2(t)\rangle_{T_s} + V_D\right) \tag{7.157}$$

The expression for the averaged current $\langle i_2(t)\rangle_{T_s}$ is given by Eq. (7.137) derived in Section 7.4.2:

$$\langle i_2(t)\rangle_{T_s} = \frac{d'(t)}{d(t)}\langle i_1(t)\rangle_{T_s} \tag{7.158}$$

Equations (7.157) and (7.158) constitute the averaged terminal relations of the switch network. An equivalent circuit corresponding to these relationships is shown in Fig. 7.52. The generators that depend on the transistor duty cycle $d(t)$ are combined into an ideal transformer with the turns ratio $d'(t):d(t)$. This part of the model is the same as in the averaged switch model derived earlier for the switch network with ideal switches. The elements R_{on}/d and V_D model the conduction losses in the switch network. This is a large-signal, nonlinear model. If desired, this model can be perturbed and linearized in the usual manner, to obtain a small-signal ac switch model.

The model of Fig. 7.52 is also well suited for computer simulations. As an example of this application, consider the buck-boost converter in Fig 7.53(a). In this converter, the transistor on-resistance is $R_{on} = 50$ mΩ, while the diode forward voltage drop is $V_D = 0.8$ V. Resistor $R_L = 100$ mΩ models the copper loss of the inductor. All other losses are neglected. Figure 7.53(b) shows the averaged circuit model of the converter obtained by replacing the switch network with the averaged switch model of Fig. 7.52.

Let's investigate how the converter output voltage reaches its steady-state value, starting from zero initial conditions. A transient simulation can be used to generate converter waveforms during the start-up transient. It is instructive to compare the responses obtained by simulation of the converter switching circuit shown in Fig. 7.53(a) against the responses obtained by simulation of the averaged circuit model shown in Fig. 7.53(b). Details of how these simulations are performed can be found in Appendix B.1. Figure 7.54 shows the start-up transient waveforms of the inductor current and the output voltage. In the waveforms obtained by simulation of the averaged circuit model, the switching ripple is removed, but other features of the converter transient responses match very closely the responses

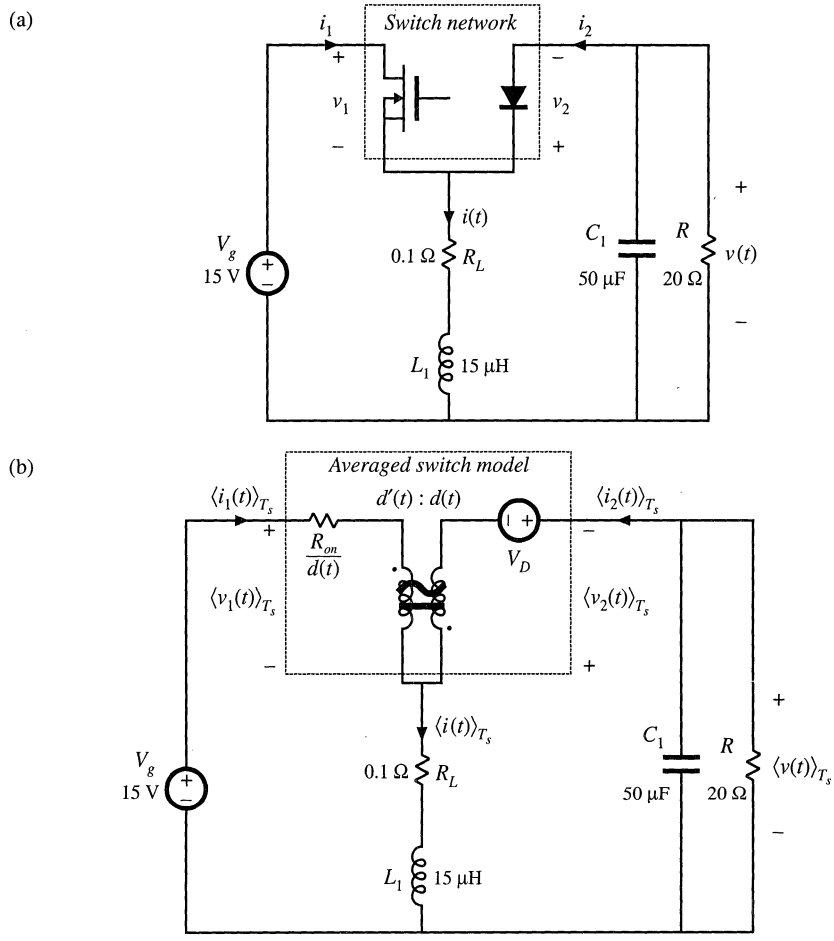

Fig. 7.53 Buck-boost converter example: (a) converter circuit; (b) averaged circuit model of the converter.

obtained from the switching circuit. Simulations of averaged circuit models can be used to predict converter steady-state and dynamic responses, as well as converter losses and efficiency.

7.4.6 Example: Averaged Switch Modeling of Switching Losses

Switching losses can also be modeled via averaged switch modeling. As an example, consider again the CCM buck converter of Fig. 7.48(a). Let us suppose that the transistor is ideal, and that the diode exhibits reverse recovery described in Section 4.3.2. The simplified switch waveforms are shown in Fig. 7.55. Initially, the diode conducts the inductor current and the transistor is in the off state. When the transistor turns on, a negative current flows through the diode so that the transistor current i_1 exceeds the inductor current. The time it takes to remove the charge Q_r stored within the diode is the reverse recovery time t_r.

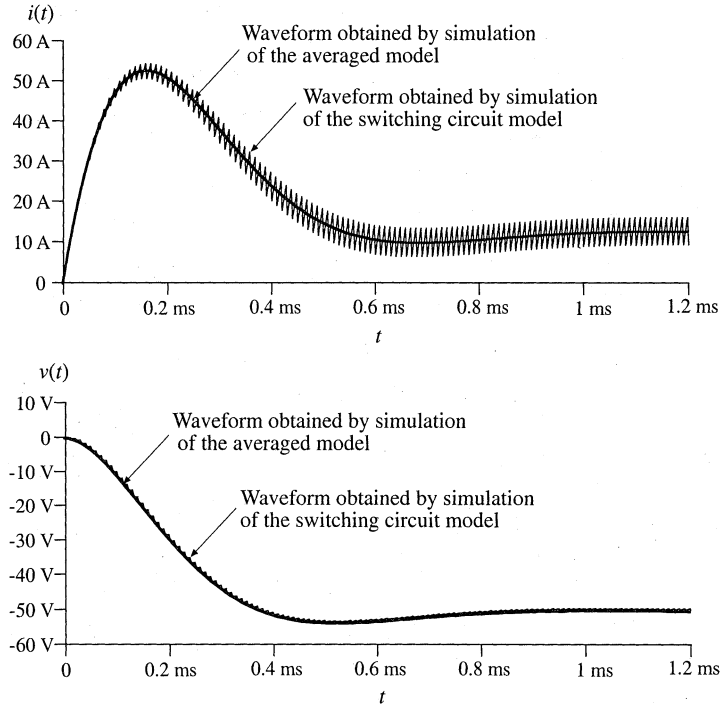

Fig. 7.54 Waveforms obtained by simulation of the switching converter circuit shown in Fig. 7.53(a) and by simulation of the averaged circuit model of Fig. 7.53(b)

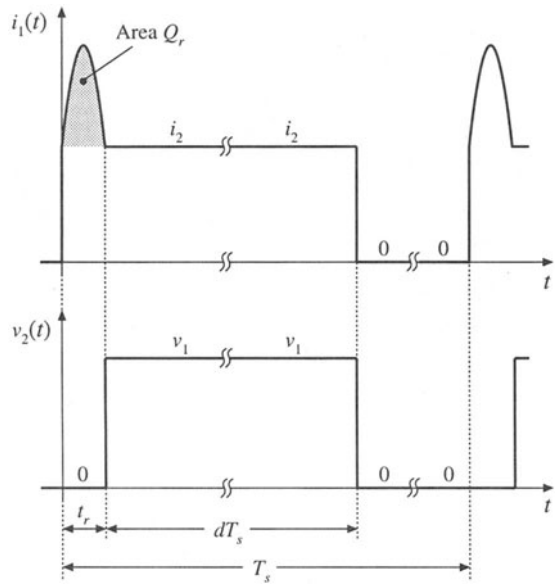

Fig. 7.55 Switch waveforms, buck converter switching loss example.

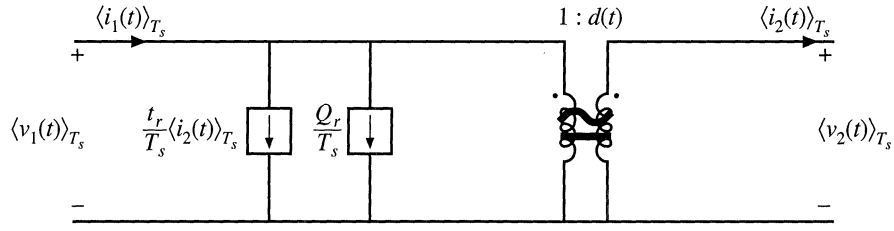

Fig. 7.56 Large-signal averaged switch model for the buck converter switching loss example.

It is assumed that the diode is "snappy," so that the voltage drop across the diode remains small during the reverse recovery time. After the diode reverse recovery is completed, the diode turns off, and the voltage v_2 across the diode quickly jumps to the input voltage $v_1 = v_g$. For this simple example, conduction losses and other switching losses are neglected.

Let us select $v_1(t)$ and $i_2(t)$ as the independent terminal variables of the two-port switch network, and derive expressions for the averaged dependent terminal waveforms $\langle i_1(t)\rangle_{T_s}$ and $\langle v_2(t)\rangle_{T_s}$. The average value of $i_1(t)$ is equal to the area under the $i_1(t)$ waveform, divided by the switching period T_s:

$$\begin{aligned}\langle i_1(t)\rangle_{T_s} &= \frac{1}{T_s}\int_0^{T_s} i_1(t)\,dt = \frac{1}{T_s}\left(Q_r + t_r\langle i_2(t)\rangle_{T_s} + dT_s\langle i_2(t)\rangle_{T_s}\right) \\ &= \frac{Q_r}{T_s} + \frac{t_r}{T_s}\langle i_2(t)\rangle_{T_s} + d\langle i_2(t)\rangle_{T_s}\end{aligned} \tag{7.159}$$

The quantity $d(t)$ is the effective transistor duty cycle, defined in Fig. 7.55 as the transistor on-time minus the reverse recovery time, divided by the switching period. The average value of $v_2(t)$ is equal to:

$$\langle v_2(t)\rangle_{T_s} = d\langle v_1(t)\rangle_{T_s} \tag{7.160}$$

Equations (7.159) and (7.160) constitute the averaged terminal relations of the switch network. An equivalent circuit corresponding to these relationships is constructed in Fig. 7.56. The generators that depend on the effective transistor duty cycle $d(t)$ are combined into an ideal transformer. To complete the model, the recovered charge Q_r and the reverse recovery time t_r can be expressed as functions of the current $\langle i_2(t)\rangle_{T_s}$ [20]. This is a large-signal averaged switch model, which accounts for the switching loss of the idealized waveforms of Fig. 7.55. If desired, this model can be perturbed and linearized in the usual manner, to obtain a small-signal ac switch model.

The model of Fig. 7.56 has the following physical interpretation. The transistor operates with the effective duty cycle $d(t)$. This is the turns ratio of the ideal dc transformer, which models the first-order switch property of lossless transfer of power from the switch input to the switch output port. The additional current generators model the switching loss. Note that both generators consume power. The total switching loss is:

$$P_{sw} = \langle v_1(t)\rangle_{T_s}\left(\frac{Q_r}{T_s} + \frac{t_r}{T_s}\langle i_2(t)\rangle_{T_s}\right) \tag{7.161}$$

These generators also correctly model how the switching loss increases the average switch input current.

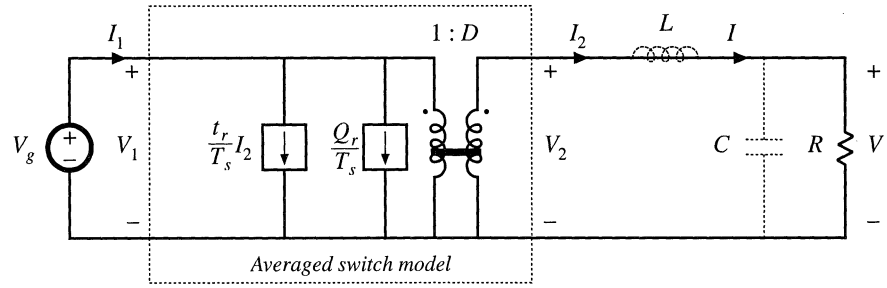

Fig. 7.57 Dc equivalent circuit model, buck converter switching loss example.

By inserting the switch model of Fig. 7.56 into the original converter circuit of Fig. 7.48(a), and by letting all waveforms be equal to their quiescent values, we obtain the steady-state model of Fig. 7.57. This model predicts that the steady-state output voltage is:

$$V = DV_g \tag{7.162}$$

To find the efficiency, we must compute the average input and output powers. The converter input power is

$$P_{in} = V_g I_1 = V_g \left(\frac{Q_r}{T_s} + \frac{t_r}{T_s} I_2 + D I_2 \right) \tag{7.163}$$

The average output power is

$$P_{out} = V I_2 = D V_g I_2 \tag{7.164}$$

Hence the converter efficiency is

$$\eta = \frac{P_{out}}{P_{in}} = \frac{1}{1 + \frac{Q_r}{DT_s I} + \frac{t_r}{DT_s}} \tag{7.165}$$

Beware, the efficiency is not simply equal to V/DV_g.

7.5 THE CANONICAL CIRCUIT MODEL

Having discussed several methods for deriving the ac equivalent circuit models of switching converters, let us now pause to interpret the results. All PWM CCM dc–dc converters perform similar basic functions. First, they transform the voltage and current levels, ideally with 100% efficiency. Second, they contain low-pass filtering of the waveforms. While necessary to remove the high-frequency switching ripple, this filtering also influences low-frequency voltage and current variations. Third, the converter waveforms can be controlled by variation of the duty cycle.

We expect that converters having similar physical properties should have qualitatively similar equivalent circuit models. Hence, we can define a *canonical circuit model* that correctly accounts for all

of these basic properties [1-3]. The ac equivalent circuit of any CCM PWM dc–dc converter can be manipulated into this canonical form. This allows us to extract physical insight, and to compare the ac properties of converters. The canonical model is used in several later chapters, where it is desired to analyze converter phenomena in a general manner, without reference to a specific converter. So the canonical model allows us to define and discuss the physical ac properties of converters.

In this section, the canonical circuit model is developed, based on physical arguments. An example is given which illustrates how to manipulate a converter equivalent circuit into canonical form. Finally, the parameters of the canonical model are tabulated for several basic ideal converters.

7.5.1 Development of the Canonical Circuit Model

The physical elements of the canonical circuit model are collected, one at a time, in Fig. 7.58. The converter contains a power input port $v_g(t)$ and a control input port $d(t)$, as well as a power output port and load having voltage $v(t)$. As discussed in Chapter 3, the basic function of any CCM PWM dc–dc converter is the conversion of dc voltage and current levels, ideally with 100% efficiency. As illustrated in Fig. 7.58(a), we have modeled this property with an ideal dc transformer, having effective turns ratio $1{:}M(D)$ where M is the conversion ratio. This conversion ratio is a function of the quiescent duty cycle D. As discussed in Chapter 3, this model can be refined, if desired, by addition of resistors and other elements that model the converter losses.

Slow variations $v_g(t)$ in the power input induce ac variations $v(t)$ in the converter output voltage. As illustrated in Fig. 7.58(b), we expect these variations also to be transformed by the conversion ratio $M(D)$.

The converter must also contain reactive elements that filter the switching harmonics and transfer energy between the power input and power output ports. Since it is desired that the output switching ripple be small, the reactive elements should comprise a low-pass filter having a cutoff frequency well below the switching frequency. This low-pass characteristic also affects how ac line voltage variations influence the output voltage. So the model should contain an effective low-pass filter as illustrated in Fig. 7.58(c). This figure predicts that the line-to-output transfer function is

$$G_{vg}(s) = \frac{\hat{v}(s)}{\hat{v}_g(s)} = M(D)\, H_e(s) \tag{7.166}$$

where $H_e(s)$ is the transfer function of the effective low-pass filter loaded by resistance R. When the load is nonlinear, R is the incremental load resistance, evaluated at the quiescent operating point. The effective filter also influences other properties of the converter, such as the small-signal input and output impedances. It should be noted that the elemental values in the effective low-pass filter do not necessarily coincide with the physical element values in the converter. In general, the element values, transfer function, and terminal impedances of the effective low-pass filter can vary with quiescent operating point. Examples are given in the following subsections.

Control input variations, specifically, duty cycle variations $\hat{d}(t)$, also induce ac variations in the converter voltages and currents. Hence, the model should contain voltage and current sources driven by $\hat{d}(t)$. In the examples of the previous section, we have seen that both voltage sources and current sources appear, which are distributed around the circuit model. It is possible to manipulate the model such that all of the $\hat{d}(t)$ sources are pushed to the input side of the equivalent circuit. In the process, the sources may become frequency-dependent; an example is given in the next subsection. In general, the sources can be combined into a single voltage source $e(s)\hat{d}(s)$ and a single current source $j(s)\hat{d}(s)$ as shown in

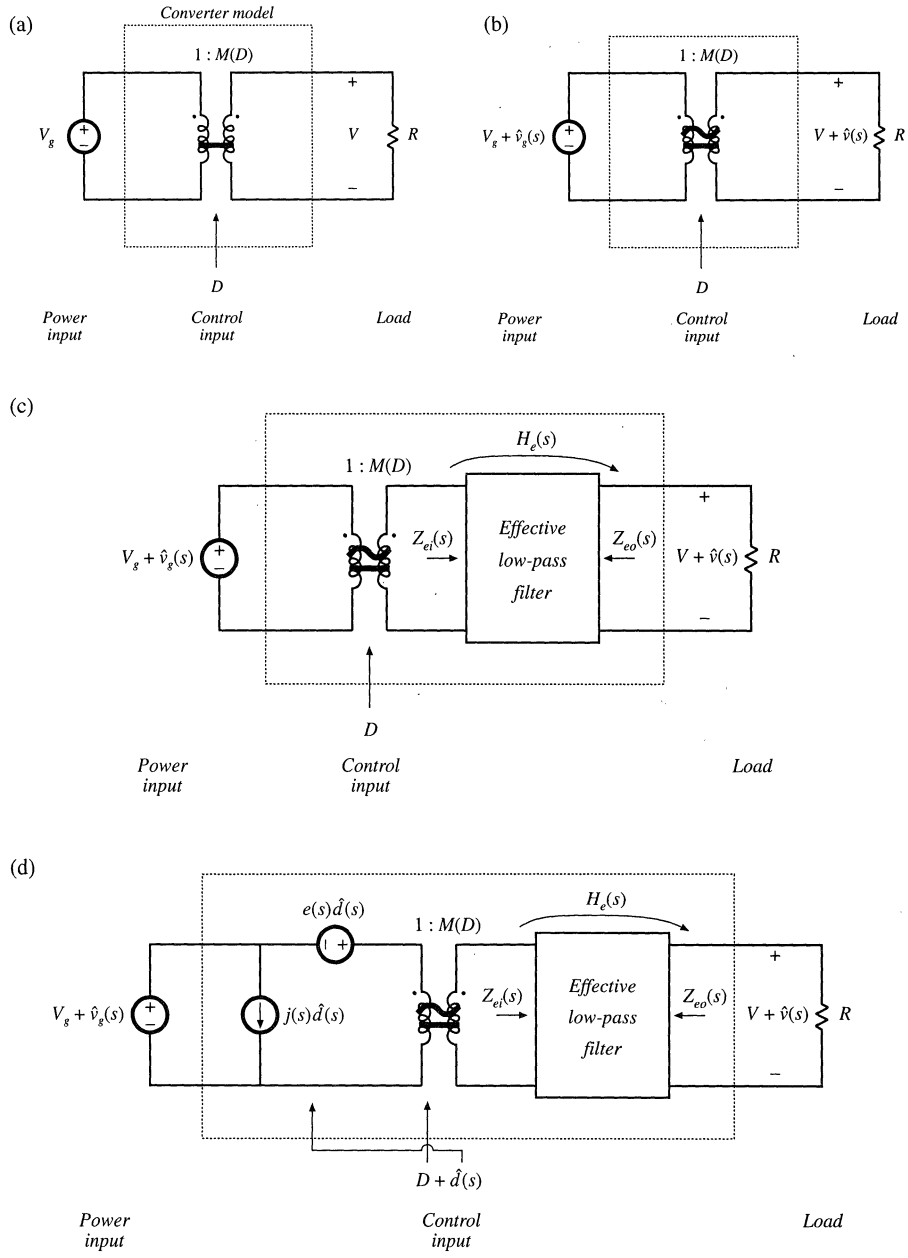

Fig. 7.58 Development of the canonical circuit model, based on physical arguments: (a) dc transformer model, (b) inclusion of ac variations, (c) reactive elements introduce effective low-pass filter, (d) inclusion of ac duty cycle variations.

Fig. 7.58(d). This model predicts that the small-signal control-to-output transfer function is

$$G_{vd}(s) = \frac{\hat{v}(s)}{\hat{d}(s)} = e(s)\, M(D)\, H_e(s) \tag{7.167}$$

This transfer function is found by setting the $\hat{v}_g(s)$ variations to zero, and solving for the dependence of $\hat{v}(s)$ on $\hat{d}(s)$. Figure 7.58(d) is the complete canonical circuit, which can model any PWM CCM dc–dc converter.

7.5.2 Example: Manipulation of the Buck-Boost Converter Model into Canonical Form

To illustrate the steps in the derivation of the canonical circuit model, let us manipulate the equivalent circuit of the buck-boost converter into canonical form. A small-signal ac equivalent circuit for the buck-boost converter is derived in Section 7.2. The result, Fig. 7.16(b), is reproduced in Fig. 7.59. To manipulate this network into canonical form, it is necessary to push all of the independent $d(t)$ generators to the left, while pushing the inductor to the right and combining the transformers.

The $(V_g - V)\hat{d}(t)$ voltage source is in series with the inductor, and hence the positions of these two elements can be interchanged. In Fig. 7.60(a), the voltage source is placed on the primary side of the $1{:}D$ ideal transformer; this requires dividing by the effective turns ratio D. The output-side $I\hat{d}(t)$ current source has also been moved to the primary side of the $D'{:}1$ transformer. This requires multiplying by the turns ratio $1/D'$. The polarity is also reversed, in accordance with the polarities of the $D'{:}1$ transformer windings.

Next, we need to move the $I\hat{d}(t)/D$ current source to the left of the inductor. This can be done using the artifice illustrated in Fig. 7.60(b). The ground connection of the current source is broken, and the source is connected to node A instead. A second, identical, current source is connected from node A to ground. The second source causes the current flowing into node A to be unchanged, such that the node equations of Figs. 7.60(a) and 7.60(b) are identical.

In Fig. 7.60(c), the parallel combination of the inductor and current source is converted into Thevenin equivalent form. The series combination of an inductor and voltage source are obtained.

In Fig. 7.60(d), the $I\hat{d}(t)/D$ current source is pushed to the primary side of the $1{:}D$ transformer. The magnitude of the current source is multiplied by the turns ratio D. In addition, the current source is pushed through the $(V_g - V)\hat{d}(t)/D$ voltage source, using the previously described artifice. The ground connection of the source is moved to node B, and an identical source is connected from node B to ground such that the circuit node equations are unchanged.

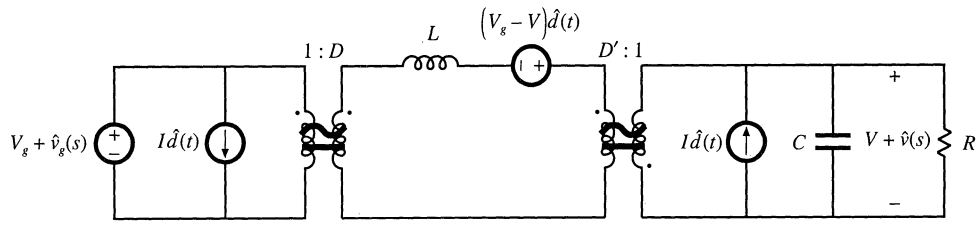

Fig. 7.59 Small-signal ac model of the buck-boost converter, before manipulation into canonical form.

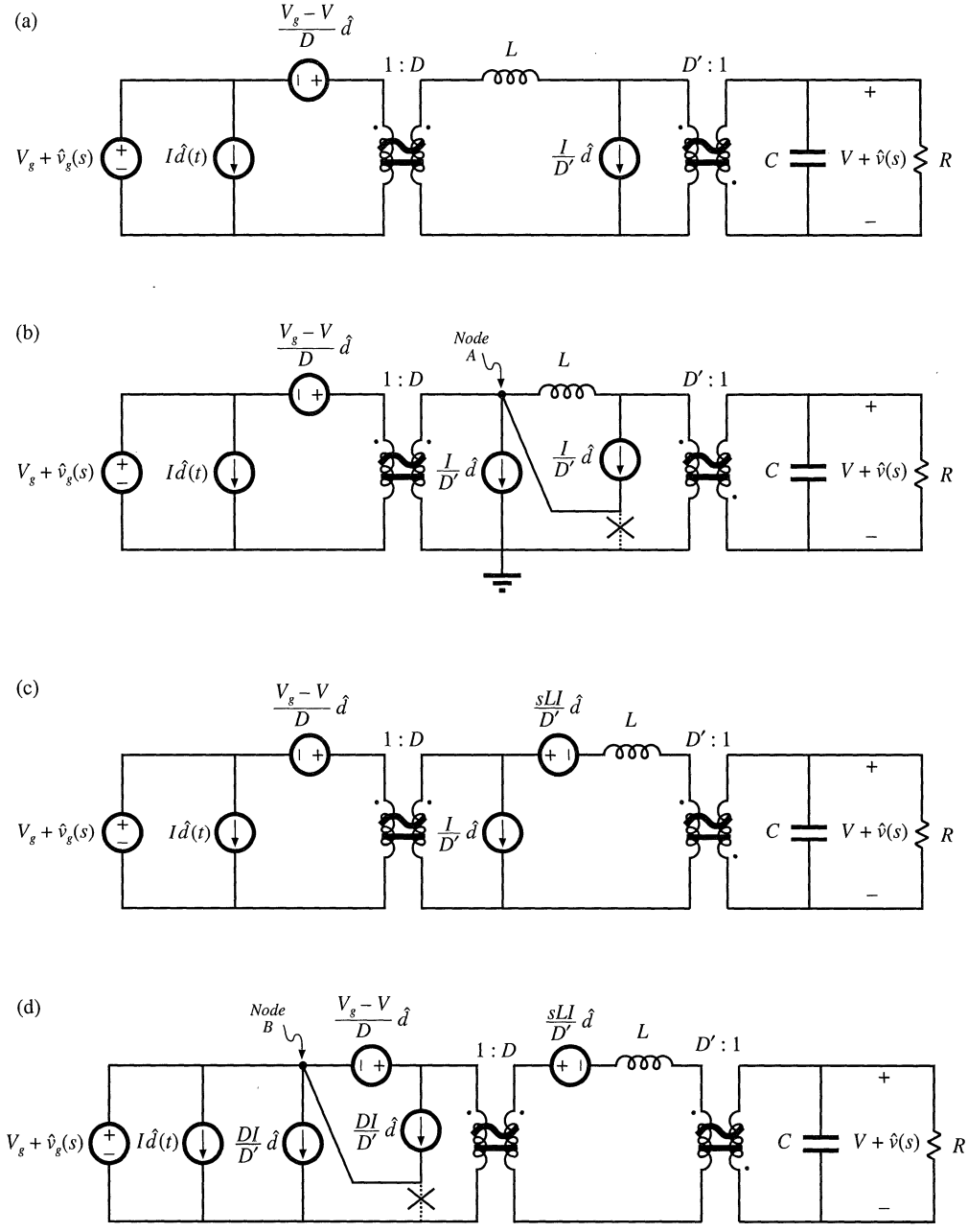

Fig. 7.60 Steps in the manipulation of the buck-boost ac model into canonical form.

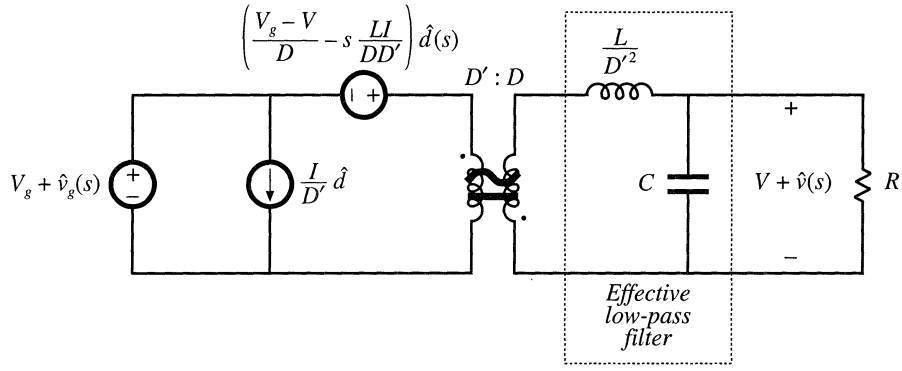

Fig. 7.61 The buck-boost converter model, in canonical form.

Figure 7.61 is the final form of the model. The inductor is moved to the secondary side of the D':1 transformer, by multiplying by the square of the turns ratio as shown. The $sLI\hat{d}(t)/D'$ voltage source is moved to the primary side of the 1:D transformer, by dividing by the turns ratio D. The voltage and current sources are combined as shown, and the two transformers are combined into a single D':D transformer. The circuit is now in canonical form.

It can be seen that the inductance of the effective low-pass filter is not simply equal to the physical inductor value L, but rather is equal to L/D'^2. At different quiescent operating points, with different values of D', the value of the effective inductance will change. In consequence, the transfer function, input impedance, and output impedance of the effective low-pass filter will also vary with quiescent operating point. The reason for this variation is the transformation of the inductance value by the effective D':1 transformer.

It can also be seen from Fig. 7.61 that the coefficient of the $\hat{d}(t)$ voltage generator is

$$e(s) = \frac{V_g - V}{D} - s\frac{LI}{DD'} \tag{7.168}$$

This expression can be simplified by substitution of the dc relationships (7.29). The result is

$$e(s) = -\frac{V}{D^2}\left(1 - s\frac{DL}{D'^2R}\right) \tag{7.169}$$

When we pushed the output-side $I\hat{d}(t)$ current source through the inductor, we obtained a voltage source having a frequency dependence. In consequence, the $e(s)\hat{d}$ voltage generator is frequency-dependent.

7.5.3 Canonical Circuit Parameter Values for Some Common Converters

For ideal CCM PWM dc–dc converters containing a single inductor and capacitor, the effective low-pass filter of the canonical model should contain a single inductor and a single capacitor. The canonical model then reduces to the circuit of Fig. 7.62. It is assumed that the capacitor is connected directly across the load. The parameter values for the basic buck, boost, and buck-boost converters are collected in Table 7.1. Again, it should be pointed out that the effective inductance L_e depends not only on the physical

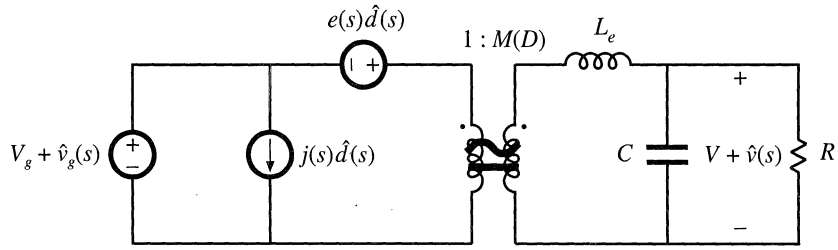

Fig. 7.62 The canonical model, for ideal CCM converters containing a single inductor and capacitor.

Table 7.1 Canonical model parameters for the ideal buck, boost and buck-boost converters

Converter	$M(D)$	L_e	$e(s)$	$j(s)$
Buck	D	L	$\frac{V}{D^2}$	$\frac{V}{R}$
Boost	$\frac{1}{D'}$	$\frac{L}{D'^2}$	$V\left(1-\frac{sL}{D'^2R}\right)$	$\frac{V}{D'^2R}$
Buck-boost	$-\frac{D}{D'}$	$\frac{L}{D'^2}$	$-\frac{V}{D^2}\left(1-\frac{sDL}{D'^2R}\right)$	$-\frac{V}{D'^2R}$

inductor value L, but also on the quiescent duty cycle D. Furthermore, the current flowing in the effective inductance L_e does not in general coincide with the physical inductor current $I + \hat{i}(t)$.

The model of Fig. 7.62 can be solved using conventional linear circuit analysis, to find quantities of interest such as the converter transfer functions, input impedance, and output impedance. Transformer isolated versions of the buck, boost, and buck-boost converters, such as the full bridge, forward, and flyback converters, can also be modeled using the equivalent circuit of Fig. 7.62 and the parameters of Table 7.1, provided that one correctly accounts for the transformer turns ratio.

7.6 MODELING THE PULSE-WIDTH MODULATOR

We have now achieved the goal, stated at the beginning of this chapter, of deriving a useful equivalent circuit model for the switching converter in Fig. 7.1. One detail remains: modeling the pulse-width modulator. The pulse-width modulator block shown in Fig. 7.1 produces a logic signal $\delta(t)$ that commands the converter power transistor to switch on and off. The logic signal $\delta(t)$ is periodic, with frequency f_s and duty cycle $d(t)$. The input to the pulse-width modulator is an analog control signal $v_c(t)$. The function of the pulse-width modulator is to produce a duty cycle $d(t)$ that is proportional to the analog control volt-

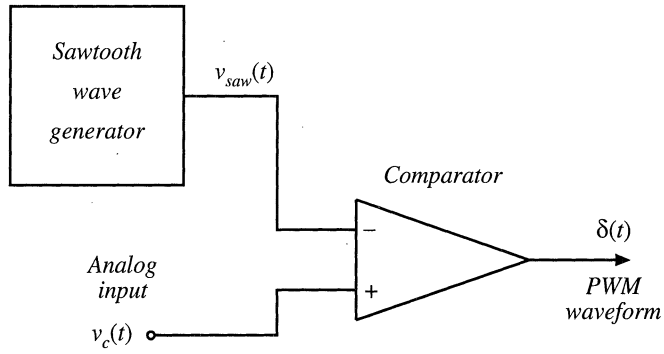

Fig. 7.63 A simple pulse-width modulator circuit.

age $v_c(t)$.

A schematic diagram of a simple pulse-width modulator circuit is given in Fig. 7.63. A sawtooth wave generator produces the voltage waveform $v_{saw}(t)$ illustrated in Fig. 7.64. The peak-to-peak amplitude of this waveform is V_M. The converter switching frequency f_s is determined by and equal to the frequency of $v_{saw}(t)$. An analog comparator compares the analog control voltage $v_c(t)$ to $v_{saw}(t)$. This comparator produces a logic-level output which is high whenever $v_c(t)$ is greater than $v_{saw}(t)$, and is otherwise low. Typical waveforms are illustrated in Fig. 7.64.

If the sawtooth waveform $v_{saw}(t)$ has minimum value zero, then the duty cycle will be zero whenever $v_c(t)$ is less than or equal to zero. The duty cycle will be $D = 1$ whenever $v_c(t)$ is greater than or equal to V_M. If, over a given switching period, $v_{saw}(t)$ varies linearly with t, then for $0 \le v_c(t) \le V_M$ the duty cycle d will be a linear function of v_c. Hence, we can write

$$d(t) = \frac{v_c(t)}{V_M} \quad \text{for } 0 \le v_c(t) \le V_M \tag{7.170}$$

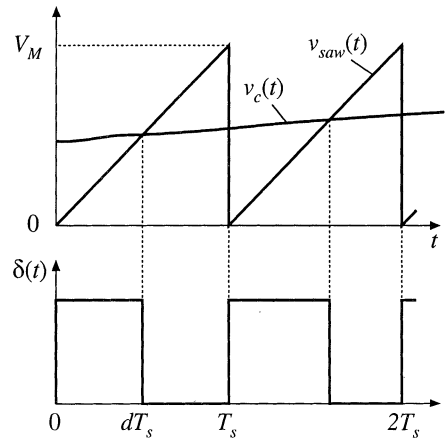

Fig. 7.64 Waveforms of the circuit of Fig. 7.63.

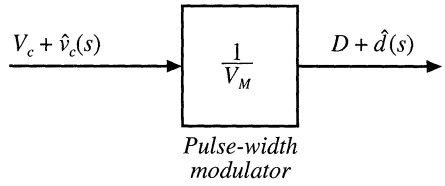

Fig. 7.65 Pulse-width modulator block diagram.

This equation is the input-output characteristic of the pulse-width modulator [2,11].

To be consistent with the perturbed-and-linearized converter models of the previous sections, we can perturb Eq. (7.170). Let

$$\begin{aligned} v_c(t) &= V_c + \hat{v}_c(t) \\ d(t) &= D + \hat{d}(t) \end{aligned} \tag{7.171}$$

Insertion of Eq. (7.171) into Eq. (7.170) leads to

$$D + \hat{d}(t) = \frac{V_c + \hat{v}_c(t)}{V_M} \tag{7.172}$$

A block diagram representing Eq. (7.172) is illustrated in Fig. 7.65. The pulse-width modulator has linear gain $1/V_M$. By equating like terms on both sides of Eq. (7.172), one obtains

$$\begin{aligned} D &= \frac{V_c}{V_M} \\ \hat{d}(t) &= \frac{\hat{v}_c(t)}{V_M} \end{aligned} \tag{7.173}$$

So the quiescent value of the duty cycle is determined in practice by V_c.

The pulse-width modulator model of Fig. 7.65 is sufficiently accurate for nearly all applications. However, it should be pointed out that pulse-width modulators also introduce sampling of the waveform. Although the analog input signal $v_c(t)$ is a continuous function of time, there can be only one discrete value of the duty cycle during every switching period. Therefore, the pulse-width modulator samples the waveform, with sampling rate equal to the switching frequency f_s. Hence, a more accurate modulator block diagram is as in Fig. 7.66 [10]. In practice, this sampling restricts the useful frequencies of the ac variations to values much less than the switching frequency. The designer must ensure that the bandwidth of the control system be sufficiently less than the Nyquist rate $f_s/2$.

Significant high-frequency variations in the control signal $v_c(t)$ can also alter the behavior of the pulse-width modulator. A common example is when $v_c(t)$ contains switching ripple, introduced by the feedback loop. This phenomenon has been analyzed by several authors [10,19], and effects of inductor current ripple on the transfer functions of current-programmed converters are investigated in Chapter 12. But it is generally best to avoid the case where $v_c(t)$ contains significant components at the switching frequency or higher, since the pulse-width modulators of such systems exhibit poor noise immunity.

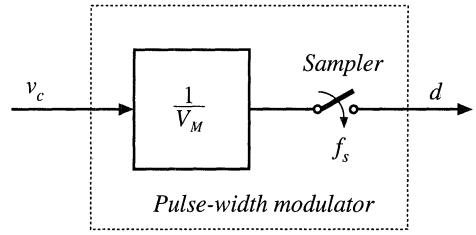

Fig. 7.66 A more accurate pulse-width modulator model, including sampling.

7.7 SUMMARY OF KEY POINTS

1. The CCM converter analytical techniques of Chapters 2 and 3 can be extended to predict converter ac behavior. The key step is to average the converter waveforms over one switching period. This removes the switching harmonics, thereby exposing directly the desired dc and low-frequency ac components of the waveforms. In particular, expressions for the averaged inductor voltages, capacitor currents, and converter input current are usually found.

2. Since switching converters are nonlinear systems, it is desirable to construct small-signal linearized models. This is accomplished by perturbing and linearizing the averaged model about a quiescent operating point.

3. Ac equivalent circuits can be constructed, in the same manner used in Chapter 3 to construct dc equivalent circuits. If desired, the ac equivalent circuits may be refined to account for the effects of converter losses and other nonidealities.

4. The state-space averaging method of Section 7.3 is essentially the same as the basic approach of Section 7.2, except that the formality of the state-space network description is used. The general results are listed in Section 7.3.2.

5. The circuit averaging technique also yields equivalent results, but the derivation involves manipulation of circuits rather than equations. Switching elements are replaced by dependent voltage and current sources, whose waveforms are defined to be identical to the switch waveforms of the actual circuit. This leads to a circuit having a time-invariant topology. The waveforms are then averaged to remove the switching ripple, and perturbed and linearized about a quiescent operating point to obtain a small-signal model.

6. When the switches are the only time-varying elements in the converter, then circuit averaging affects only the switch network. The converter model can then be derived by simply replacing the switch network with its averaged model. Dc and small-signal ac models of several common CCM switch networks are listed in Section 7.4.4. Conduction and switching losses can also be modeled using this approach.

7. The canonical circuit describes the basic properties shared by all dc–dc PWM converters operating in the continuous conduction mode. At the heart of the model is the ideal $1{:}M(D)$ transformer, introduced in Chapter 3 to represent the basic dc–dc conversion function, and generalized here to include ac variations. The converter reactive elements introduce an effective low-pass filter into the network. The model also includes independent sources that represent the effect of duty cycle variations. The parameter values in the canonical models of several basic converters are tabulated for easy reference.

8. The conventional pulse-width modulator circuit has linear gain, dependent on the slope of the sawtooth waveform, or equivalently on its peak-to-peak magnitude.

REFERENCES

[1] R. D. MIDDLEBROOK and SLOBODAN ĆUK, "A General Unified Approach to Modeling Switching-Converter Power Stages," *International Journal of Electronics*, Vol. 42, No. 6, pp. 521-550, June 1977.

[2] SLOBODAN ĆUK, "Modeling, Analysis, and Design of Switching Converters," Ph.D. thesis, California Institute of Technology, November 1976.

[3] R. D. MIDDLEBROOK AND SLOBODAN ĆUK, "Modeling and Analysis Methods for Dc-to-Dc Switching Converters," *Proceedings of the IEEE International Semiconductor Power Converter Conference*, 1977 Record, pp. 90-111, March 1977. Reprinted in *Advances in Switched-Mode Power Conversion*, Vol. 1, Irvine: Teslaco, 1983.

[4] G. W. WESTER and R. D. MIDDLEBROOK, "Low-Frequency Characterization of Switched Dc-Dc Converters," *IEEE Transactions an Aerospace and Electronic Systems*, Vol. AES-9, pp. 376-385, May 1973.

[5] DANIEL M. MITCHELL, *Dc–Dc Switching Regulator Analysis*, New York: McGraw-Hill, 1988.

[6] SETH R. SANDERS and GEORGE C. VERGESE, "Synthesis of Averaged Circuit Models for Switched Power Converters," *IEEE Transactions on Circuits and Systems*, Vol. 38, No. 8, pp. 905-915, August 1991.

[7] P. T. KREIN, J. BENTSMAN, R. M. BASS, and B. C. LESIEUTRE, "On the Use of Averaging for the Analysis of Power Electronic Systems," *IEEE Transactions on Power Electronics*, Vol. 5, No. 2, pp. 182-190, April 1990.

[8] B. LEHMAN and R. M. BASS, "Switching Frequency Dependent Averaged Models for PWM DC-DC Converters," *IEEE Transactions on Power Electronics*, Vol. 11, No. 1, pp. 89-98, January 1996.

[9] R. M. BASS and J. SUN, "Averaging Under Large-Ripple Conditions," *IEEE Power Electronics Specialists Conference*, 1998 Record, pp. 630-632, May 1998.

[10] ARTHUR R. BROWN and R. D. MIDDLEBROOK, "Sampled-Data Modeling of Switching Regulators," *IEEE Power Electronics Specialists Conference*, 1981 Record, pp. 349-369, June 1981.

[11] R. D. MIDDLEBROOK, "Predicting Modulator Phase Lag in PWM Converter Feedback Loops," *Proceedings of the Eighth National Solid-State Power Conversion Conference* (Powercon 8), April 1981.

[12] A. KISLOVSKI, R. REDL, AND N. SOKAL, *Dynamic Analysis of Switching-Mode DC/DC Converters*, New York: Van Nostrand Reinhold, 1994.

[13] R. TYMERSKI and V. VORPERIAN, "Generation, Classification and Analysis of Switched-Mode DC-to-DC Converters by the Use of Converter Cells," *Proceedings of the 1986 International Telecommunications Energy Conference* (INTELEC'86), pp. 181-195, October 1986.

[14] V. VORPERIAN, R. TYMERSKI, and F. C. LEE, "Equivalent Circuit Models for Resonant and PWM Switches," *IEEE Transactions on Power Electronics*, Vol. 4, No. 2, pp. 205-214, April 1989.

[15] V. VORPERIAN, "Simplified Analysis of PWM Converters Using the Model of the PWM Switch: Parts I and II," *IEEE Transactions on Aerospace and Electronic Systems*, Vol. AES-26, pp. 490-505, May 1990.

[16] S. FREELAND and R. D. MIDDLEBROOK, "A Unified Analysis of Converters with Resonant Switches," *IEEE Power Electronics Specialists Conference*, 1987 Record, pp. 20-30.

[17] ARTHUR WITULSKI and ROBERT ERICKSON, "Extension of State-Space Averaging to Resonant Switches —and Beyond," *IEEE Transactions on Power Electronics*, Vol. 5, No. 1, pp. 98-109, January 1990.

[18] D. MAKSIMOVIĆ and S. ĆUK, "A Unified Analysis of PWM Converters in Discontinuous Modes," *IEEE Transactions on Power Electronics*, Vol. 6, No. 3, pp. 476-490, July 1991.

[19] D. J. SHORTT and F. C. LEE, "Extensions of the Discrete-Average Models for Converter Power Stages," *IEEE Power Electronics Specialists Conference*, 1983 Record, pp. 23-37, June 1983.

[20] O. AL-NASEEM and R.W. ERICKSON, "Prediction of Switching Loss Variations by Averaged Switch Modeling," *IEEE Applied Power Electronics Conference*, 2000 Record, pp. 242-248, February 2000.

PROBLEMS

7.1 An ideal boost converter operates in the continuous conduction mode.

(a) Determine the nonlinear averaged equations of this converter.

(b) Now construct a small-signal ac model. Let

$$\begin{aligned} \langle v_g(t) \rangle_{T_s} &= V_g + \hat{v}_g(t) \\ d(t) &= D + \hat{d}(t) \\ \langle i(t) \rangle_{T_s} &= I + \hat{i}(t) \\ \langle v(t) \rangle_{T_s} &= V + \hat{v}(t) \end{aligned}$$

where V_g, D, I, and V are steady-state dc values; $\hat{v}_g(t)$ and $\hat{d}(t)$ are small ac variations in the power and control inputs; and $\hat{i}(t)$ and $\hat{v}(t)$ are the resulting small ac variations in the inductor current and output voltage, respectively. Show that the following model results:

Large-signal dc components

$$\begin{aligned} 0 &= -D'V + V_g \\ 0 &= D'I - \frac{V}{R} \end{aligned}$$

Small-signal ac components

$$\begin{aligned} L\frac{d\hat{i}(t)}{dt} &= -D'\hat{v}(t) + V\hat{d}(t) + \hat{v}_g(t) \\ C\frac{d\hat{v}(t)}{dt} &= D'\hat{i}(t) - I\hat{d}(t) - \frac{\hat{v}(t)}{R} \end{aligned}$$

7.2 Construct an equivalent circuit that corresponds to the boost converter small-signal ac equations derived in Problem 7.1(b).

7.3 Manipulate your boost converter equivalent circuit of Problem 7.2 into canonical form. Explain each step in your derivation. Verify that the elements in your canonical model agree with Table 7.1.

7.4 The ideal current-fed bridge converter of Fig. 2.31 operates in the continuous conduction mode.

(a) Determine the nonlinear averaged equations of this converter.

(b) Perturb and linearize these equations, to determine the small-signal ac equations of the converter.

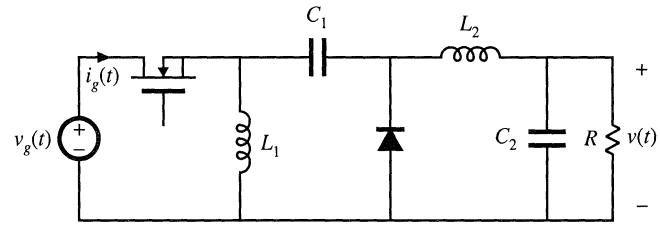

Fig. 7.67 Inverse SEPIC, Problem 7.7.

(c) Construct a small-signal ac equivalent circuit model for this converter.

7.5 Construct a complete small-signal ac equivalent circuit model for the flyback converter shown in Fig. 7.18, operating in continuous conduction mode. The transformer contains magnetizing inductance L, referred to the primary. In addition, the transformer exhibits significant core loss, which can be modeled by a resistor R_C in parallel with the primary winding. All other elements are ideal. You may use any valid method to solve this problem. Your model should correctly predict variations in $i_g(t)$.

7.6 Modeling the Ćuk converter. You may use any valid method to solve this problem.

(a) Derive the small-signal dynamic equations that model the ideal Ćuk converter.

(b) Construct a complete small-signal equivalent circuit model for the Ćuk converter.

7.7 Modeling the inverse-SEPIC. You may use any valid method to solve this problem.

(a) Derive the small-signal dynamic equations that model the converter shown in Fig. 7.67.

(b) Construct a complete small-signal equivalent circuit model for the inverse-SEPIC.

7.8 Consider the nonideal buck converter of Fig. 7.68. The input voltage source $v_g(t)$ has internal resistance R_g. Other component nonidealities may be neglected.

(a) Using the state-space averaging method, determine the small-signal ac equations that describe variations in i, v, and i_g, which occur owing to variations in the transistor duty cycle d and input voltage v_g.

(b) Construct an ac equivalent circuit model corresponding to your equations of part (a).

(c) Solve your model to determine an expression for the small-signal control-to-output transfer function.

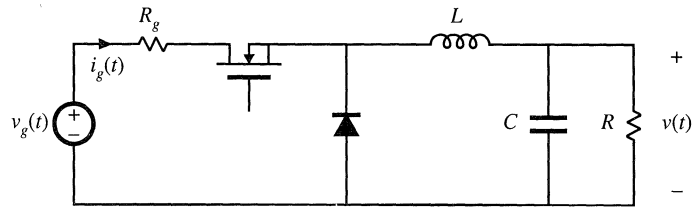

Fig. 7.68 Nonideal buck converter, Problem 7.8.

7.9 Use the circuit-averaging technique to derive the dc and small-signal ac equivalent circuit of the buck converter with input filter, illustrated in Fig. 2.32. All elements are ideal.

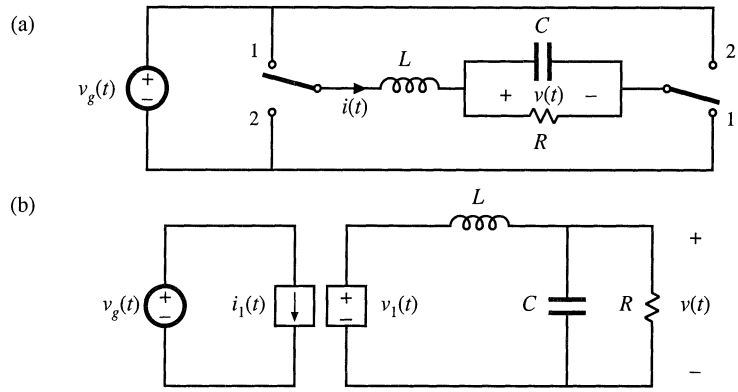

Fig. 7.69 Bridge inverter, Problem 7.11: (a) circuit, (b) large-signal averaged model.

7.10 A flyback converter operates in the continuous conduction mode. The MOSFET switch has on-resistance R_{on}, and the secondary-side diode has a constant forward voltage drop V_D. The flyback transformer has primary winding resistance R_p and secondary winding resistance R_s.

(a) Derive the small-signal ac equations for this converter.

(b) Derive a complete small-signal ac equivalent circuit model, which is valid in the continuous conduction mode and which correctly models the above losses, as well as the converter input and output ports.

7.11 Circuit averaging of the bridge inverter circuit of Fig. 7.69(a).

(a) Show that the converter of Fig. 7.69(a) can be written in the electrically identical form shown in Fig. 7.69(b). Sketch the waveforms $i_1(t)$ and $v_1(t)$.

(b) Use the circuit-averaging method to derive a large-signal averaged model for this converter.

(c) Perturb and linearize your circuit model of part (b), to obtain a single equivalent circuit that models dc and small-signal ac signals in the bridge inverter.

7.12 Use the circuit averaging method to derive an equivalent circuit that models dc and small-signal ac signals in the buck-boost converter. You may assume that the converter operates in the continuous conduction mode, and that all elements are ideal.

(a) Give a time-invariant electrically identical circuit, in which the switching elements are replaced by equivalent voltage and current sources. Define the waveforms of the sources.

(b) Derive a large-signal averaged model for this converter.

(c) Perturb and linearize your circuit model of part (b), to obtain a single equivalent circuit that models dc and small-signal ac signals in the buck-boost converter.

7.13 The two-output flyback converter of Fig. 7.70(a) operates in the continuous conduction mode. It may be assumed that the converter is lossless.

(a) Derive a small-signal ac equivalent circuit for this converter.

(b) Show that the small-signal ac equivalent circuit for this two-output converter can be written in the generalized canonical form of Fig. 7.70(b). Give analytical expressions for the generators $e(s)$ and $j(s)$.

7.14 A pulse-width modulator circuit is constructed in which the sawtooth-wave generator is replaced by a triangle-wave generator, as illustrated in Fig. 7.71(a). The triangle waveform is illustrated in Fig. 7.71(b).

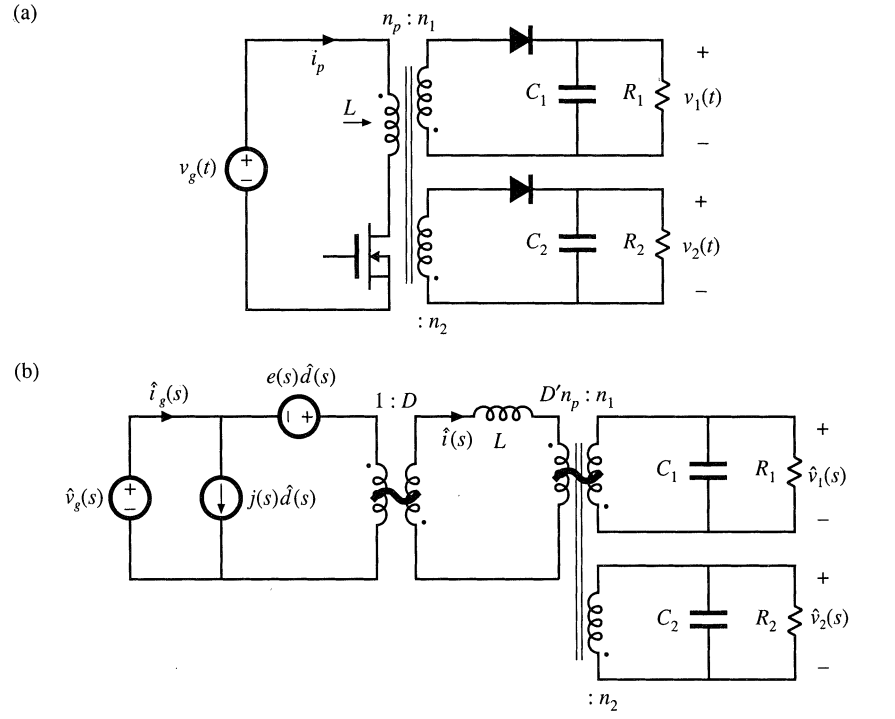

Fig. 7.70 Two-output flyback converter, Problem 7.13: (a) converter circuit, (b) small-signal ac equivalent circuit.

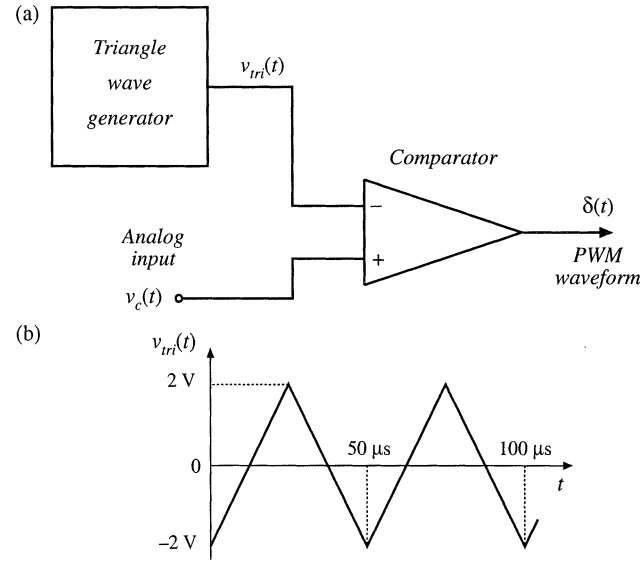

Fig. 7.71 Pulse-width modulator, Problem 7.14.

(a) Determine the converter switching frequency, in Hz.

(b) Determine the gain $d(t)/v_c(t)$ for this circuit.

(c) Over what range of v_c is your answer to (b) valid?

7.15 Use the averaged switch modeling technique to derive an ac equivalent circuit model for the buck-boost converter of Fig. 7.31:

(a) Replace the switches in Fig. 7.31 with the averaged switch model given in Fig. 7.50(c).

(b) Compare your result with the model given in Fig. 7.16(b). Show that the two models predict the same small-signal line-to-output transfer function $G_{vg}(s) = \hat{v}/\hat{v}_g$.

7.16 Modify the CCM dc and small-signal ac averaged switch models of Fig. 7.50, to account for MOSFET on-resistance R_{on} and diode forward voltage drop V_D.

7.17 Use the averaged switch modeling technique to derive a dc and ac equivalent circuit model for the flyback converter of Fig. 7.18. You can neglect all losses and the transformer leakage inductances.

(a) Define a switch network containing the transistor Q_1 and the diode D_1 as in Fig. 7.39(a). Derive a large-signal averaged switch model of the switch network. The model should account for the transformer turns ratio n.

(b) Perturb and linearize the model you derived in part (a) to obtain the dc and ac small-signal averaged switch model. Verify that for $n = 1$ your model reduces to the model shown in Fig. 7.39(d).

(c) Using the averaged switch model you derived in part (b), sketch a complete dc and small-signal ac model of the flyback converter. Solve the model for the steady-state conversion ratio $M(D) = V/V_g$.

(d) The averaged switch models you derived in parts (a) and (b) could be used in other converters having an isolation transformer. Which ones?

7.18 In the flyback converter of Fig. 7.18, the transistor on-resistance is R_{on}, and the diode forward voltage drop is V_D. Other losses and the transformer leakage inductances can be neglected. Derive a dc and small-signal ac averaged switch model for the switch network containing the transistor Q_1 and the diode D_1. The model should account for the on-resistance R_{on}, the diode forward voltage drop V_D, and the transformer turns ratio n.

7.19 In the boost converter of Fig. 7.72(a), the $v_1(t)$ and $i_2(t)$ waveforms of Fig. 7.72(b) are observed. During the transistor turn-on transition, a reverse current flows through the diode which removes the diode stored charge. As illustrated in Fig. 7.72(b), the reverse current spike has area $-Q_r$ and duration t_r. The inductor winding has resistance R_L. You may neglect all losses other than the switching loss due to the diode stored charge and the conduction loss due to the inductor winding resistance.

(a) Derive an averaged switch model for the boost switch network in Fig. 7.72(a).

(b) Use your result of part (a) to sketch a dc equivalent circuit model for the boost converter.

(c) The diode stored charge can be expressed as a function of the current I_1 as:

$$Q_r = k_q\sqrt{I_1}$$

while the reverse recovery time t_r is approximately constant. Given $V_g = 100$ V, $D = 0.5$, $f_s = 100$ kHz, $k_q = 100$ nC/A$^{1/2}$, $t_r = 100$ ns, $R_L = 0.1\ \Omega$, use a dc sweep simulation to plot the converter efficiency as a function of the load current I_{LOAD} in the range:

$$1\text{ A} \le I_{LOAD} \le 10\text{ A}$$

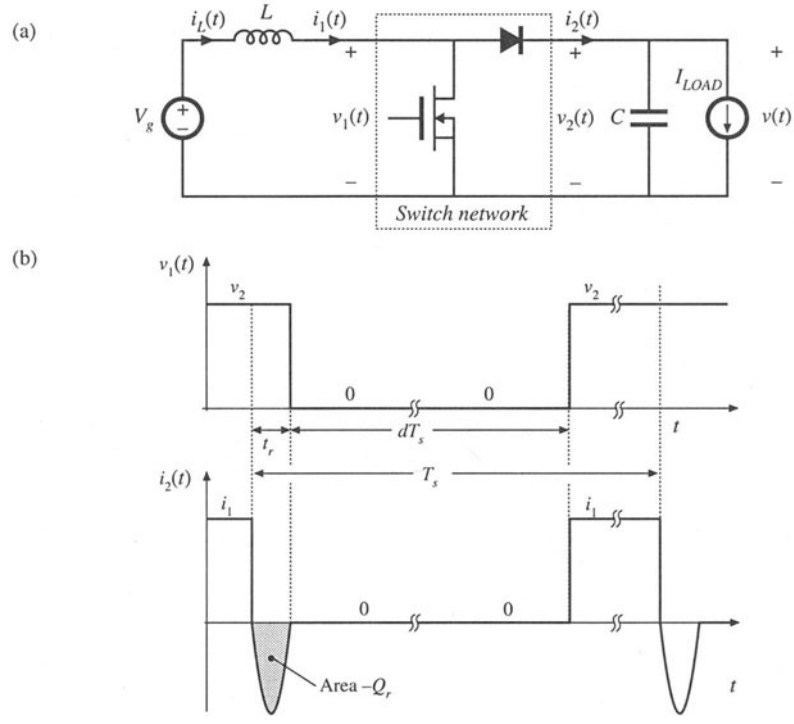

Fig. 7.72 Boost converter and waveforms illustrating reverse recovery of the diode. Averaged switch modeling in this converter is addressed in Problem 7.19.